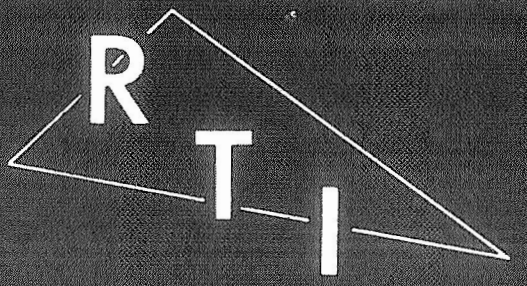

RESEARCH TRIANGLE INSTITUTE

NASA CR-111848

EVALUATION OF A GAS DISCHARGE TRANSDUCER AND ASSOCIATED INSTRUMENTATION NECESSARY FOR THE ASTEROID BELT METEOROID EXPERIMENT

February 1971

Prepared under Contract No. NAS1-9420 by
RESEARCH TRIANGLE INSTITUTE
Research Triangle Park, N. C.

for Langley Research Center

NATIONAL AERONAUTICS AND SPACE ADMINISTRATION

NASA CR-111848

EVALUATION OF A GAS DISCHARGE TRANSDUCER AND ASSOCIATED INSTRUMENTATION NECESSARY FOR THE ASTEROID BELT METEOROID EXPERIMENT

By C. D. Parker

Prepared under Contract No. NAS 1-9420 by
RESEARCH TRIANGLE INSTITUTE
Research Triangle Park, N. C.

for Langley Research Center

NATIONAL AERONAUTICS AND SPACE ADMINISTRATION

FOREWORD

This report was prepared by The Research Triangle Institute, Research Triangle Park, N. C., on NASA Contract NAS1-9420, "Evaluation of a Gas-Discharge Transducer and Associated Instrumentation Necessary For The Asteroid Belt Meteoroid Experiment". The contract was monitored by L. R. McMaster of the Instrument Research Division, Langley Research Center.

This investigation was performed by the Engineering and Environmental Sciences Divsion of the Research Triangle Institute under the general direction of Dr. R. M. Burger. Mr. J. B. Tommerdahl was Laboratory Supervisor and C. D. Parker was Project Leader. Other Institute staff members who contributed significantly to this work are Dr. J. J. Wortman, C. E. Moore, S. R. Stilley, J. H. White and Dr. H. G. Richter.

In addition to L. R. McMaster, numerous other Langley Research Center personnel contributed significantly to this investigation. These included R. L. O'Neal and John Thomson.

Abstract

EVALUATION OF A GAS DISCHARGE TRANSDUCER AND ASSOCIATED INSTRUMENTATION NECESSARY FOR THE ASTEROID BELT METEOROID EXPERIMENT

By C. D. Parker

Research Triangle Institute
Research Triangle Park, N. C.

An electrode assembly located inside a gas filled pressure cell as a pressure transducer was characterized in order to adapt this assembly to a meteoroid experiment for Pioneer F/G. Numerous pressurizing gases were investigated, and a mixture of 75 percent argon and 25 percent nitrogen was selected as suitable for the meteoroid experiment. Additionally, it was necessary to add an initial ionization source to the pressure transducers to achieve reliability and Ni^{63} was electroplated on the transducer electrodes for this purpose. Experiments were conducted to gain confidence in their reliability of the meteoroid experiment.

A preliminary design of a compatible electronic system was completed early in this investigation. This effort was terminated in favor of an electronic system designed and fabricated at Langley Research Center.

CONTENTS

LIST OF ILLUSTRATIONS

LIST OF ILLUSTRATIONS (continued)

LIST OF ILLUSTRATIONS (continued)

EVALUATION OF A GAS DISCHARGE TRANSDUCER AND ASSOCIATED INSTRUMENTATION NECESSARY FOR THE ASTEROID BE T METEOROID EXPERIMENT

By C. D. Parker
Research Triangle Institute

SECTION I

INTRODUCTION

In February or March of 1972, a spacecraft, Pioneer F, will be launched from Cape Kennedy on a voyage to the vicinity of the Planet Jupiter. By midsummer, approximately 140 days from Earth, Pioneer F will enter the 150 million mile wide Asteroid Belt. Pioneer F will spend approximately 200 days traversing the Asteroid Belt, and approach within approximately 80,000 miles of Jupiter between December 1973 and March 1974. While Pioneer F is in transit to Jupiter, Pioneer G will embark on a similar journey about March of 1973 (ref. 1). Both Pioneer F and Pioneer G will carry a Langley Research Center (LaRC) experiment designed to provide a measure of the density of micrometeoroids in the 10^{-9} g mass range between Earth and Jupiter, and especially in the Asteroid Belt. The investigations described in this report have been in direct support of these two experiments, the Meteoroid Experiment For Pioneer F and Pioneer G (MEPF/G).

The MEPF/G experiment consists of a group of pressurized cells exposed so as to impact with meteoroids during the Pioneer F/G flights. Each of these sealed cells enclose a pressure transducer that functions through associated circuitry to provide a count of the number of cells penetrated. Figure 1 is a simplified block diagram of the experiment. The pressurized cells are located in twelve (12) pressure panels mounted on the back of the Pioneer instrument package, and each panel is compartmented into eighteen (18) individual cells. The transducer circuitry supplies the required high voltage to the transducers, provides a suitable signal to the counters when a transducer fires and limits power consumed by a firing transducer. The time control counter functions to advance the event counter by only one count whenever a transducer fires and provides time for the transducer to see a vacuum before counting additional firings. The event counter is a recycling counter that is serially read out to the spacecraft by the multiplexer upon receipt of the word gate and bit rate commands. The power converter receives 28 Vdc from the spacecraft and supplies the voltages required by the experiment. The power converter can be turned ON and OFF on command from the spacecraft. Figure 2 is a photograph of the MEPF/G Design Verification Unit (DVU)

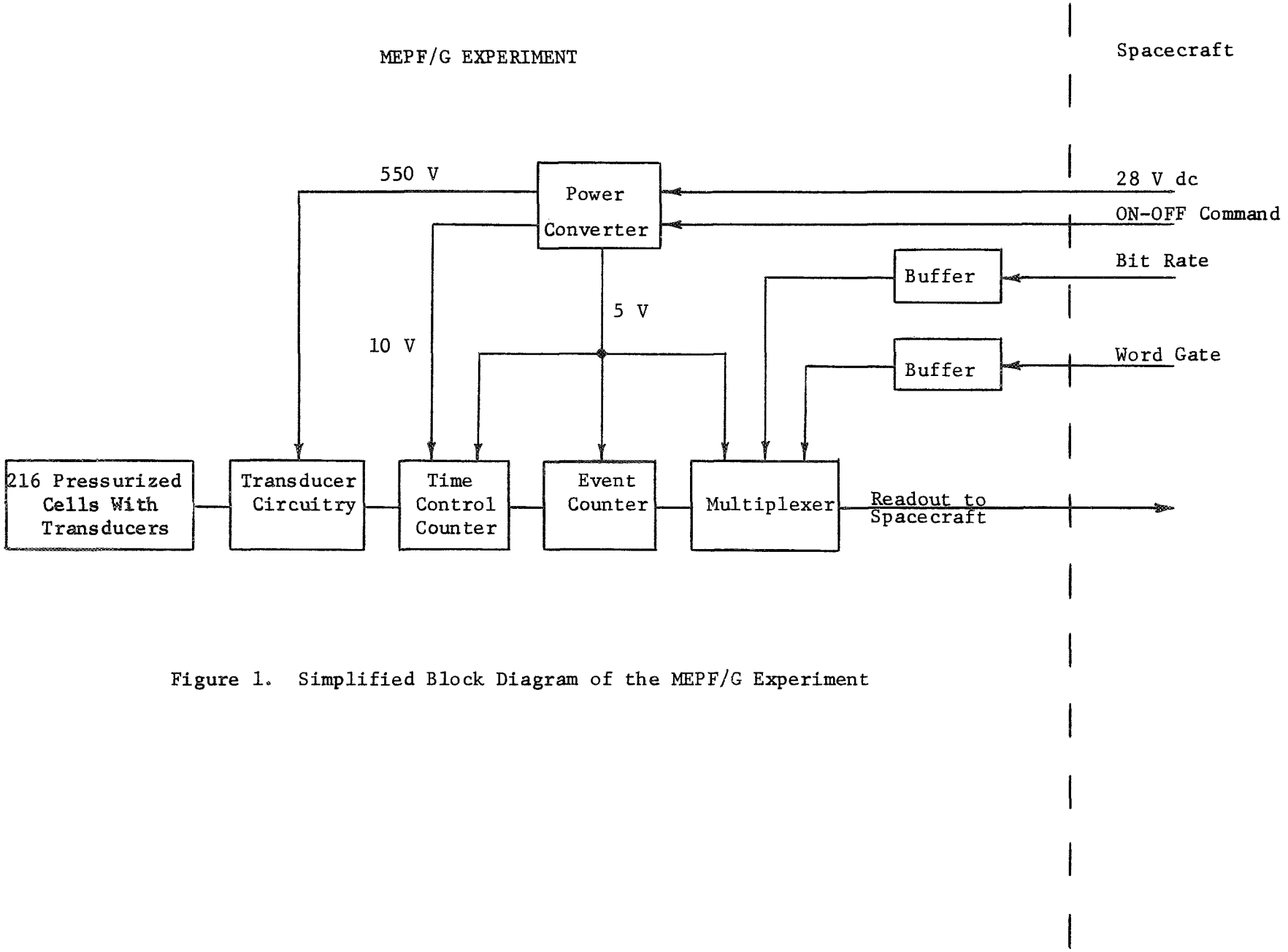

Figure 1. Simplified Block Diagram of the MEPF/G Experiment

NASA
L-70-5581

Figure 2. MEPF/G Design Verification Unit

fabricated at LaRC. The 12 panels of 18 pressurized cells each are in evidence, and all of the electronics is located in the single chassis box. The particular configuration of the MEPF/G experiment reflects limitations on power, weight and size. Of these limitations, weight is the most significant and largely dictated the other features of the experiment. The MEPF/G experiments were allotted 3.9 lb, one watt of electric power and the electronic package was restricted to a 3" x 3" x 3" cube. Numerous other restrictions and limitations were imposed by existing Pioneer documents (ref. 2).

A Sequence of Events

The initial objectives of this project were to characterize the transducers previously selected for the MEPF/G experiment and design an electronic package to provide the required readout. Some characteristics of the transducers were readily determined and progress with the electronic design was possible. The most significant characteristic of these transducers, however, was an unacceptable reliability, and an improvement in reliability became the most important consideration for the project. Investigations into the reliability problem required, improvements in the test facilities and alterations in the transducer cleaning and mounting procedures. Alternate electrode geometries and materials were also investigated. Concurrent with these investigations, the gas pressurizing the cells was changed to accommodate another experiment on the spacecraft. This change required that some of the preceding characterization work be repeated.

The solution to the basic reliability problem involved the electroplating of a radioactive material on the transducer electrodes and a flight quality procedure for cleaning, plating and counting radioactivity had to be evolved.

The second gas, selected for the pressure cells on the basis of desirable thermal properties, ultimately proved to be unsatisfactory, and the identification of a suitable pressurizing gas became a priority objective. This investigation led to the gas mixture used in the MEPF/G experiment, and a final characterization of the transducer.

Most of the flight hardware for the MEPF/G experiment were fabricated at LaRC. The pressure panels were designed and fabricated with the basic transducer purchased as an off-the-shelf item. RTI electroplated the transducer electrodes with a radioactive isotope of Nickel, Ni^{63}. The electronic instrumentation flight package was designed and fabricated at LaRC. A parallel effort at RTI resulted in a very similar design, and a model of this design was proved to be reliable through extensive testing. A power converter required for the experiment was subcontracted from RTI to Wilmore Electronics Company, Durham, N. C.

In order to expedite fabrication of this MEPF/G experiment, it was necessary to make commitments concerning the power converter early in the design effort. The voltage to be supplied to the transducers was specified before the final pressurizing gas was selected, and it had to be changed with each change in gas.

SECTION II

THE MEPF/G EXPERIMENT

The Pressure Cells

The MEPF/G pressure cells are fabricated at LaRC from sheets of 1 mil and 2 mils stainless steel. A 1 mil sheet is placed over a 2 mil sheet and the two sheets are seam-welded together to form the 18 individual cells. Fig. 3 is a photograph of a completed pressure panel showing the 18 cells with transducers and wiring in place. Adjacent cells have transducer attachments at opposite ends to provide space for wiring, and two folds are symmetrically located on the panel for stress relief. The transducers, illustrated in Fig. 4 and shown photographically in Fig. 5, consist of a pair of electrodes located in each pressure cell. The electrodes are of tin-plated kovar and set in thermally matched glass. Fig. 6 illustrates the method of mounting the transducer in the pressure cell.

It is perhaps a misnomer to refer to these electrode assemblies as a transducer. The electrode-pressure cell combination actually comprises a cold cathode discharge tube that "fires" to conduct current under favorable conditions. When the pressure cell is fully pressurized, only a negligible leakage conduction occurs. If the cell leaks gas to a surrounding vacuum, as it would if penetrated by a micrometeoroid in space, the gas pressure will decrease until the electrodes can "breakdown" or "fire" and conduct significant current. As pressure is further decreased, the conduction will extinguish and again become negligible. The term transducer will be used in this report to refer to the electrode-pressure cell combination functioning as a cold cathode discharge tube.

Cold Cathode Discharge Tubes

The electrical characteristics of a cold cathode discharge tube are a complex function of many variables including gas pressure; cathode geometry, material and surface conditions; temperature; gas properties; and the amount and type of ionizing radiation within the device. An excellent discussion of the cold cathode discharge phenomena can be found in Acton and Swift (ref. 3). Only those aspects of the theory that are pertinent to the MEPF/G application are discussed in this report.

The I-V characteristic of a cold cathode device with parallel plate electrodes and constant pressure and temperature is illustrated in Fig. 7. As voltage is increased, a small current flows due to the mobility of residual electrons and positive ions in the pressurizing gas. Residual ions and electrons result from photons or radioactive additives,

NASA
L-70-5457

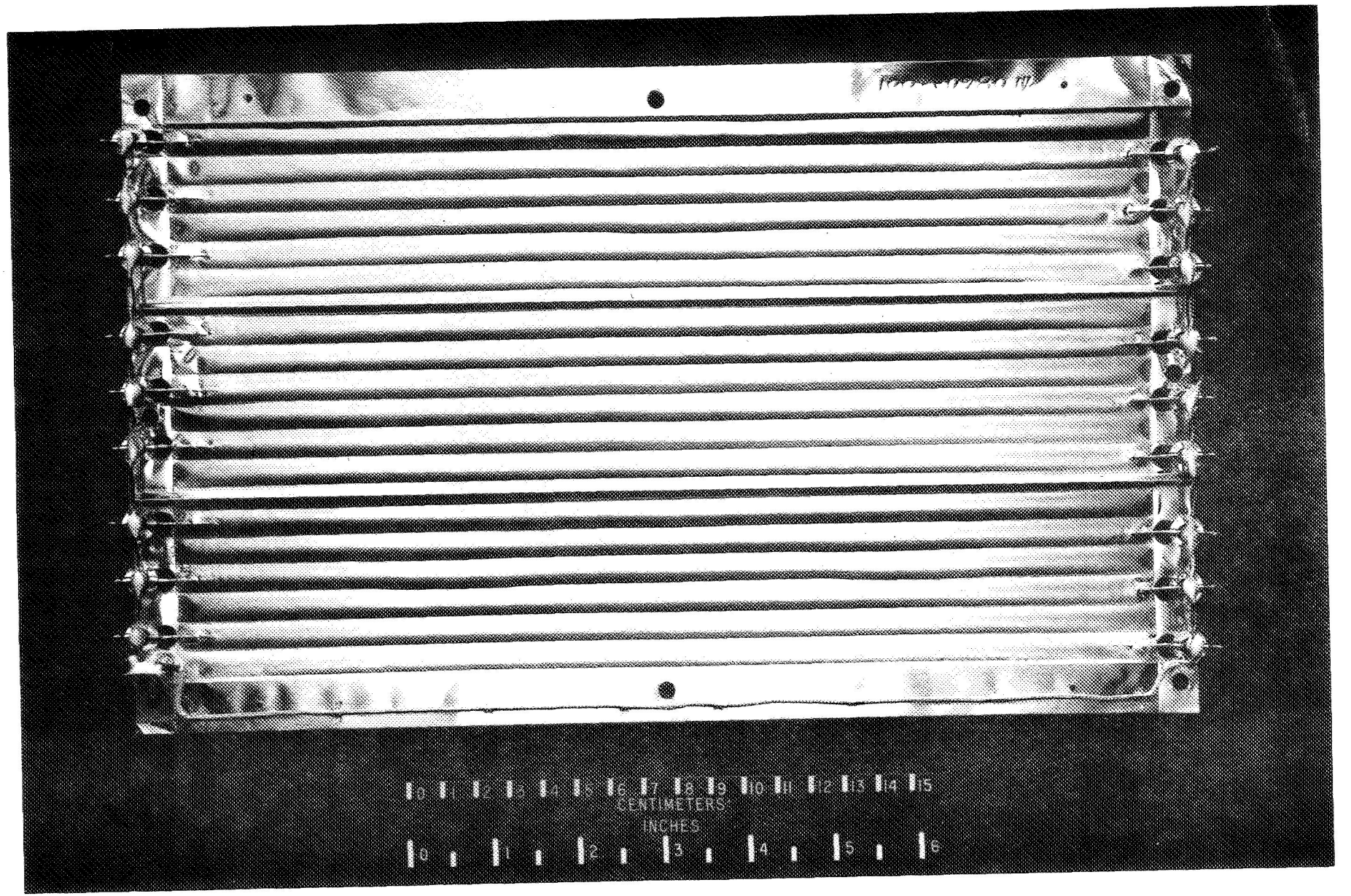

Figure 3. A Complete MEPF/G Pressure Panel

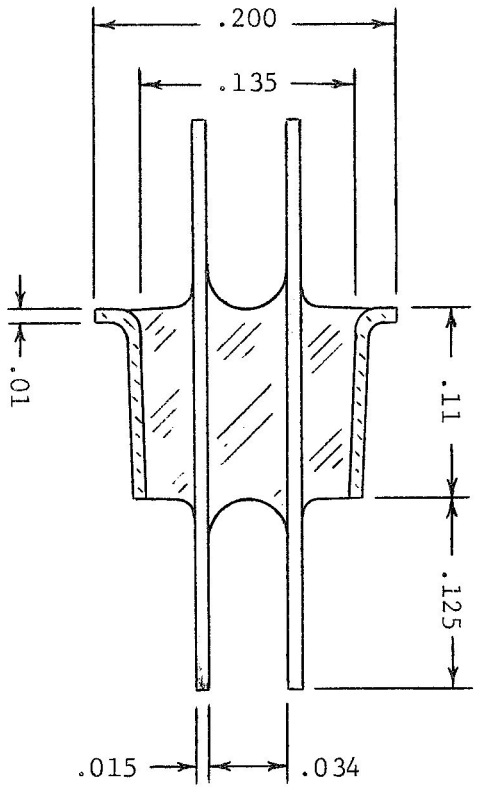

Figure 4. Illustration of the MEPF/G Transducer

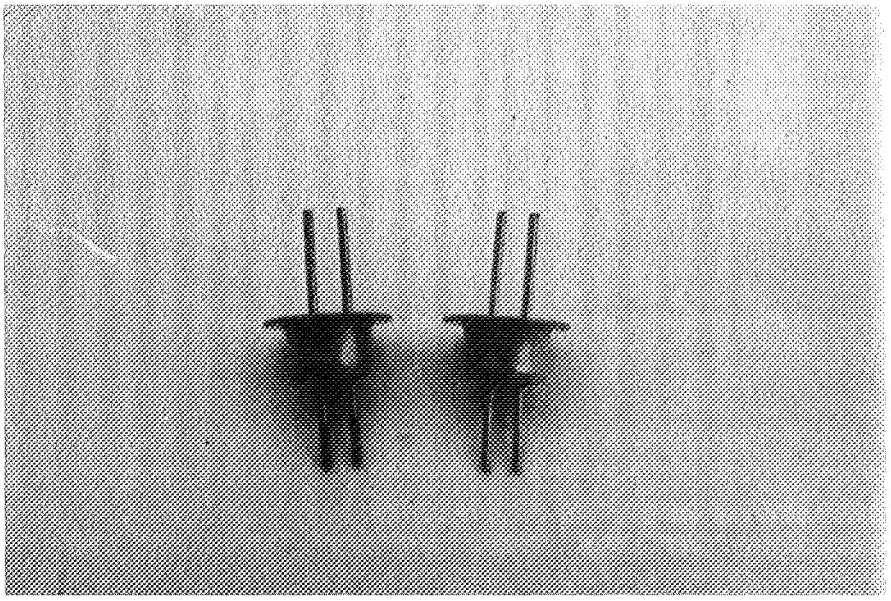

Figure 5. MEPF/G Pressure Transducers
(Unit on left has been plated with Ni^{63})

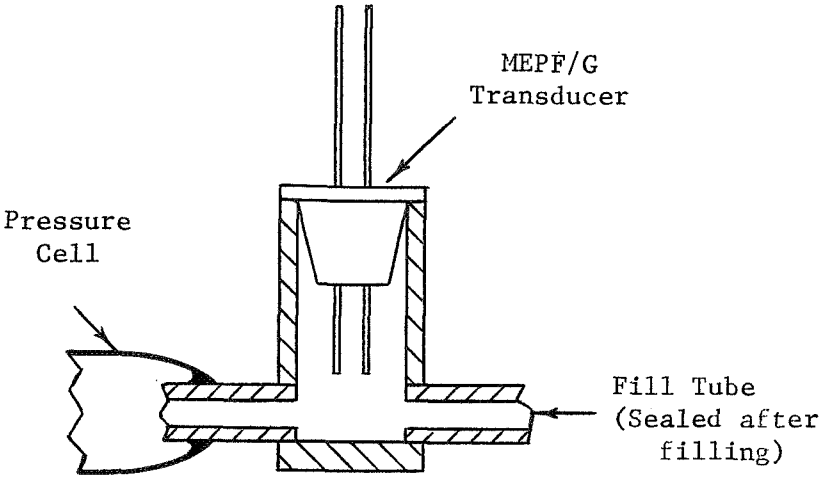

Figure 6. Illustration of a Transducer Mounted in a Pressure Cell

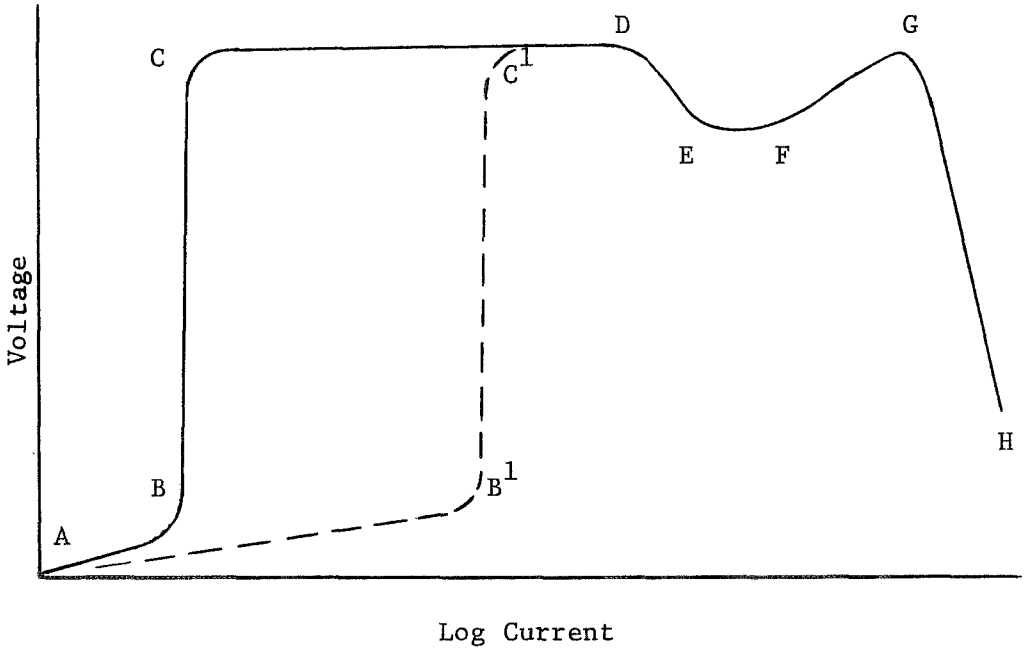

Figure 7. Log Current-Voltage Characteristics of a Cold Cathode Discharge Tube

for example, and are usually present in any gas. This residual current appears as segment AB of Fig. 7. As voltage is further increased, a constant current region, segment BC is reached in which all of the residual ions and electrons are being collected and the voltage can be significantly increased without any further increases in current. Beyond this constant current region, a cold cathode device may enter the Townsend Discharge region in which a rapid increase in current results from further voltage increases. This increase of current is due to electron avalanche; i.e., a condition in which a primary electron causes further ionization in collisions with gas atoms. The Townsend Discharge region, segment CD in Fig. 7, is not self-maintaining and conduction will cease if the source of the residual ionization is removed.

If voltage across the electrodes is increased to the negative resistance region, i.e., beyond D in Fig. 7, the cold cathode device will "breakdown" and the gas will glow. The voltage at which this occurs is the breakdown, striking or firing voltage and is of special interest to the MEPF/G Experiment. After breakdown, the cold cathode device will move through the negative resistance region to the normal glow region, segment EF in Fig. 7. In this region, the gas surrounding the negative electrode glows and the voltage across the electrode reaches a minimum value, i.e., the running voltage. The running voltage and the cathode surface area covered by the glow varies with the current. A cold cathode device operating in the glow region is commonly known as a glow tube. Beyond the normal glow region lies the abnormal glow region, segment FG, and the Arc Discharge region, segment GH. The abnormal glow is a permissible region of operation. It differs from normal glow in the distribution of the electric field between anode and cathode.

There are numerous applications of cold cathode devices which operate to the left of the firing voltage in Fig. 7, i.e., to the left of D. An important example is the Geiger-Muller Counter. Most cold cathode devices utilize the breakdown and glow regions of the I-V characteristics, however, as does the MEPF/G experiment.

The dotted curves in Fig. 7 illustrate a mode of operation that can occur if the initial ionization level is sufficiently high. An increasing voltage will continue to yield an increasing current due to the availability of residual ions and electrons. This is an undersirable mode for the MEPF/G application in that a significantly greater leakage current flows prior to breakdown.

The Ionization Cycle. - The breakdown or firing characteristics of a cold cathode discharge device can be analyzed in terms of an ionization cycle. Consider, for example, a cold cathode device with plane, parallel electrodes, a constant gas pressure and a constant applied

voltage. If an electron is produced at the cathode by external illumination or a radioactive source, for example, it will be accelerated toward the anode by the electric field. In transit toward the anode, the electron may obtain sufficient energy to cause further ionization when colliding with gas atoms or molecules. Positive ions thus created will be accelerated toward the cathode and may cause secondary emission of electrons when striking the cathode. If the energy attained by the ion is sufficient, the secondary emission may consist of two electrons, for example, one to neutralize the atom and one to be accelerated toward the cathode. This process is referred to as an ionization cycle, and the efficiency of the process will determine if current in a given cold cathode device will continue to increase or if the ionization cycle is self-quenching.

The efficiency of the ionization cycle can be examined by considering several parameters descriptive of the cycle. An important parameter is the ionization coefficient of the pressurizing gas, η_i, which is defined as the number of ion pairs created by an electron in moving through a potential difference of one volt in an electric field. The greater the ionization coefficient, the more efficient the ionization cycle and the more probable it is that current in the device will continue to increase. The ionization coefficient is a characteristic of the pressurizing gas for the accelerating electron must attain an energy of V_i to ionize the gas atom or molecule. The ionization coefficient also varies with the gas pressure. At high pressure the accelerated electron will experience numerous elastic collisions and probably will not attain sufficient energy between these collisions to ionize a gas atom. As pressure is reduced, η_i will increase to a maximum value and then decrease. The decrease of η_i at low pressures is due to the decreasing probability of a collision between the electron and a gas molecule.

A second parameter of considerable importance is the secondary emission coefficient, γ, which is defined as the number of electrons released from the cathode per positive ion striking the cathode. It is a characteristic of cathode material, surface condition and geometry. It also depends upon the electric field and gas pressure. An electron emitted from the cathode may be drawn away by the electric field or reflected back to the cathode by gas molecules.

Acton and Swift (ref. 3) have examined the ionization cycle mathematically for the plane, parallel electrode geometry. From the definition of the ionization coefficient, a current of i/e electrons per second will be increased by an amount

$$\delta\left(\frac{i}{e}\right) = \left(\frac{i}{e}\right) \eta_i \cdot \delta V$$

in passing through a potential difference of δV volts, where i is the

electron current, e is the electronic charge and η_i is the ionization coefficient. From the above equation, the following can be developed:

$$di = i\,\eta_i\,dV\ ,$$

$$\frac{di}{i} = \eta_i\,dV\ ,$$

$$\ln i = \int_o^{V_a} \eta_i\,dV\ ,$$

$$i = \exp \int_o^{V_a} \eta_i\,dV\ . \qquad (1)$$

In the plane, parallel electrode configuration, η_i can be considered a constant once the electrons leaving the cathode have been accelerated enough to take part in the ionization cycle. It is assumed, therefore, that η_i is zero until the electrons are accelerated through V_i volts and constant from that point to the anode, where V_i is the ionization potential of the pressurizing gas. Therefore, Eq. (1) can be rewritten as

$$i = \exp \int_{V_i}^{V_a} \eta_i \cdot dV\ ,$$

$$= \exp\, \eta_i(V_a - V_i)\ .$$

Therefore, an electron current, i_k, leaving the cathode will arrive at the anode as

$$i_a = i_k \exp\, \eta_i(V_a - V_i)\ . \qquad (2)$$

The electron current contributed by ionization per second is equal to the difference between the anode and cathode electron currents per second and is given by

$$i_a - i_k = i_k \left[\exp\, \left(\eta_i(V_a - V_i)\right) - 1\right]\ . \qquad (3)$$

A positive ion is also created for every electron created. These will

flow to the cathode and produce additional electrons through secondary emission. These secondary electrons are given by

$$\gamma\, i_k\, [\exp \eta_i(V_a - V_i) - 1] \tag{4}$$

where γ is the secondary emission coefficient of the cathode.

Equations (3) and (4) provide for an analysis of the ionization cycle. Consider an electron current, $i_k(t)$, leaving the cathode at time, t. After a time, t_e, the average time for $i_k(t)$ to produce ionization, a positive ion current of

$$i_k(t)\, [\exp \eta_i(V_a - V_i) - 1]$$

will flow toward the cathode. After a time, t_i, this positive ion current will strike the cathode and cause an electron current of

$$\gamma\, i_k(t)\, [\exp \eta_i(V_a - V_i) - 1]$$

to leave the cathode. Thus, the electron current of $i_k(t)$ at time, t, has caused a current at time $(t + t_e + t_i)$ of

$$i_k(t + t_e + t_i) = i_k(t)\, \gamma\, [\exp \eta_i(V_a - V_i) - 1]. \tag{5}$$

Observing that $t_i >> t_e$, and that $\exp \eta_i(V_a - V_i) >> 1$, Eq. (5) can be approximated by

$$i_k(t + t_i) = i_k(t)\, \gamma \exp \eta_i(V_a - V_i)\ . \tag{6}$$

This is the most fundamental relationship in the theory of the cold cathode devices. If

$$\gamma \exp \eta_i(V_a - V_i) > 1;\ i_k(t + t_i) > i_k(t)\ ,$$

and if

$$\gamma \exp \eta_i(V_a - V_i) < 1;\ i_k(t + t_i) < i_k(t)\ .$$

Essentially stated, the cathode current increases or decreases with time as $\gamma \exp \eta_i(V_a - V_i)$ is greater or less than unity, respectively. If

$$\gamma \exp \eta_i(V_a - V_i) = 1\ , \tag{7}$$

current will neither increase or decrease. This is defined as the maintenance condition.

To further consider the breakdown or firing of a cold cathode device, it is necessary to consider variations in η_i and γ. Since γ remains nearly constant for a given gas-cathode configuration, variations in γ with voltage and pressure can be reasonably neglected. This is not the case with η_i. In addition to variations with pressure, η_i, has been found to increase rapidly at a certain value of current density (approximately 10^{-3} mA/cm^2) (ref. 3). This increase results from a distortion of the electric field by the space charge of the positive ions in the current stream. An increase in η_i means that a lower value of V_a is required to meet the current maintenance condition in Eq. (7).

Assume, for example, that a slowly increasing voltage is applied across the electrodes of the cold cathode device. At low values of V_a,

$$\gamma \exp \eta_i(V_a - V_i) < 1 ,$$

and the device will not fire. As V_a continues to increase, a condition will be reached such that

$$\exp \eta_i(V_a - V_i) > 1 ,$$

and the electron current will increase. If current continues to increase, as it will if neither γ, η_i nor V_a decreases, the critical value of current will be reached and the device will avalanche into breakdown. In fact, external circuitry must be used to prevent a cold cathode device from destroying itself. (In practice, a series resistor is usually employed to cause a decrease in V_a when the current increases.)

From the preceding discussion, it is evident that an ideal condition is for the maintenance condition to be met when the current density is small and η_i is increasing with current. If these conditions are met, the cold cathode device will avalanche into the normal glow region (assuming proper use of external circuitry) and is said to have fired. It is the firing of the device that is exploited by the MEPF/G experiment. External circuitry is used to cause the device to cease conducting or turn-off rather than remain in the normal glow region.

When the maintenance condition of Eq. (7) is met, conditions are such that the cold cathode device can fire and the voltage across the electrodes is called the firing voltage, V_f. An equation for the firing

voltage can be obtained from Eq. (7) by setting the V_a equal to V_f and solving for V_f:

$$\gamma \exp[\eta_i(V_f - V_i)] = 1 ,$$

therefore,

$$V_f = V_i + \frac{1}{\eta_i} \ln \frac{1}{\gamma} . \tag{8}$$

Equation (8) is useful in that values of η_i and $\ln 1/\gamma$ have been tabulated in various texts for certain gases and cathodes. (See, for example, ref. 3). These tabulations correspond to parallel plate geometries, however, and do not yield acceptable values for the MEPF/G configuration.

In Eq. (8), the ionization potential of the gas, V_i, is a constant and the secondary emission coefficient, γ, is a property of the cathode and the positive ion striking the cathode. The ionization coefficient, η_i, varies with gas pressure and has a maximum value, η_m. (The fact that η_i also varies with current density is of no consequence when considering the firing voltage.) When η_i is a maximum value, the striking voltage reaches a minimum value, V_{fm}, given by

$$V_{fm} = V_i + \frac{1}{\eta_m} \ln \frac{1}{\gamma} . \tag{9}$$

Paschen Characteristics. - Paschen's law states that for a given gas and cathode material, the firing voltage of a parallel plate, cold cathode device depends upon the product of gas pressure and electrode separation, i.e.,

$$V_f = f(px) ,$$

where p is the gas pressure and x is the separation between the electrodes. Plots of V_f versus (px) are called Paschen curves, and these characteristics are useful to the MEPF/G experiment. Experimentally determined Paschen characteristics of the MEPF/G transducer with numerous gases were used to select the pressurizing gas. Since the electrode spacing was controlled within specified limits by screening practices, Paschen curves for the MEPF/G transducers were plotted with only pressure on the abscissa. Numerous examples are included in this report.

Equation (9) states that the firing voltage minimum is independent of electrode separation, and Paschen's law shows the firing voltage to

depend upon the product of pressure and separation. It is concluded, therefore, that variations in the electrode spacing will not change the minimum firing voltage, but only change the pressure at which it occurs.

Paschen curves can be represented by the equation

$$V_f = V_{sm} + B(px) \quad , \tag{10}$$

where B is an empirical constant chosen to give the best fit between $V_f = 2\ V_{fm}$ and $V_f = 4\ V_{fm}$ (ref. 3). The empirical constant, B, in Eq. (10), can be considered a Figure-of-Merit for the purposes of the MEPF/G experiment since a high value of B corresponds to a firing voltage above the minimum value.

Figure 8 illustrates the Paschen characteristics of a hypothetical gas at both room and liquid nitrogen (LN_2) temperature. Two points are defined in Fig. 8 that are critically important in the selection of a pressurizing gas for the MEPF/G experiment. Since 16.7 psia (864 mm Hg) is the sealing pressure at room temperature, it is critical that the voltage applied to these transducers not exceed the firing voltage corresponding to 864 mm Hg at room temperature. (Fabrication of the MEPF/G pressure panels is significantly simplified if the gas pressures sealed into the cells is approximately one atmosphere.) Figure 8 illustrates a significantly different Paschen characteristic at LN_2 temperature. It is likely that gas density is a more realistic abscissa for the Paschen characteristic, however, and gas density in the sealed pressure cells does not change appreciably with temperature. (Some references suggest using density for pressure whenever temperature variations must be considered.) Regardless of whether or not the actual Paschen characteristics change with density, a valid, worst-case interpretation of a critical high voltage is to select the lower value of V_f corresponding to 864 mm Hg on the room temperature curve or V_f corresponding to 222 mm Hg on the LN_2 temperature curve. (A panel sealed at 864 mm Hg at room temperature and cooled to LN_2 temperature will have a pressure of 222 mm Hg.) The lower value of these two voltages is defined as V_{hi} and is an upper bound on the voltage that can be applied to the MEPF/G transducers. A second critical voltage corresponds to the minimum firing voltage, V_{lo}, on the LN_2 temperature curve. It is critical that the voltage applied to the MEPF/G transducers always stay within these bounds. As a matter of good engineering practice, it is desirable that the pressurizing gas have Paschen characteristics with a large difference between V_{hi} and V_{lo}, and that the power supply voltage provide for a reasonable safety margin within these bounds.

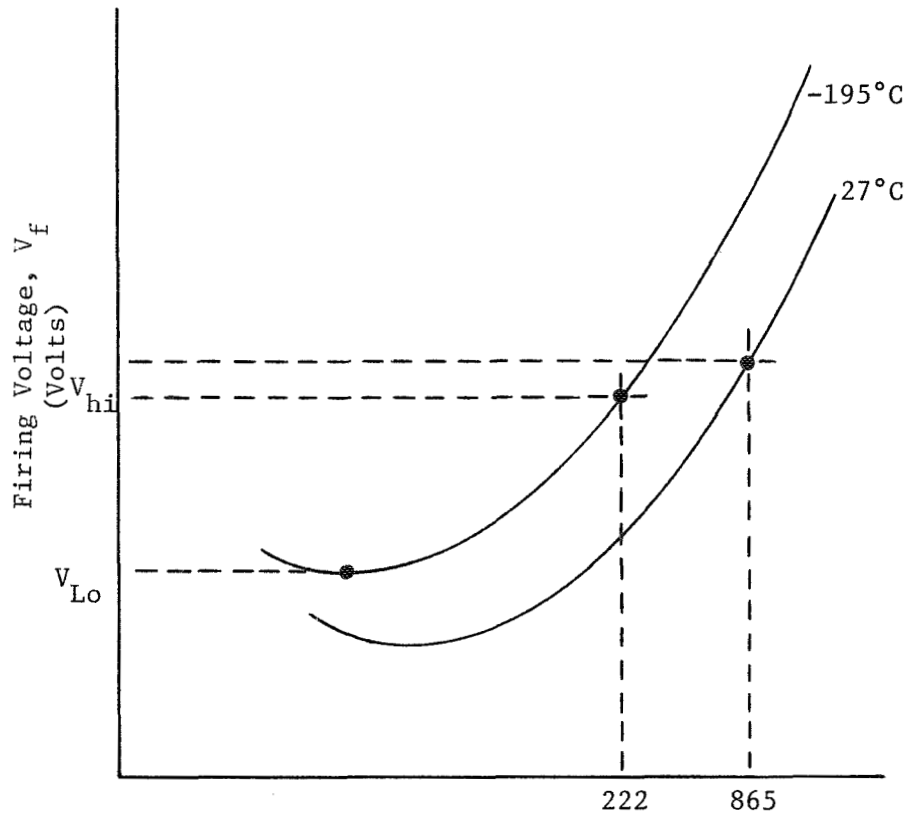

Figure 8. A Hypothetical Paschen Curve

Electrode Spacing

Paschen's law, as stated by Eq. 10, suggests that V_{hi} can be increased without changing the minimum firing voltage by increasing the electrode spacing. Several problems are encountered when applying this principle to shape the characteristics of the MEPF/G transducer. The geometry of the transducer limits the separation that can be achieved. Policy and good engineering practice require that the pressure cells (and transducer housing) be at ground potential, and one of the electrodes is also at ground potential. If the two electrode geometry is to remain symmetrical, the 34 mil spacing shown in Fig. 4 is near a maximum. Any increase in the spacing between electrodes will decrease the approximately 35 mils electrode-housing spacing.

It is of interest to the MEPF/G experiment to consider how the electric field between the two electrodes varies with separation. The electric field must accelerate free electrons to an energy level sufficient to cause additional gas ionization before a firing event can occur. For a given gas density (and mean-free-path), the higher the electric field, the more probable it is that an electron can attain the energy necessary for ionization. Significant physical insight into the nature of the electric field between the electrodes can be gained by considering the following idealized geometry. The electric field between two long, parallel conducting cylinders is a classical problem in many texts (ref. 4). The electric potential and gradient will be a maximum along a line passing between two such cylinders. Along this line, the electric potential is given by

$$\phi = \frac{Vo}{4\ \mathrm{Cosh}^{-1}\ (d/R)}\ \ell n\ \frac{(x-a)^2}{(x+a)^2}\ , \tag{11}$$

where $a = \sqrt{d^2 - R^2}$,

Vo = Voltage between the electrodes,

2d = spacing between the electrode centers,

R = radius of the two electrodes, and

x = distance between the midpoint of the line segment connecting the electrode centers and the point in question.

The electric field, E, is obtained by differentiating Eq. (11).

$$E = \frac{d\phi}{dx} = \frac{a\ Vo}{\mathrm{Cosh}^{-1}\ (d/R)}\ \frac{1}{(x^2-a^2)} \tag{12}$$

By setting the deriative of Eq. (12) to zero, it is observed that the minimum value of the electric field occurs at x = 0 (centered exactly between the electrodes) and is given by

$$E_{min} = -\frac{Vo}{a\ \mathrm{Cosh}^{-1}\ d/R} \tag{13}$$

The maximum value of the electric field occurs at the electrodes and is calculated by solving Eq. (12) with x = d - R. Maximum and minimum values of the electric field have been calculated for values of Vo, d and R corresponding to the geometry of the MEPF/G Transducers. These results are plotted in Fig. 9 for E_{max} and E_{min} where abscissa is the separation of the inside surface of the electrodes or 2d - 2R. The

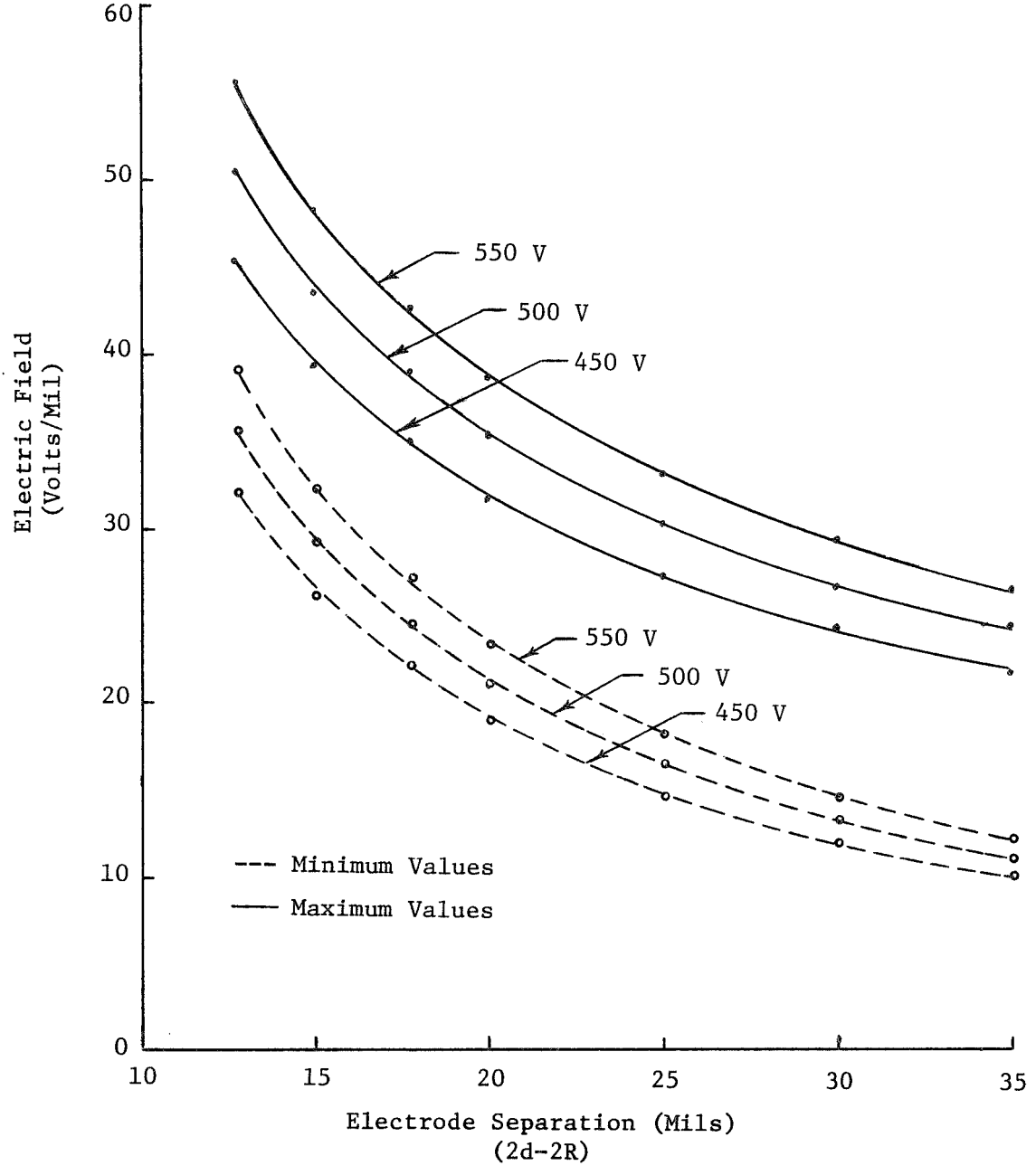

Figure 9. Calculated Values of the Electric Field

average value is simply the voltage divided by the separation and falls between the maximum and minimum values in each case. These curves illustrate that altering the electrode spacing can have a significant effect if the spacing is small, but is of less significance as spacing is increased. It is concluded that the slope of the Paschen curves can be increased by increasing the separation between the electrodes, but the separation is near optimum in the MEPF/G transducer. With separation on the order of 30 mils, for example, there is little to be gained by further increases. Following sections of this report will support these conclusions with experimental results.

Gas Mixtures. - When a mixture of gases is used in a cold cathode tube, the firing mechanism can become significantly more involved. The effects of some mixtures are such that minute traces of the second gas can completely change the Paschen characteristics of a cold cathode

TABLE I

METASTABLE ENERGIES (V_m) AND FIRST IONIZATION ENERGIES (V_i) OF SEVERAL ELEMENTS*

Element	V_m (eV)	V_i (eV)
He	19.8	24.5
Ne	16.6	21.5
A	12.5	15.6
Kr	9.5	13.5
Xe	7.0	12.0
H_2		15.9
N	9.8	16.7
O		13.5
Hg	5.4	10.4
	4.6	
H_2O		13.2

*From 1) Acton and Swift, COLD CATHODE DISCHARGE TUBES (Ref. 3)
2) Cobine, GASEOUS CONDUCTORS (Ref. 5
3) REFERENCE DATA FOR RADIO ENGINEERS, 4th Ed. (Ref. 6)

tube. Consequently, it is imperative that high purity gases and clean techniques be used in fabricating the MEPF/G pressure cell since impurities can easily constitute a trace quantity of a second gas.

The ionization cycle discussed in a preceding section of this report required that an electron attain sufficient energy to ionize a gas atom in order for firing to occur. A second mechanism is possible in some gas mixtures, i.e., an atom of one gas can be ionized by a metastable atom of the second gas. The ionization coefficient of such a mixture is increased and the firing voltage is significantly decreased. Gas mixtures in which this firing mechanism occurs are called Penning mixtures, and the lowering of the ionization coefficient is called the Penning effect. Table I tabulates ionization and metastable energies for numerous gases and is useful in predicting the properties of certain mixtures. Helium and neon are examples of gases that are likely to become Penning mixtures if other gases are present since their metastables are capable of ionizing most of the gases in Table I. In a collision between a metastable of one gas and an atom of the second, the probability of an ionizing event occurring increases as the difference between the potential energies before and after the collision decreases. Referring again to Table I, a 16.6 eV neon metastable is more likely to create a 15.6 eV argon ion than a 13.5 eV krypton ion.

There are other important mechanisms that occur in gas mixtures that influence the firing and/or glow characteristics of cold cathode tubes, but none of these were of significance to the MEPF/G experiment.

Testing Considerations. - Most of the experimental data to be presented in this report were determined with the circuit of Fig. 10. In this circuit the capacitor charges to the power supply voltage through the 10^7 ohm resistor, R_1. When the transducer is caused to fire, the cathode discharges through the transducer, R_2 and R_3; and a read-out pulse is available across R_3. The amplitude of the read-out pulse and the output impedance of the circuit are readily adjustable with R_2 and R_3. After the capacitor discharges, the transducer ceases to conduct due to the current limiting role of R_1. This circuit was designed to limit power dissipation by preventing a transducer from glowing and is essentially identical to the circuit to be flown on the MEPF/G. Factors which influenced the design of this circuit other than power restrictions are weight restrictions and certain properties of the transducers coupled with Pioneer ground. Weight limitations necessitated placing many of the pressure transducers in parallel so as to limit the wires to be run from the electronic package (Power Converter) to the transducers. A large value of R_1 was necessary to limit power dissipation, and the parasitic capacitance of the wires to the transducer was sufficient to

cause the circuit to oscillate. The voltage polarity of Fig. 10 reflects the fact that the transducer housing and one electrode is at ground potential, and it is desirable that the second electrode be negative since the electric field will be greater there.

The transducer test facility was altered frequently to facilitate different types of tests. Basically, the configuration indicated in Fig. 11 was used in most tests. It provided for controlling the pressure and temperature of the transducers under test.

Experiments with Helium

Helium was originally specified as the pressurizing gas for the MEPF/G experiment. Helium was a reasonable choice. It is chemically inert, has a boiling temperature below nitrogen (the specified low temperature for the experiment), has a small atom so as to more readily leak through a small hole and a helium leak is easily detected. The metastable and ionization energies of helium shown in Table I indicate that any number of impurities in helium could prove troublesome, but high-purity gas and ultra-clean procedures were to be used.

Satisfactory Paschen curves were not obtained with helium although hundreds of firings were recorded. Plots of firing voltages versus pressure yielded such a random distribution of data points that a Paschen curve could not be fitted to the data. Even more disturbing were numerous failures-to-fire, and eliminating this unreliability became the projects most pressing problem. In a continuing effort to improve the reliability of the helium-filled transducer, the test facility was improved by careful upgrading cleanliness, and the electrode geometry and finish were altered. These changes did not alter the experimental results.

The introduction of an initial ionization source completely solved the failure-to-fire problem. No failures were ever observed when a mCi, Co^{60} source was unsheathed in the vicinity of a transducer under test. The use of radioactivity was to be avoided except as a last resort, however, to avoid conflict with the Pioneer specifications limiting its use.

While the unreliability of the helium transducer was still a pending problem, helium was banned as a pressurizing gas for the MEPF/G experiment. Another experiment scheduled for the Pioneer F/G flights was sensitive to helium and thus incompatible with helium as a pressurizing gas. In retrospect, it is likely that the difficulties that eventually forced the abandonment of neon as a pressurizing gas would also have been evident in helium.

An "approximate" Paschen characteristic for the MEPF/G transducer with helium is shown in Fig. 12. This curve is supported by numerous

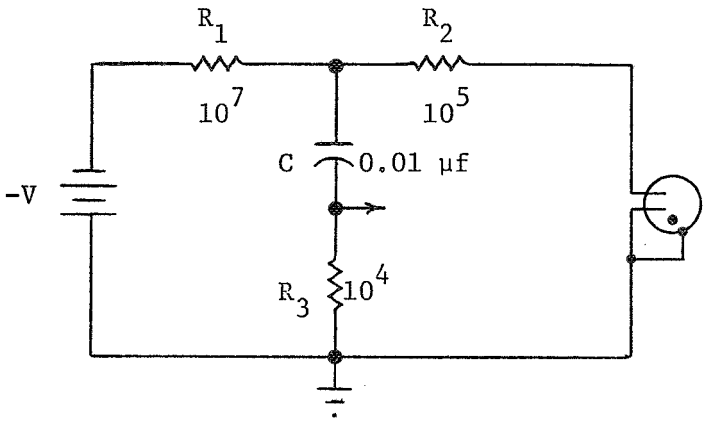

Figure 10. Transducer Circuitry

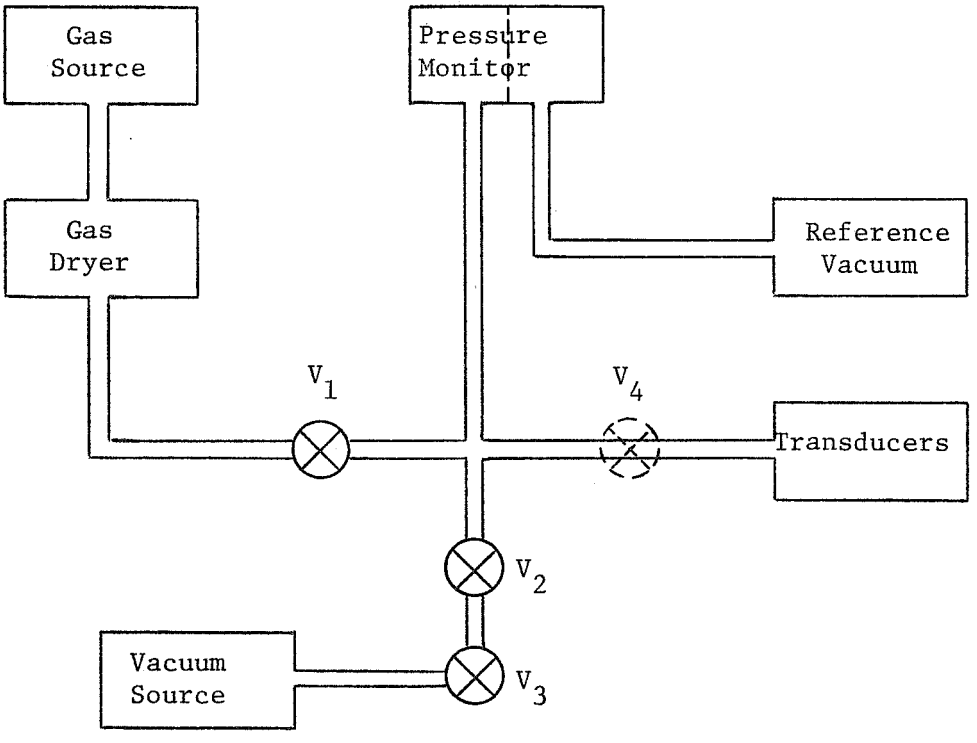

Figure 11. A Transducer Test Facility

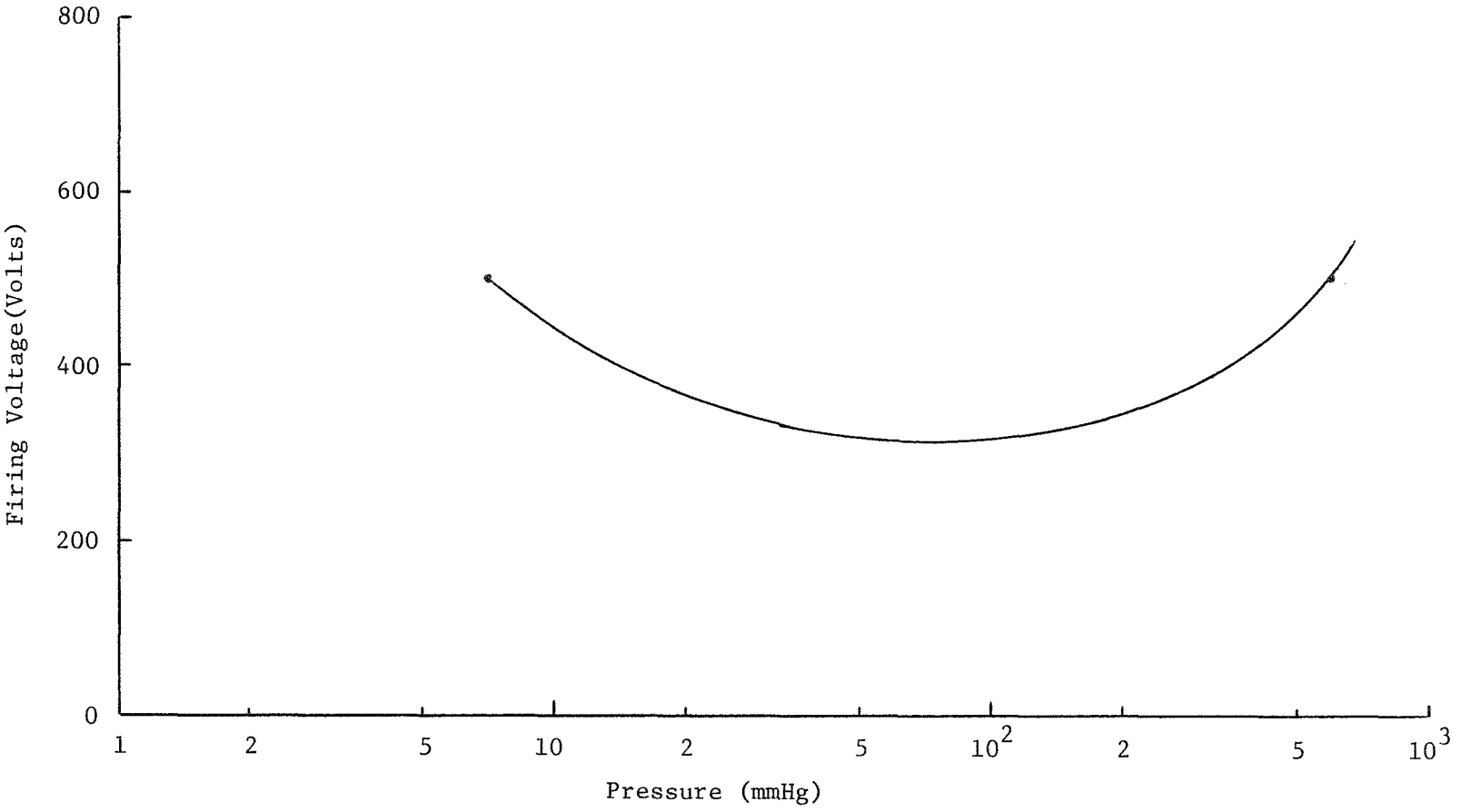

Figure 12. Helium Paschen Curve

firings at 500 volts. When a Co^{60} ionization source was used, helium-filled transducers were observed to fire at about 600 mmHg and continued to fire until the pressure reduced to less than 7 mmHg. Without Co^{60}, helium transducers were observed to fire at voltages between these end points. Other points for this curve were deduced from a review of much data.

Figure 13, is a series of oscillograms showing the output of the transducers circuitry for a helium-filled transducer firing at various pressures. These are "first" firing events and the waveforms are all similar. Figure 14 includes three oscillograms taken during a single pressure-lowering event. First is the initial firing, and the others were taken at lower pressures as the transducer continued to oscillate.

Experiments with Neon

Neon was chosen to replace helium as a pressurizing gas primarily because of its thermal properties. Pioneer specifications require that the MEPF/G panels function at LN_2 temperature (-195°C), and neon and helium are the only rare gases with lower boiling points than nitrogen. At the time neon was selected, the pressure was to be 25 PSIA.

The ionization and metastable energy levels tabulated in Table I suggest that neon is likely to be very sensitive to many impurities, and it is especially likely to interact with nitrogen and argon. It was assumed that high-purity gas and clean procedures would preclude any difficulties with impurities. When neon was first used, the reliability or failure-to-fire problem associated with helium experiments still existed and precluded other investigations. Several approaches to solving these failures include alterations to the electrode geometry and finish. Two of the configurations tried; i.e., the U-shaped and spark plug geometries, are illustrated in Fig. 15. Other efforts to enhance reliability was to amalgamate the tin-plate with mercury. Among other properites, mercury is easily ionized. Generally speaking, these actions produced only minor improvements and no satistically significant statements can be made about the results. Failures continued to occur frequently. As with helium the use of a radioactive material was demonstrated to be a solution to the reliability problem.

Nickel-63. - A thorough investigation into the reliability problem demonstrated that a radioactive material to provide initial ionization was the only suitable means of achieving reliability in the MEPF/G transducers. A suitable isotope was selected in view of the following criteria:

1) The half-life of the selected isotope must be long so as to insure an adequate activity throughout the mission. (Ground storage plus transient time to Jupiter extends the mission time to more than five years.)

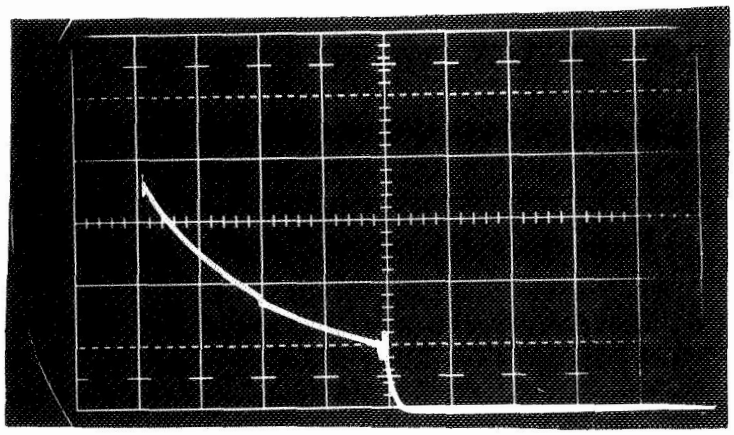

250 mmHg

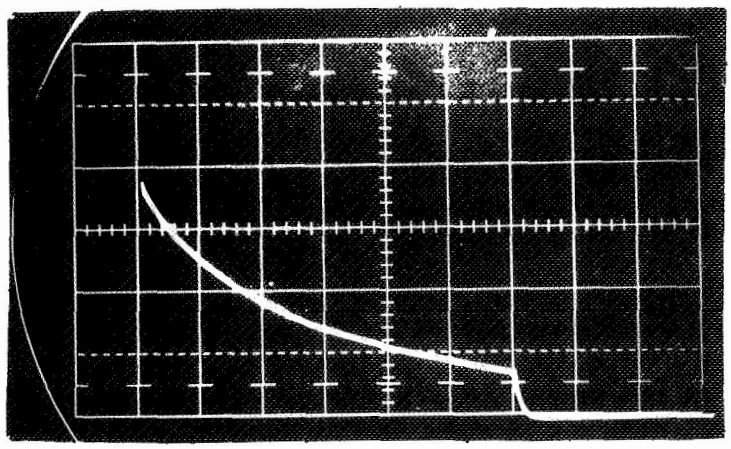

200 mmHg

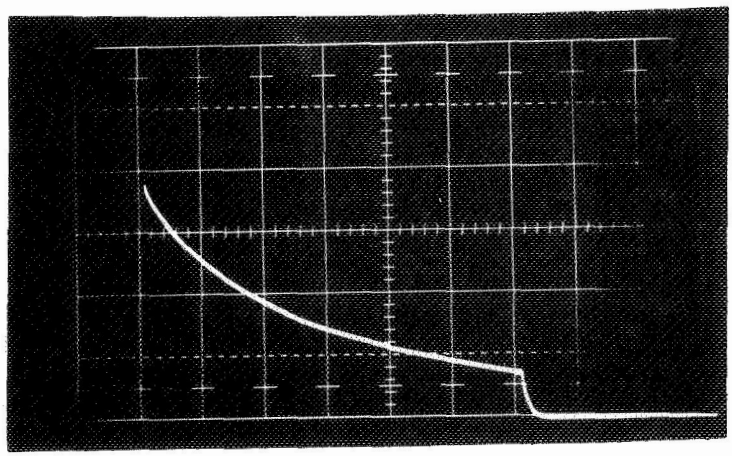

150 mmHg

Vertical Scale: 2 V/cm
Horizontal Scale : 1 mS/cm
V = 400 V

Figure 13. Oscillograms of First Firing Events in Helium

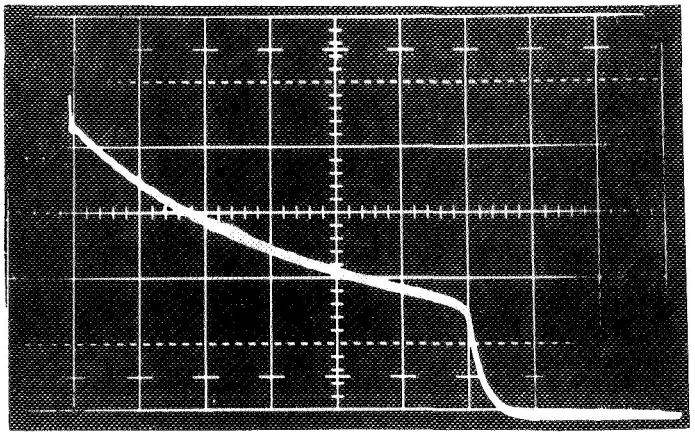

1st Firing Event
600 mmHg
2V/div.
0.5 mS/div.

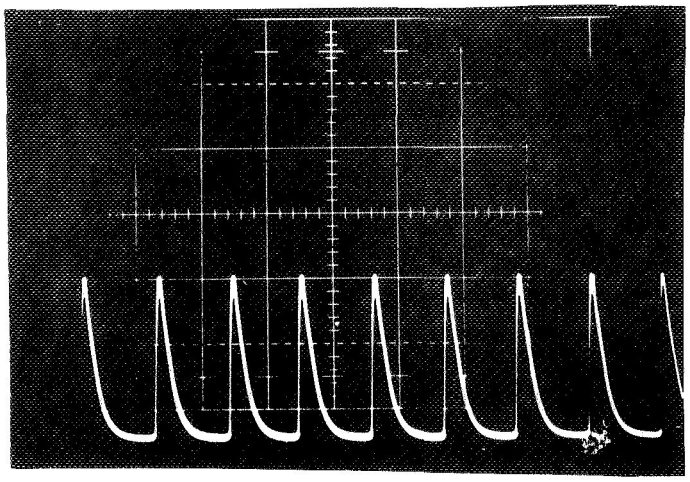

50 mmHg
0.5V/div.
0.5 mS/div.

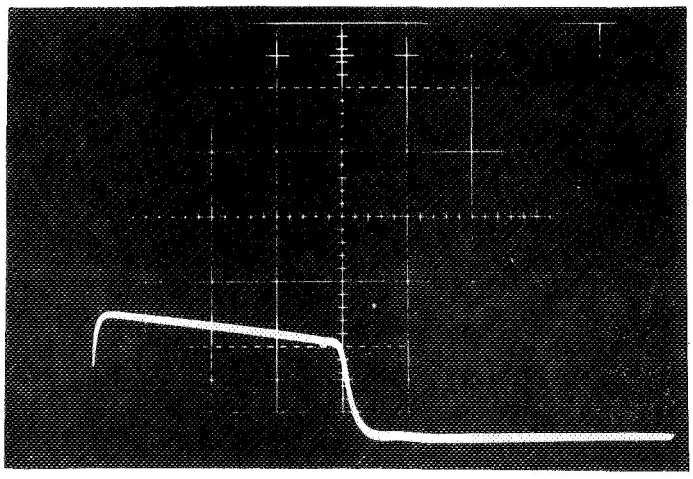

18 mmHg
0.5V/div.
0.5 mS/div.

V = 500 V

Figure 14. Oscillograms of the Transducer Circuitry Output at Various Pressures During a Single Pressure-Lowering Event.

Figure 15. An Illustration of the U-Shaped and Spark-Plug Geometries

2) The range of the particle emitted must be such as to pose no hazard to ground personnel and long relative to interelectrode spacing.

3) A stable daughter is desirable in the interest of simplicity, and

4) The material must be available in a convenient form, compatible with the experiment.

Additionally, Pioneer specifications imposed the restrictions that (ref. 2):

1) No gamma emitters be used,

2) that the particle emission energy not exceed 7 MeV, and

3) that the total activity level not exceed 1 μCi.

Restrictions on the total activity required that each of the 216

transducers in the experiment use less than 1/216 or 0.00463 μ Ci, and increases the importance of selecting an isotope with a convenient, controllable form. At the time this selection was made the possibility of using 16 panels with 18 cells each existed, and the radioactivity level was limited to 0.00341 μ Ci per cell to provide for that possibility.

Nickel-63 was selected from a tabulation of isotopes as the most suitable for the MEPF/G experiment (ref. 7). It has a half-life of 92 years, is a beta emitter with a decay of 67 keV, a suitable range of approximately five cm in air and one-half mil in copper, and a stable daughter (Cu^{63}). It poses no problem related to health hazards or AEC regulations. A most important attribute is that it can be easily electroplated on the transducers electrodes in precisely controlled, minute quantitites. Appendix A discusses the Ni^{63} plating process and summarizes the Ni^{63} properties. Appendix B discusses the health-related aspects of using Ni^{63}.

The decision to use Ni^{63} followed the completion of an experiment designed to demonstrate the necessity of an initial source of ionization. The experiment consisted of a comparison of Ni^{63} plated transducers with transducers using the spark-plug geometry and spark-plug transducers with Hg amalgamated on the electrodes. Neon was the pressurizing gas and the experiments were conducted at LN_2 temperature. These three groups of transducers were mounted and cleaned, and the test facility was thoroughly cleaned and flushed with the pressurizing gas. Basically the steps of the experiment were as follows:

1) Each test cell was pressurized to 25 PSIA and cooled to LN_2 temperature. The initial firing voltage was determined by setting the voltage across the electrodes to 525 V and slowly reducing the pressure. If the tube failed to fire, the voltage was increased in 50 V steps and the process repeated until the tube did fire.

2) After the initial firing voltage was recorded, each transducer was stored at 25 PSIA, 525 V and LN_2 temperature for one hour. After the one hour interval, each unit was exercised by slowly reducing the pressure to a vacuum and monitoring the unit for a firing event. This procedure was repeated five times.

3) Following the one-hour interval test of Step 2, the procedure was continued except the storage interval

was increased to three hours. These three-hour interval tests were repeated ten times.

4) Following the three-hour interval tests of Step 3, the tests were continued, with the Ni^{63} plated units only, for periods of 12, 24 and 48 hours.

The results of these tests, summarized in Table II, demonstrate the reliability of the Ni^{63} plated units and the unreliability of the others.

A second factor evident from these tests is the decrease in the percentages of successful firings as the storage interval is increased. This decrease was evident in a qualitative sense prior to this experiment and is the reason different time intervals were included. A related observation was recently reported by Wollan, et al (ref. 7). They reported a rise with time in the striking voltage of a cold cathode device left at a given gas pressure. They observed a rise of approximately 40 V in four hours and approximately 100 V in ten hours. When a radioactive source was added to provide initial ionization, the voltage rise with time was significantly reduced.

TABLE II

A COMPARISON OF THE RELIABILITY OF THREE CONFIGURATIONS

Transducer	Initial Firing Voltages (Volts)	One-Hour Intervals (Firing/Trials)	3-Hour Intervals
Spark Plug Geometry (Two Sets)	575, 575, 725 725, 1000, 625, 1000, 675	29/55 (53%)	2/10 (20%)
Spark Plug Geometry With Hg	525, 575, 1000, 1000, 1000	25/25 (100%)	19/55 (35%)
Parallel Geometry With 0.005 C Ni^{63}	525 (All)	25/25 (100%)	63/63 (100%) Includes 12, 24 & 48-Hour Intervals

A potential problem with the use of Ni^{63} is that betas leaving the cathode and arriving at the anode constitute a leakage current in the MEPF/G transducers. A worst-case consideration of this factor is to assume that all the emission of one μ Ci of Ni^{63} contributes to the leakage current. From the definition of a curie and an ampere, one can show the leakage current to be a negligible 6×10^{-15} A.

The addition of the Ni^{63} plating on the transducer probes solved the failure-to-fire problem and enabled progress with the transducer characterization effort. The first gas investigated with the Ni^{63} plated transducers was neon. Besides helium, neon was the only rare gas with a boiling point below nitrogen, and nitrogen was known to have a relatively high minimum firing voltage.

The experimental results included in this section were determined in the transducer circuitry of Fig. 10, and the test apparatus was similar to that of Fig. 11. The low temperature data were obtained by submerging the transducer in LN_2, and an experiment was conducted to demonstrate that the gas in the transducer actually reached LN_2 temperature. Referring to Fig. 11, argon was used to pressurize the manifold between V_1, V_2, V_4 and the pressure monitor. When V_2 was opened to allow the gas to flow to the transducer, the manifold pressure dropped to 200 mmHg absolute which is approximately the vapor pressure of argon at LN_2 temperature (-195°C). When more gas was added to the manifold, the pressure remained constant.

Neon Paschen Curves. - Many transducers were tested in neon to determine their Paschen characteristics. The initially encouraging results were not repeatable, however, and the investigation of transducer characteristics entered a new phase, i.e., stabilizing the transducer became the most important objective. The obvious, first approach was to ensure that the gas-pressure cell-transducer system was not contaminated, and every effort was made in this regard. A consideration of the metastable and ionization energies in Table I illustrates that neon is sensitive to contamination. Traces of argon in neon is a very serious contaminant, for example, and even 5 ppm will significantly lower the firing voltage at higher pressures. Referring again to Table I, several contaminants other than argon could be serious in neon. Additionally, electronegatives such as fluorine, oxygen or chlorine, for example, are usually serious since their affinity for electrons tends to interrupt the ionization cycle.

The lack of stability or repeatability with neon-filled transducers emphasizes that no typical Paschen curve can be presented in this report. Figure 16 is a "good" Paschen curve for neon in that these characteristics

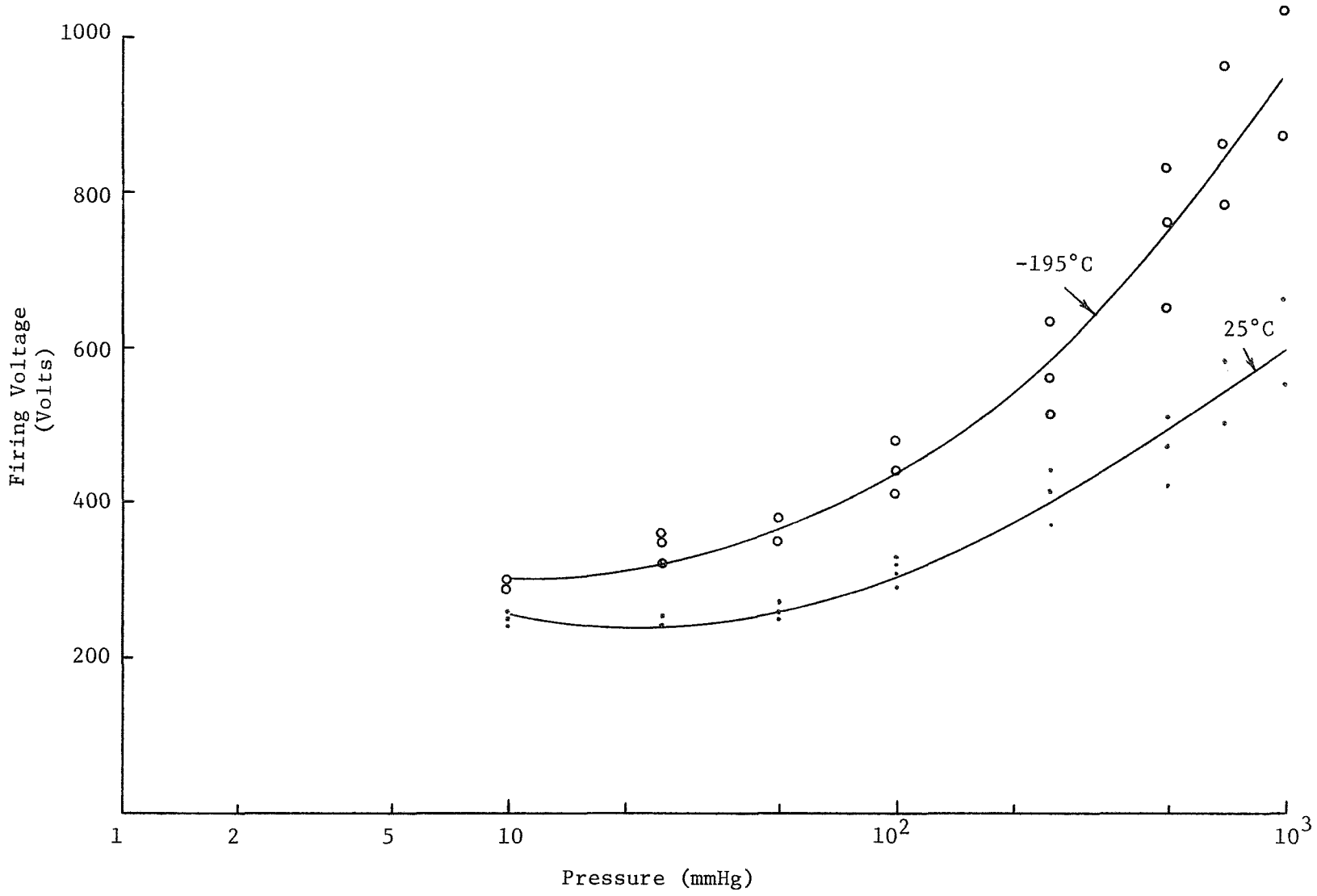

Figure 16. Neon Paschen Curves, Transducer No. 540

are acceptable for the MEPF/G objectives. Many equally good or better curves were plotted from neon experimental data, and it appeared that neon would be a suitable gas. The V_{hi} and V_{lo} voltages, as defined in Fig. 8, corresponding to Fig. 16 are 600 volts and 300 volts, respectively. (The sealing pressure was to be 1290 mmHg or 25 PSIA at room temperature.)

The difficulty with neon is illustrated in several of the following figures. Figure 17, for example, included Paschen curves for a single transducer as determined over a period of several days. At the sealing pressure of 1290 mmHg, the firing voltages differ by approximately 300 volts. There is no correlation between the order of the curves and time. The one curve that is a "cross-over" (defined by the square symbol) is an anomaly that occurred frequently with neon.

Figures 18, 19 and 20 are included to further illustrate the results achieved with neon. In each of these figures, data points obtained during a single experiment and used to define one of the curves are identified. Other data points, which could define other curves, are included as triangles. These additional curves are not included so as to avoid clutter. In general, these data were taken on separate occasions, spanning days or weeks of time.

Figure 18 includes additional Paschen curve data for the transducer of Fig. 16. These, too, are separate data. Note that V_{lo} is approximately 300 V, a value observed throughout the neon experimental effort. V_{hi} varied from transducer to transducer and from experiment to experiment. From the data in Fig. 18, V_{hi} is approximately 390 V. The data shown in Fig. 19 and Fig. 20 are also neon Paschen curve data taken under similar conditions. In these data, V_{lo} is again about 300 V and V_{hi} is 400 V in one case and 500 V in the other. The neon Paschen curves plotted in Fig. 21 are very similar to those of the preceding figures, but the data were taken approximately four months later. As before, V_{lo} is about 300 V, and V_{hi} is about 450 V.

Data for numerous neon Paschen curves on each of numerous transducers were determined during these investigations. Any of the curves presented could be considered as typical. The critical, minimum firing voltage, V_{lo}, is approximately 300 V, and V_{hi} was found to vary significantly with values from about 380 V to about 600 V. The most frequent value for V_{hi} was between 400 and 500 Volts. Acceptably high values for V_{hi} occurred frequently enough to encourage the continued investigation into neon as a pressurizing gas. The observed variations would have been acceptable if the "median" high value had not been too low. (V_{hi} and V_{lo} are defined on page 17 as useful figures-of-merit.)

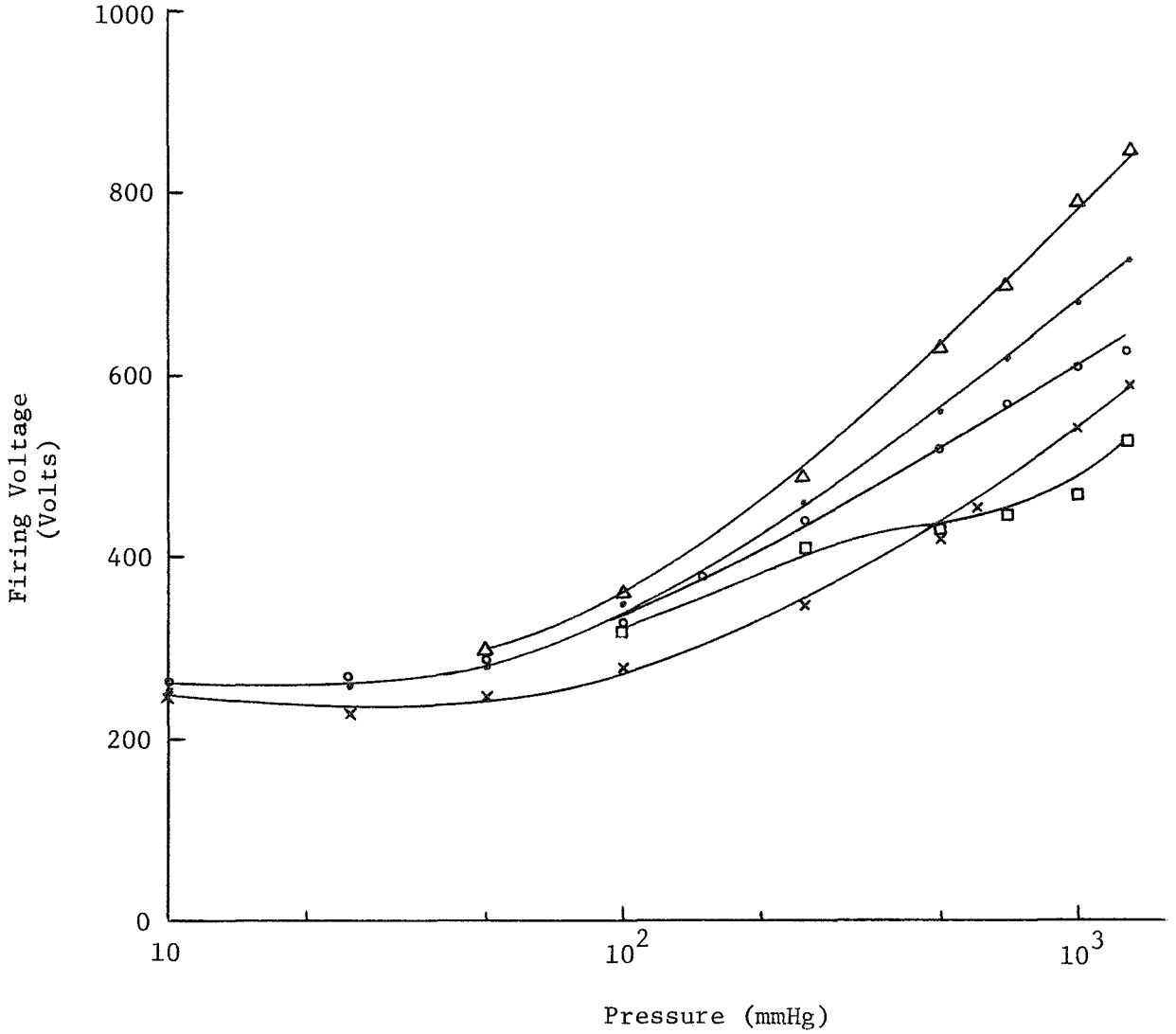

Figure 17. Neon Paschen Characteristics, Transducer No. 534

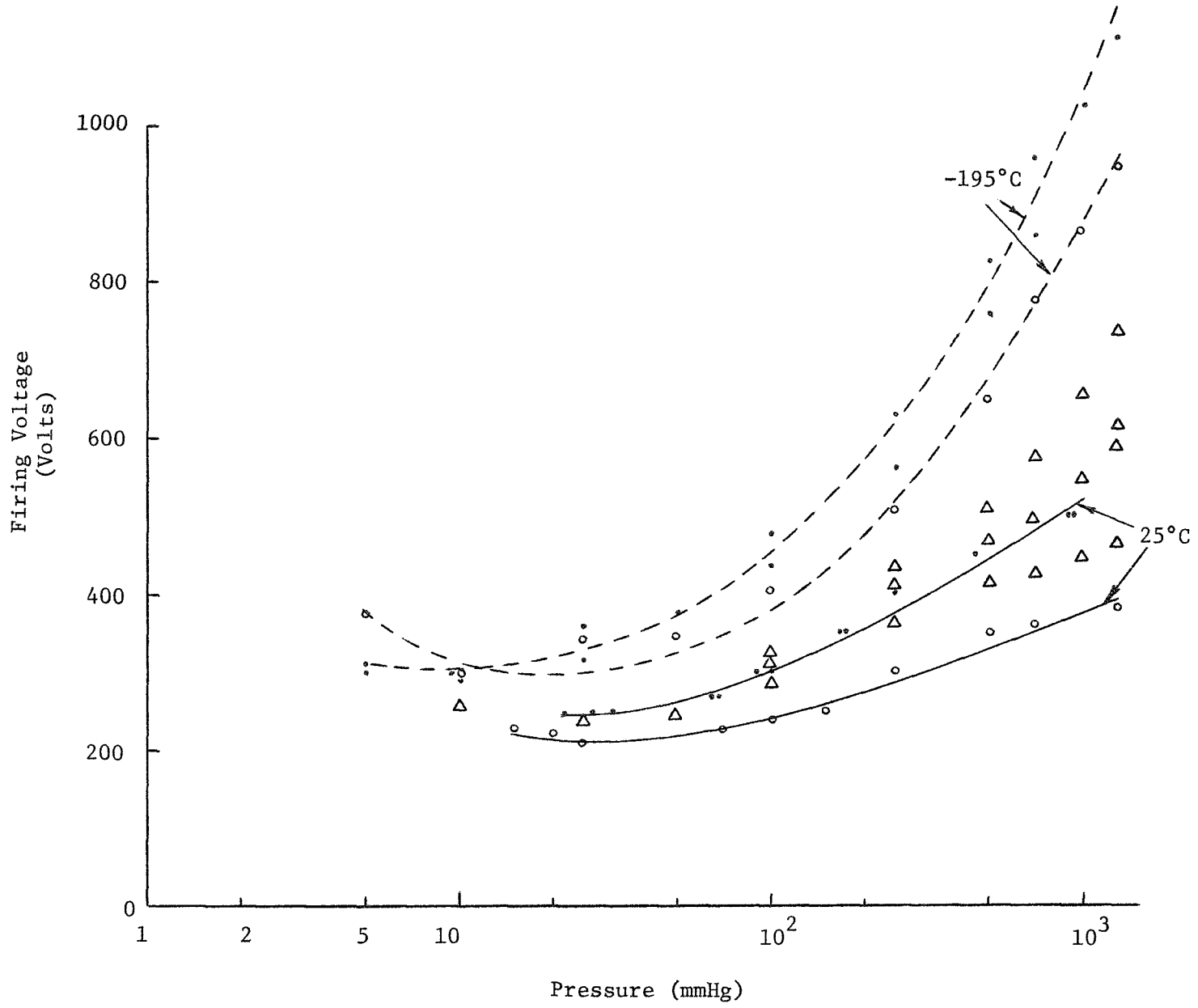

Figure 18. Additional Neon Paschen Characteristics, Transducer No. 540

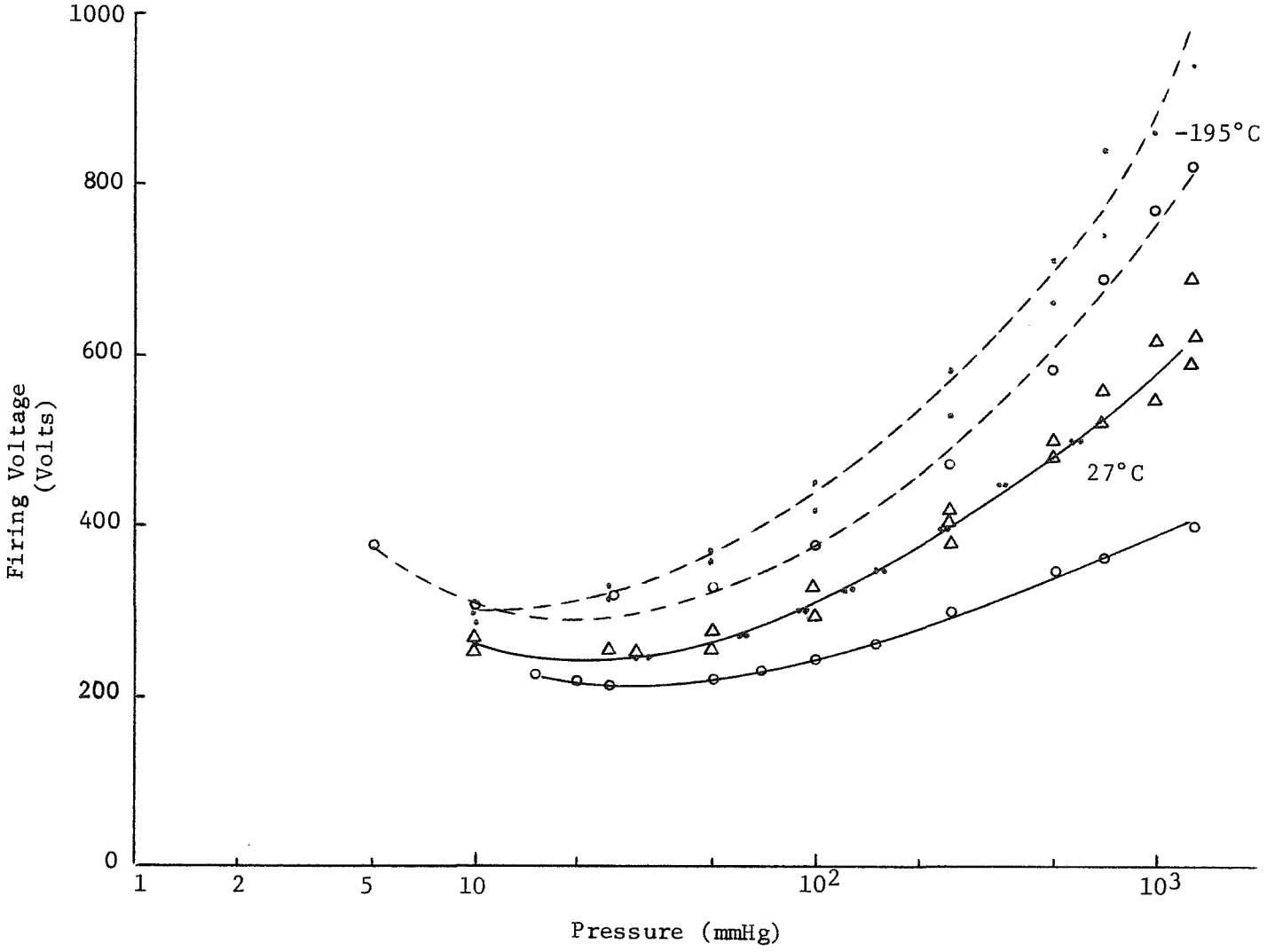

Figure 19. Neon Paschen Characteristics, Transducer No. 536

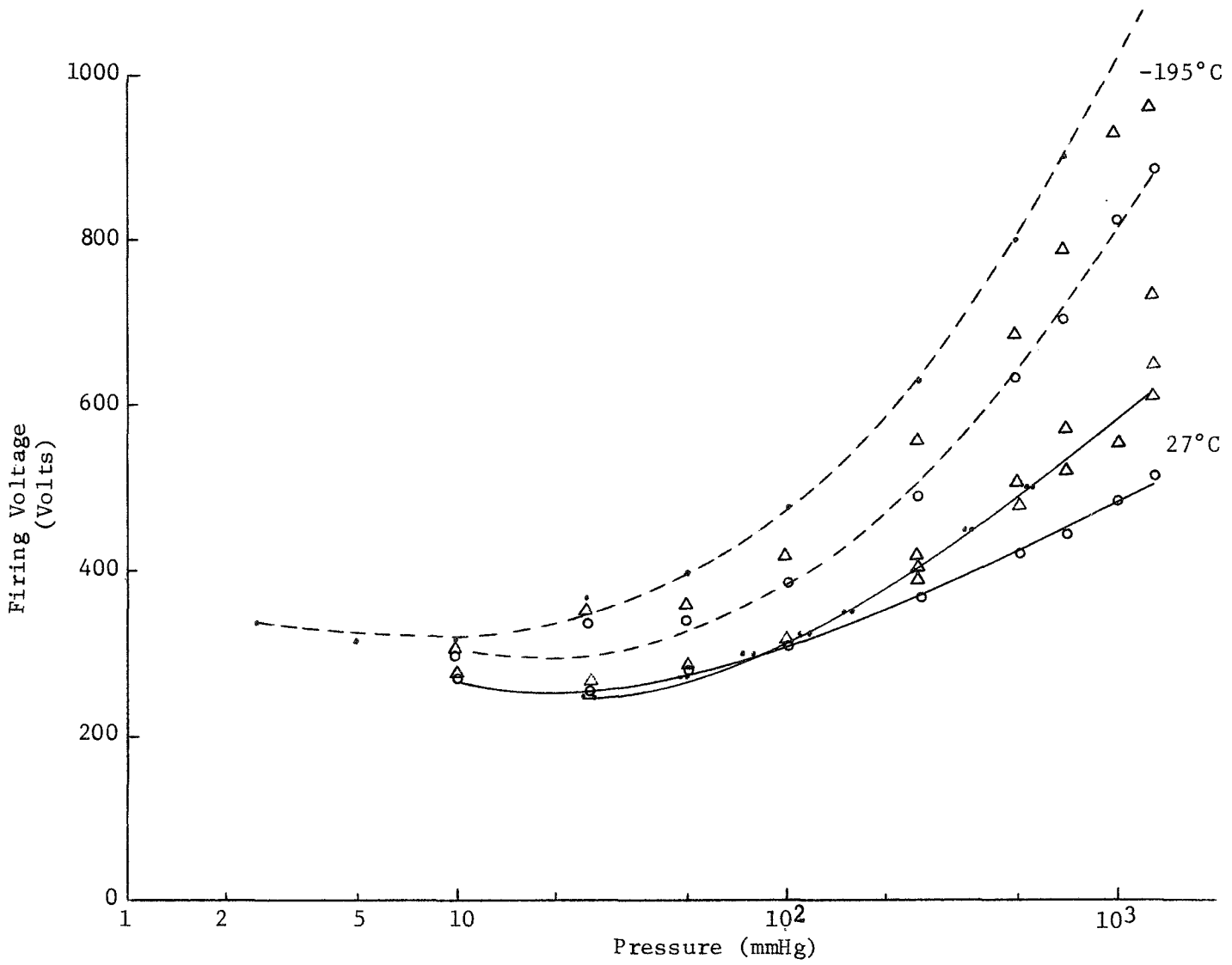

Figure 20. Neon Paschen Characteristics, Transducer No. 537

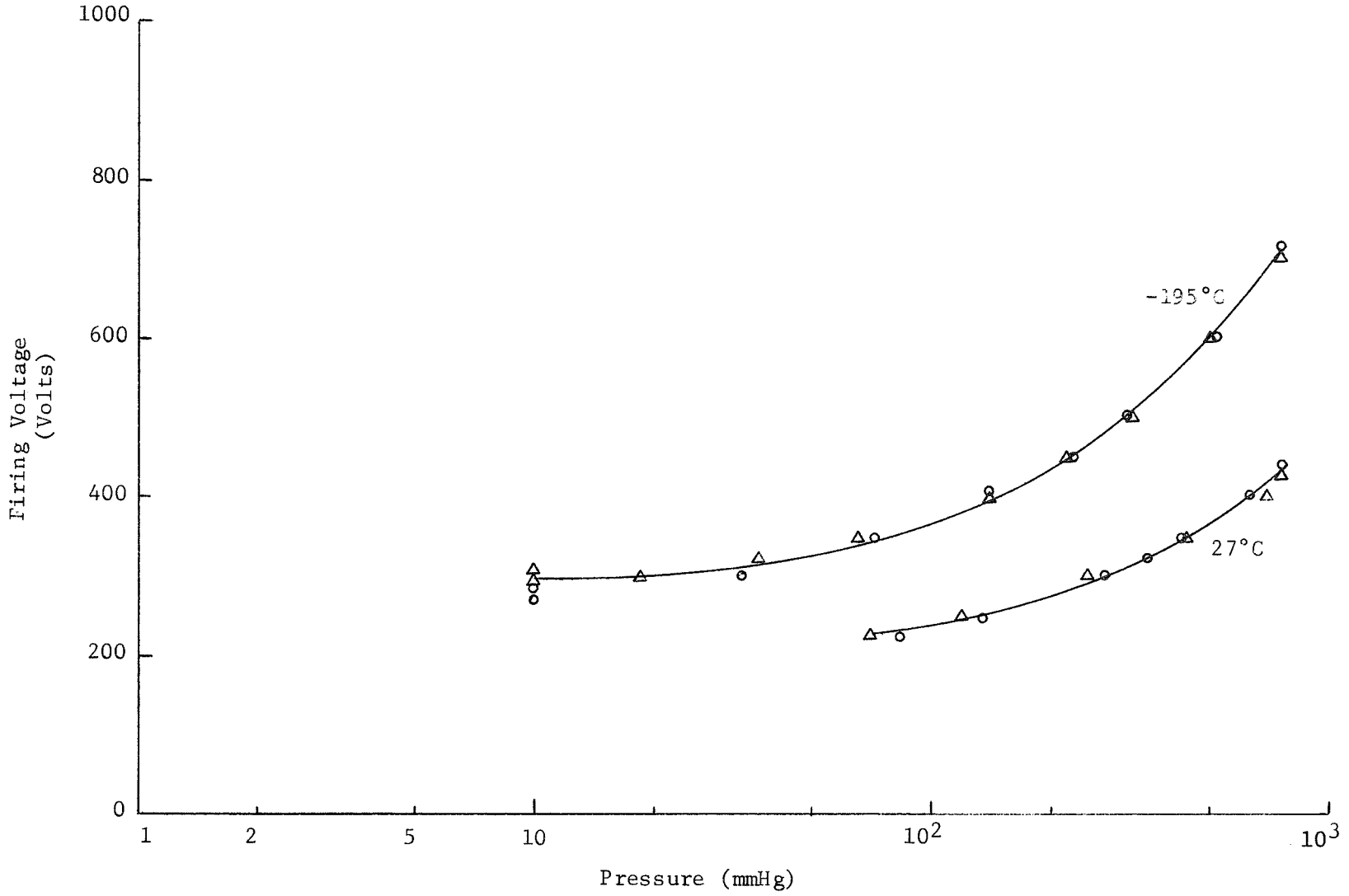

Figure 21. Neon Paschen Characteristics, Transducer Nos. 718, 719

Power Supply Voltage. - In order to meet Design Verification Unit (DVU) delivery schedules, it became necessary to specify a power supply voltage for the transducers while neon was still being characterized as a pressurizing gas. The voltage specified had to account for reasonable power supply variations and provide for an adequate safety margin within the V_{hi} and V_{lo} limits. At the time, V_{hi} was not defined and frequently measured to be an unacceptably low value. V_{lo} was well defined as 300 V. The power supply voltage was specified as 375 volts. This provided for $\pm$ 10% variation in the unregulated power supply, for example, plus a safety margin of 38 V. It was felt that this was a minimum value in view of the value of V_{lo}. On the high voltage side, 375 V plus 10% plus 10 volts to account for the inductive spike on the transformer required a V_{hi} voltage of at least 422 V, plus some safety margin. Measured values of 500 V or more were not uncommon, and it was felt that V_{hi} could eventually be fixed near or above that value.

Materials and Techniques. - Contamination was judged to be the most likely cause for the observed variations in the neon transducers, and every effort was extended to eliminate contaminants. The transducers, housings and test apparatus were cleaned frequently, thoroughly and by a variety of techniques. Different solders and fluxes were tried in the fabrication, and epoxies were substituted for solder. None of these efforts yielded a significant improvement. In fact, it is subjectively concluded that as more care and attention was given to eliminating every source of contaminants, the measured values of V_{lo} tended to be more consistently low. It is likely that the best materials and techniques left trace quantities of contaminants in the neon gas such that the Penning effect influenced the transducer characteristics. It is known that 10 ppm of argon in neon is a serious contamination and will significantly alter its firing characteristics. The threshold for argon and other contaminants are not known. Some nitrogen was in the neon gas, and Table I suggests that nitrogen may also be a serious contaminant for neon. An analysis from one of the neon gas bottles used in these experiments is as follows:

Helium	< 2 ppm
Nitrogen	< 4 ppm
Oxygen	< 1 ppm
Hydrogen	< 0.5 ppm
Carbon Dioxide	< 0.5 ppm
Hydrocarbon	< 0.5 ppm
Dew Point	< 105°F

In addition to altering the transducer geometry as described in an eariler paragraph, the cathode was altered in both material and finish in an effort to stabilize the characteristics of the MEPF/G transducer with neon. The electrodes were etched to expose a smoother, kovar finish, and electroplated with both copper and gold. None of these actions significantly altered or stabilized the transducer.

Several different electrical connections to the MEPF/G transducers were investigated as shown in Fig. 22. Characteristics for the connections illustrated in (1) and (2) were essentially identical. V_{hi} was slightly reduced for the connection in (3), and still further reduced for the connection in (4). The connection illustrated in (2) is used by MEPF/G experiment and yields the most desirable results.

Experiments with Sealed Units. - In addition to the neon Paschen curves presented earlier in this section, numerous experiments were conducted with transducers which were sealed in pressure cells. Many of these cells were fabricated by simply filling the transducer housing with gas and sealing the ends of the fill tubes. Some were soldered to copper tubing and others were sealed in MEPF/G pressure cells at LaRC. The method of mounting and sealing did not influence experimental results. These cells were sealed at different pressures (most were sealed at 1290 mm Hg) and room temperature and tested over long periods of time by fixing the temperature and increasing the applied voltage until a firing event occurred. The conclusions to be drawn from these numerous firing events are: 1) that significant variations occur between neon units fabricated in the laboratory under identical conditions, 2) a given transducer can change significantly over a period of time, and 3) the value of V_{hi} for many of these units are unacceptably low.

Some experimental results with sealed pressure cells are illustrated in Table III for three transducers firing at LN_2 temperatures. These are typical in that large variations were observed in most of these units with time. The firing voltages are not significantly correlated with time, i.e., the last firing observed frequently compared favorably with the first. Some higher and lower firings were observed in other transducers; often in a single transducer. Many of these sealed cells were opened for inspection and later resealed to fire consistently at lower voltages. Transducers 501 and 504, for example, consistently fired at high voltages. When opened, cleaned and resealed, they tended to fire lower voltages. Leaking cells were easily detected. When immersed in LN_2, their firing voltages increased to a high value since nitrogen leaked into the cells.

Experiments with the sealed units provided an opportunity to investigate the firing voltage variations with temperature at a constant

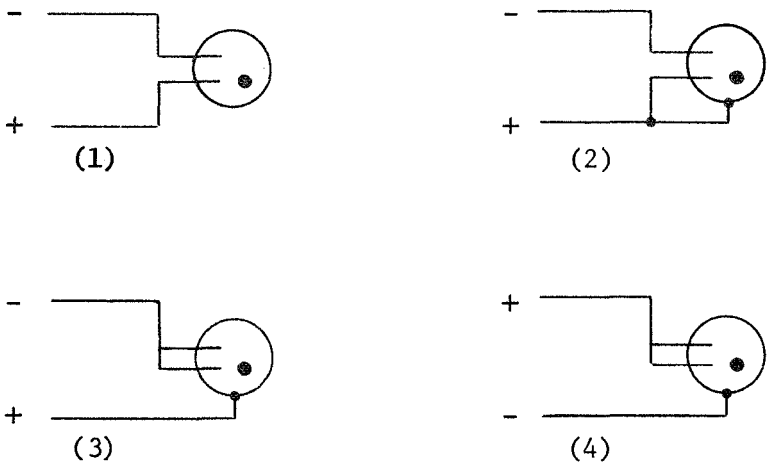

Figure 22. Electrical Connections for the MEPF/G Transducers

TABLE III

A SUMMARY OF EXPERIMENTAL RESULTS WITH SEALED TRANSDUCERS

	Transducer No.		
	625	627	628
High Firing Voltage	450	530	780
Low Firing Voltage	290	340	370
Medium Firing Voltage	370	430	580
Average Firing Voltage	360	450	590
Number of Samples	104	72	84

gas density. "Typical" firing voltages of sealed transducers at LN_2, room and + 225°F temperatures are 300 V, 400 V and 500 V, respectively. It is important to observe that the firing voltage of a sealed transducer increases with temperature.

Conclusions. - The Paschen characteristics of MEPF/G transducers with neon as a pressurizing gas are unacceptable for the MEPF/G experiment. The occasional good results led to an extended investigation into the characteristics of the transducer with neon. As these investigations continued, experimental results more consistently reflected a low value for V_{hi}. It is probable that contaminants had a detrimental effect to the neon transducers. It was concluded that a more stable transducer with a consistently high value for V_{hi} was essential to the experiment and other gases should be investigated in the interest of achieving this goal. If contaminants were responsible for the undesirable characteristics of the neon transducers, it is likely that similar of greater contamination would result in a production environment.

Experiments With Other Gases

As investigations into other gases began, it was decided to seek a gas such that the initial room temperature sealing pressure would be reduced and thus ease some fabrication problems with the MEPF/G pressure cells. The pressure finally selected was 16.7 PSIA or 865 mmHg

Nitrogen. - Nitrogen was first investigated as a replacement gas for neon. Its boiling point is satisfactory, of course, for LN_2

temperature. Paschen curves for the MEPF/G transducer with nitrogen are shown in Fig. 23. These curves result from several experiments on five different transducers. For an initial pressure of 865 mmHg, V_{hi} is greater than 1000 V and V_{lo} is approximately 500 V. These results show that nitrogen could be used, but it was desirable to provide for a lower value of V_{lo}.

The oscillograms of Fig. 24 show the voltage output from the transducer circuit of Fig. 10 for a typical nitrogen transducer. These were obtained by setting the voltage to the value indicated and lowering the pressure until a firing event occurred. The gas was at room temperature.

Results from another interesting experiment performed with nitrogen are shown in Fig. 25. Paschen curves were determined at room temperature with four different transducers in which the electrode separation was a parameter. The electrodes were arranged with 10, 16, 20 and 32 mil spacings. The curve corresponding to 10 mils is significantly lower than the others. However, there is little difference in the transducers with separations of 16 mils or greater. These results were predictable from the curves of Fig. 9 which shows electric field variations with electrode spacing.

Argon. - A room temperature Paschen curve for argon is shown in Fig. 26. Argon was not seriously considered as a pressurizing gas since its boiling point is above that of nitrogen. At LN_2 temperature, the argon liquifies and pressure drops to 200 mmHg, the vapor pressure of argon at LN_2 temperature. A gas that liquifies is unsuitable for the MEPF/G pressure cell since gas that condenses out on the walls of the pressure cell cannot play a role in the ionization cycle.

Mixtures of Neon and Nitrogen. - Mixtures of neon and nitrogen were investigated as a pressurizing gas since the boiling points of these mixtures were below that of nitrogen. It was observed that even small quantities of nitrogen in neon would significantly alter the firing characteristics of the transducer. Paschen curves for 50% neon/50% nitrogen and 75% neon/25% nitrogen mixtures are shown in Figs. 27 and 28, respectively. For the 50%/50% mixture, V_{lo} is approximately 400 V and V_{hi} is greater than 1000 V. For the 75%/25% mixture of Fig. 28, V_{lo} is approximately 375 V and V_{hi} is again greater than 1000 V. Oscillograms of the voltage output of the transducer's circuitry for these two mixtures are shown in Fig. 29. It was concluded from these results that neon/nitrogen mixtures are suitable for pressurizing the MEPF/G transducer. However, due to prior difficulties with neon, investigations into other gases were continued.

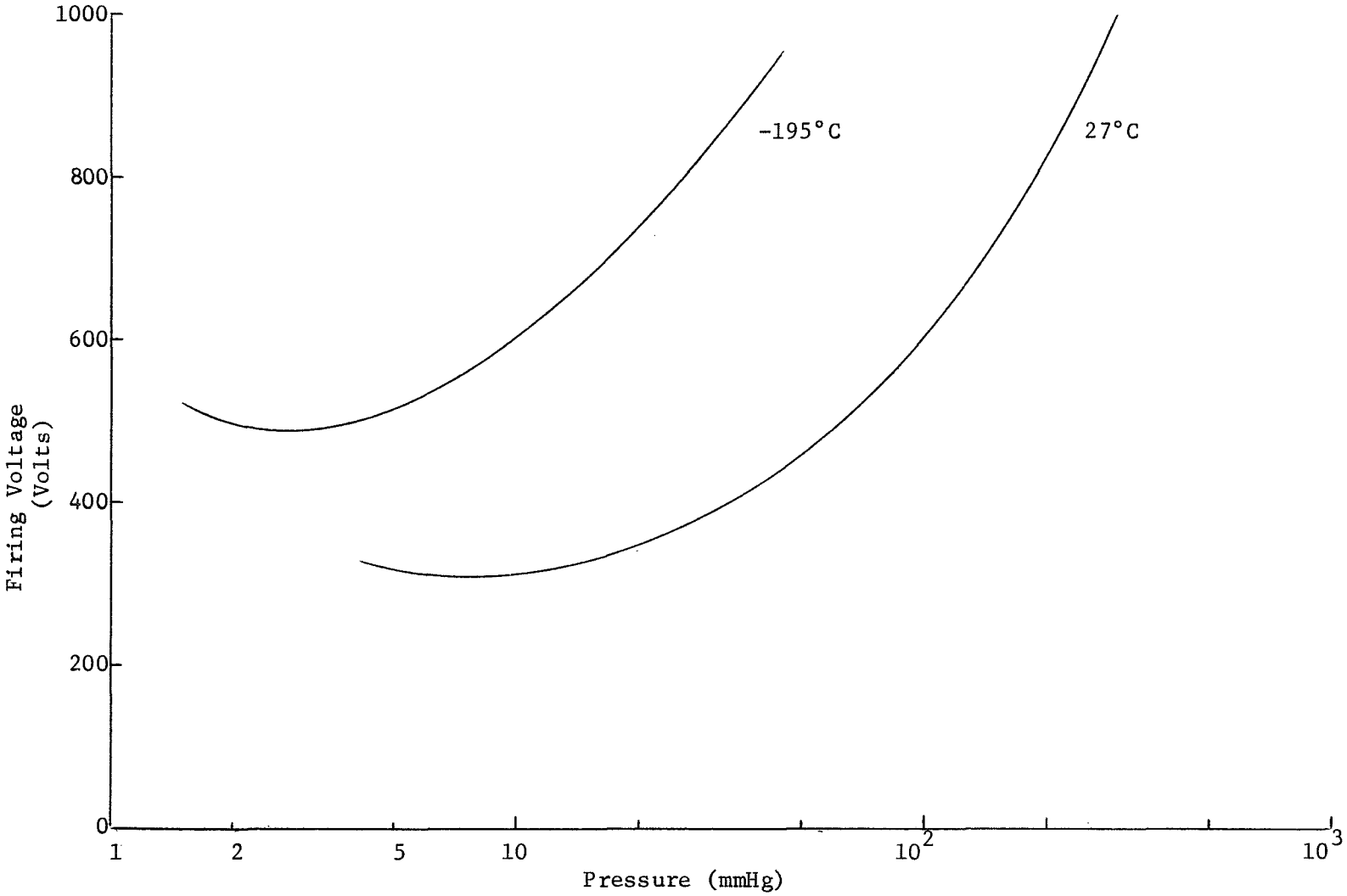

Figure 23. Nitrogen Paschen Curves

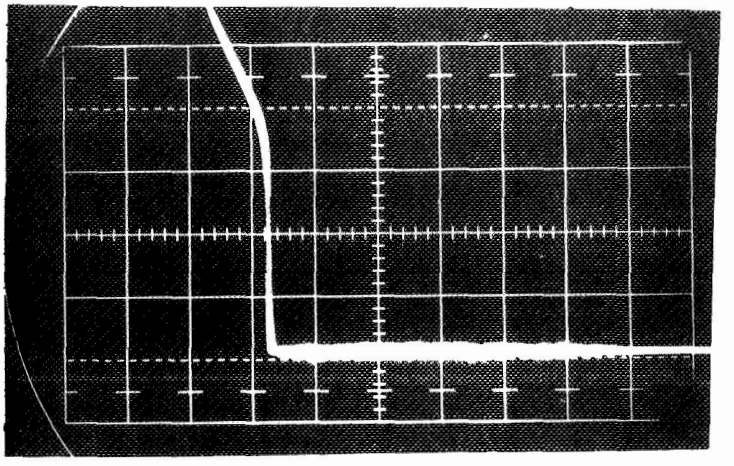

V_f = 500 V
P = 80 mmHg

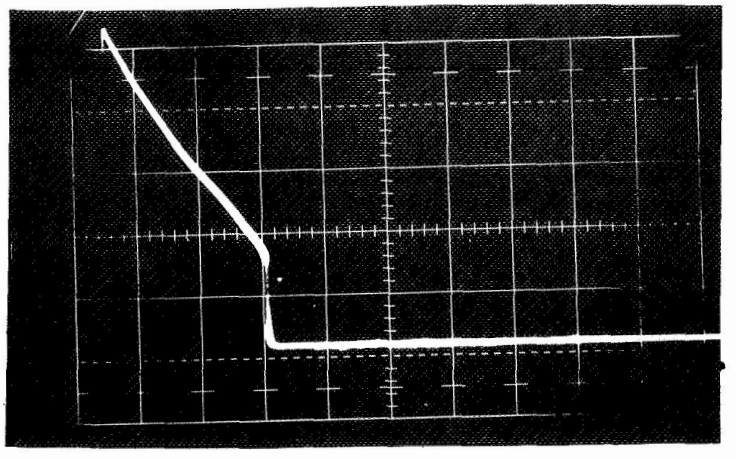

V_f = 375 V
P = 31 mmHg

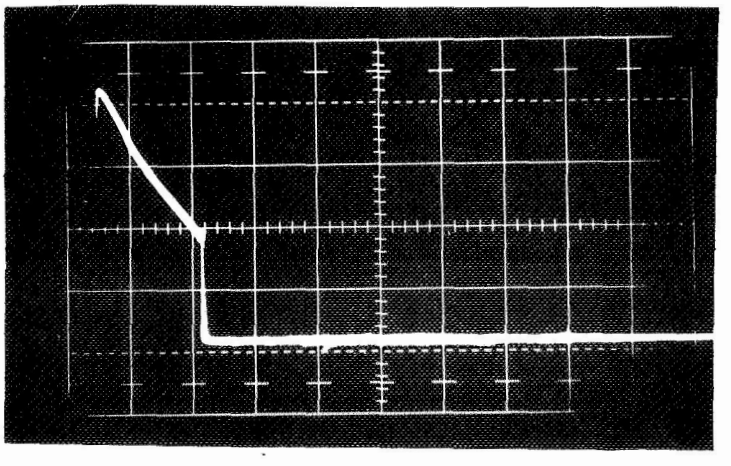

V_f = 325 V
P = 17 mmHg

Vertical Scale: 1 V/cm
Horizontal Scale: 0.5 mS/cm

Figure 24. Oscillograms of Transducer Firings with Nitrogen

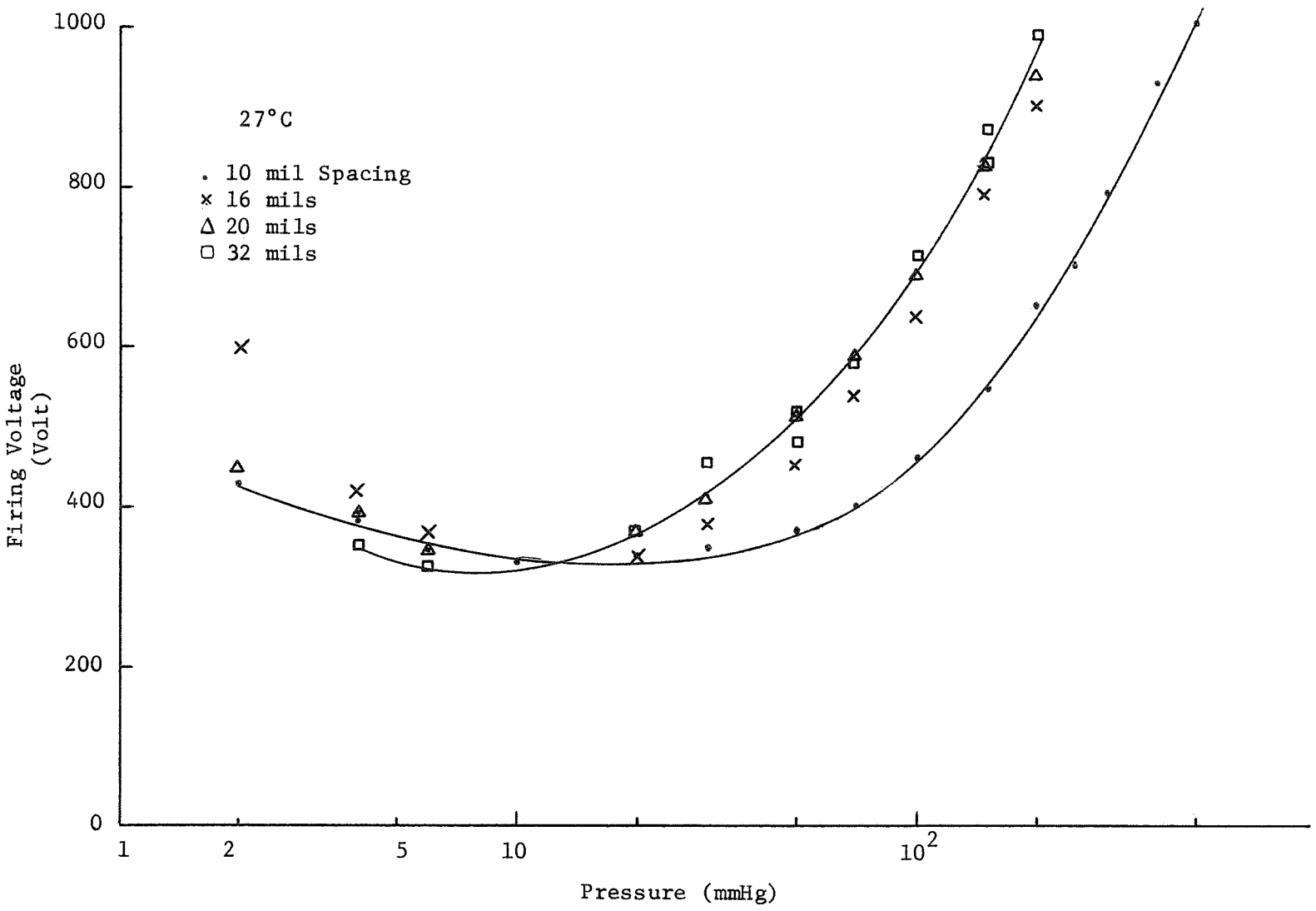

Figure 25. Nitrogen Paschen Curves with Variable Electrode Spacings

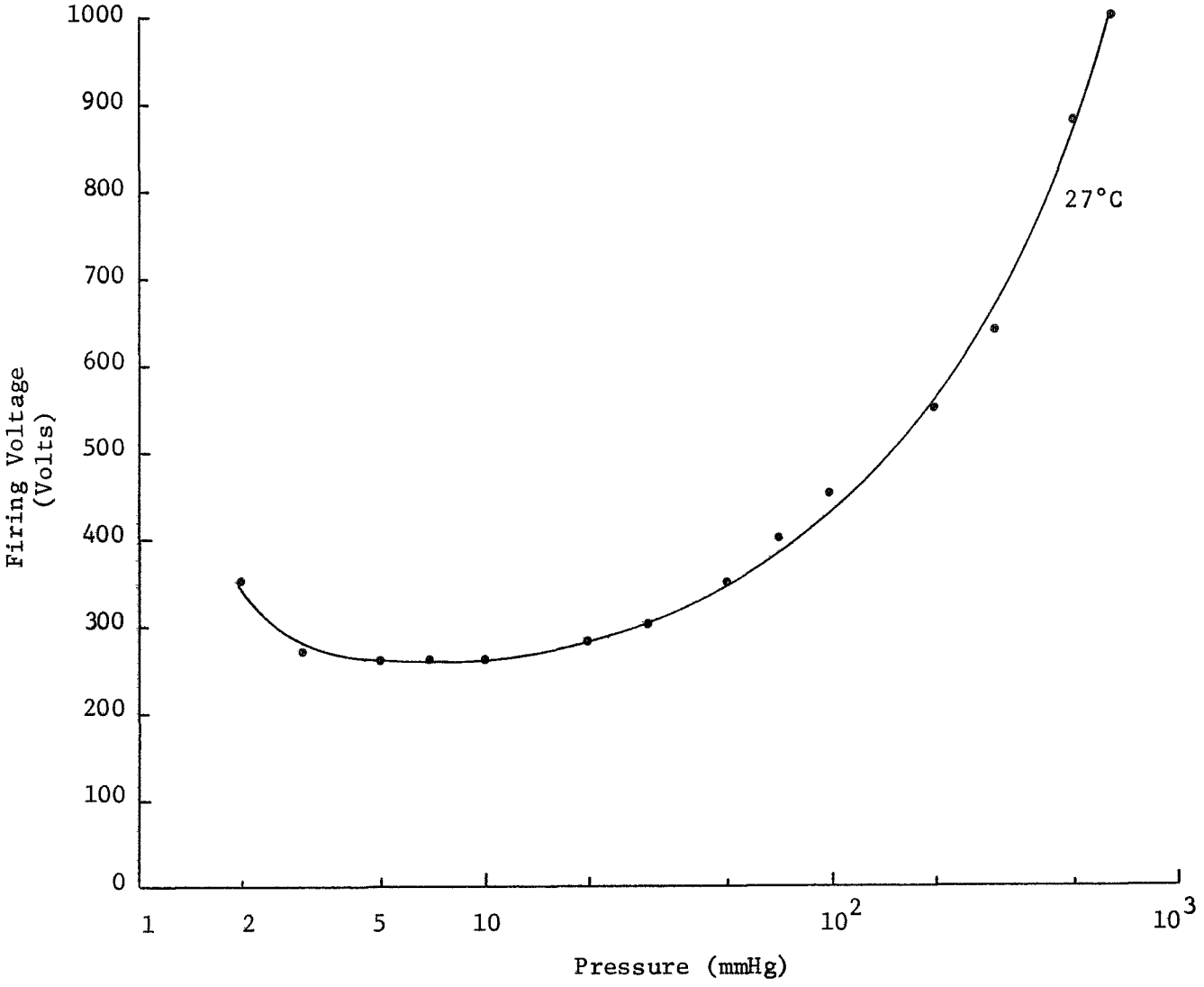

Figure 26. Argon Paschen Curves

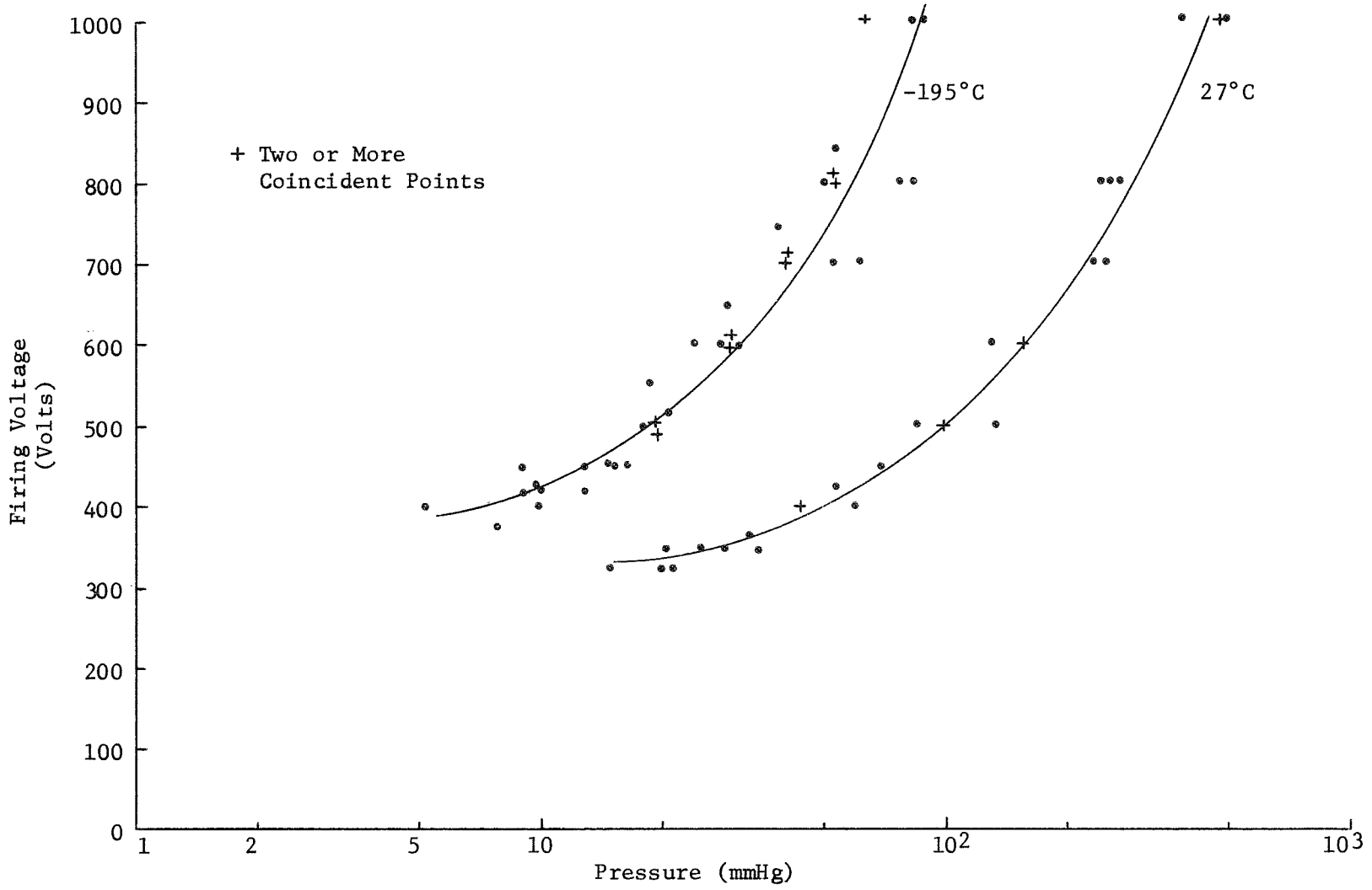

Figure 27. Paschen Curves for 50% Neon-50% Nitrogen Gas

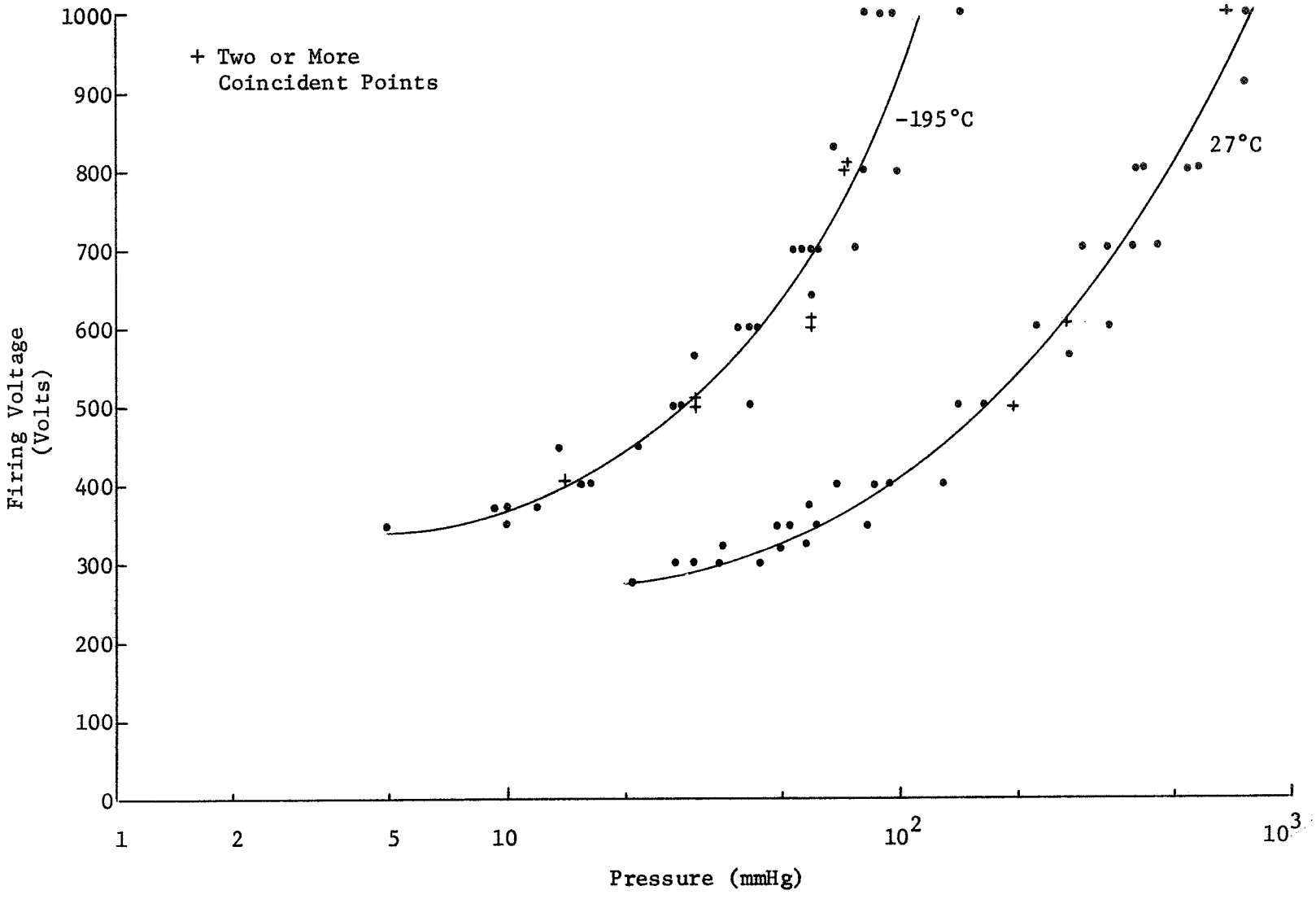

Figure 28. Paschen Curves for 75% Neon-25% Nitrogen Gas

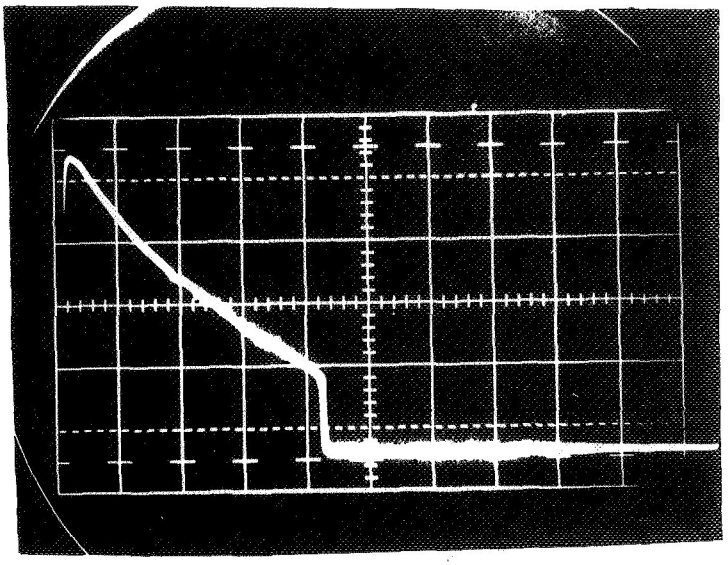

50% Neon-50% Nitrogen
V_f = 500 V
P = 18 mmHg
LN_2 Temperature

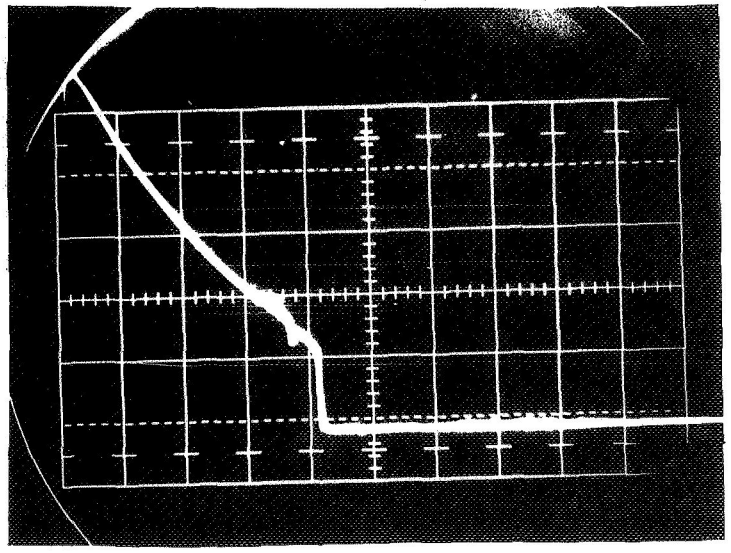

75% Neon-25% Nitrogen
V_f = 500 V
P = 28 mmHg
LN_2 Temperature

Vertical Scale: 2V/cm
Horizontal Scale: 0.5 mS/cm

Figure 29. Oscillograms of Transducer Firings with Neon-Nitrogen Gas Mixtures.

Mixtures of Argon and Nitrogen. - Concurrent with the initial investigations into neon-nitrogen mixtures, argon-nitrogen mixtures were also considered as a pressurizing gas. Mixtures with 75% or less of argon have an adequately low boiling point so as not to liquify if the initial sealing pressure at room temperature is 865 mmHg or less. Initial experimental results with argon-nitrogen mixtures are illustrated in Figs. 30 and 31. (These data were taken with the same transducers that were used for the neon-nitrogen mixtures of Figs. 27 and 28.) These experiments were conducted using the circuitry and test facility previously described by applying a fixed voltage to the transducer circuitry and lowering the pressure until a firing event occurred. Care was exercised in keeping the partial pressure of argon low such that it would not condense in the pressure cell. (The vapor pressure of argon is 200 mmHg at LN_2 temperature.)

Paschen curves for a mixture of 50% argon-50% nitrogen are shown in Fig. 30, and for a 75% argon-25% nitrogen mixture in Fig. 31. In both cases, V_{hi} is greater than 1000 V. For the 50%/50% mixture, V_{lo} is approximately 400 V, and for the 75%/25% mixture it is approximately 375V. Oscillograms of the output of the transducer circuitry of Fig. 10 for argon-nitrogen mixtures are essentially identical to those for the neon-nitrogen mixtures shown in Fig. 29. On the basis of these results, the 75% argon-25% nitrogen mixture was selected for the MEPF/G experiment. A characterization program was started with this mixture to gain confidence that it was satisfactory for the MEPF/G experiment.

During this initial investigation into argon-nitrogen mixtures, the electrode spacing experiment conducted previously with nitrogen was repeated with similar results. The 10 mil spacing yielded a slightly lower curve, but the other curves were nearly identical.

With the selection of a new pressurizing gas, it was necessary to again change the high voltage specified for the power converter. It was changed back to the original 525 V; however, part selection and screening procedures complicated the change. These problems will be discussed later in this report.

The Argon-Nitrogen Mixtures

Following the selection of a 75% argon-25% nitrogen mixture for the MEPF/G pressure cells, an extensive experimental program was carried out to further demonstrate that this mixture was satisfactory and to gain confidence in its stability. Numerous Paschen curves were determined at room and LN_2 temperatures, and with several gas mixtures that were varied about the 75%/25% mixtures specified. Additionally, these mixtures were deliberately doped with air in order to evaluate the result of an inadvertent leak during the filling process.

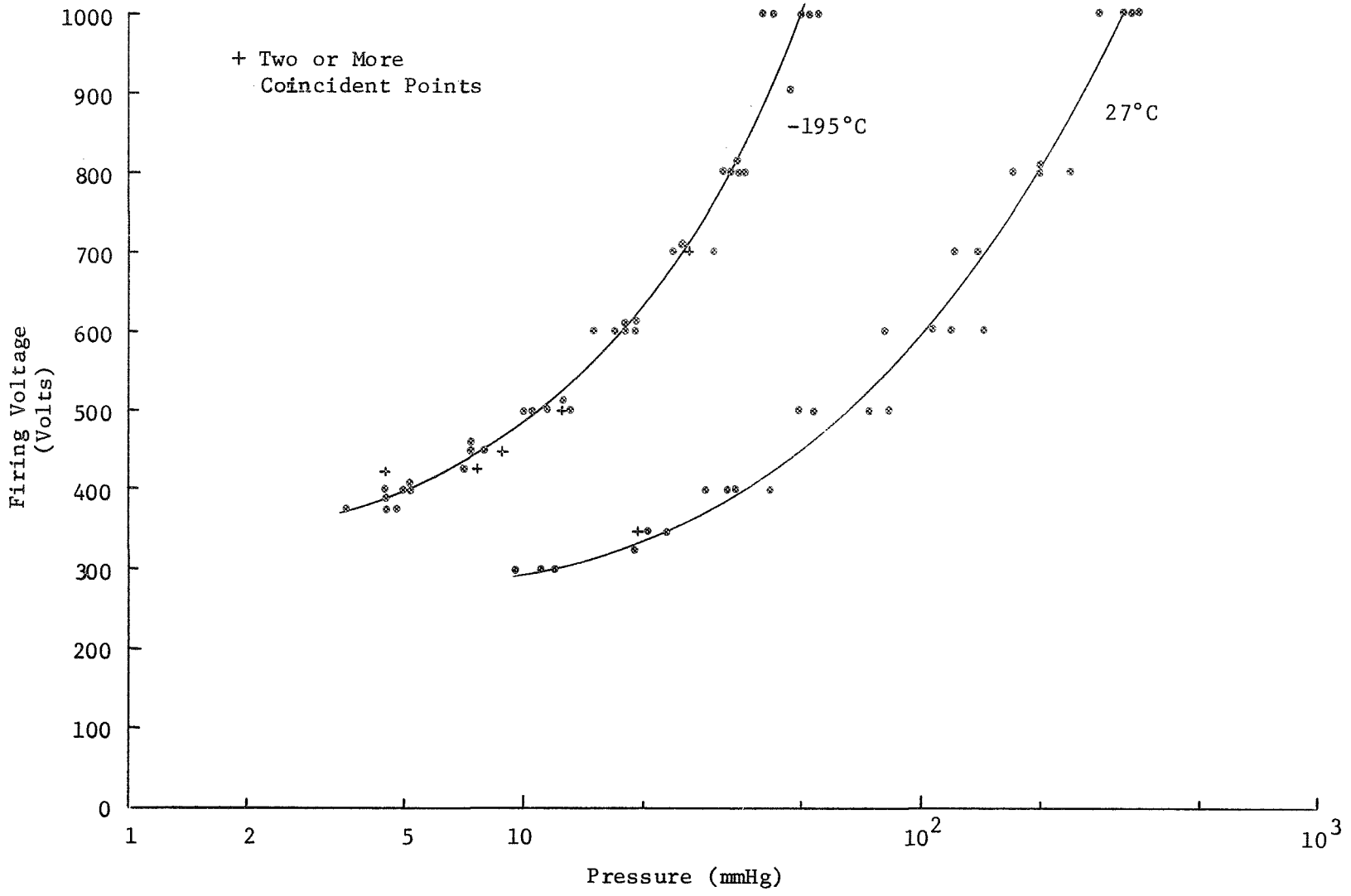

Figure 30. Paschen Curves for 50% Argon-50% Nitrogen Gas

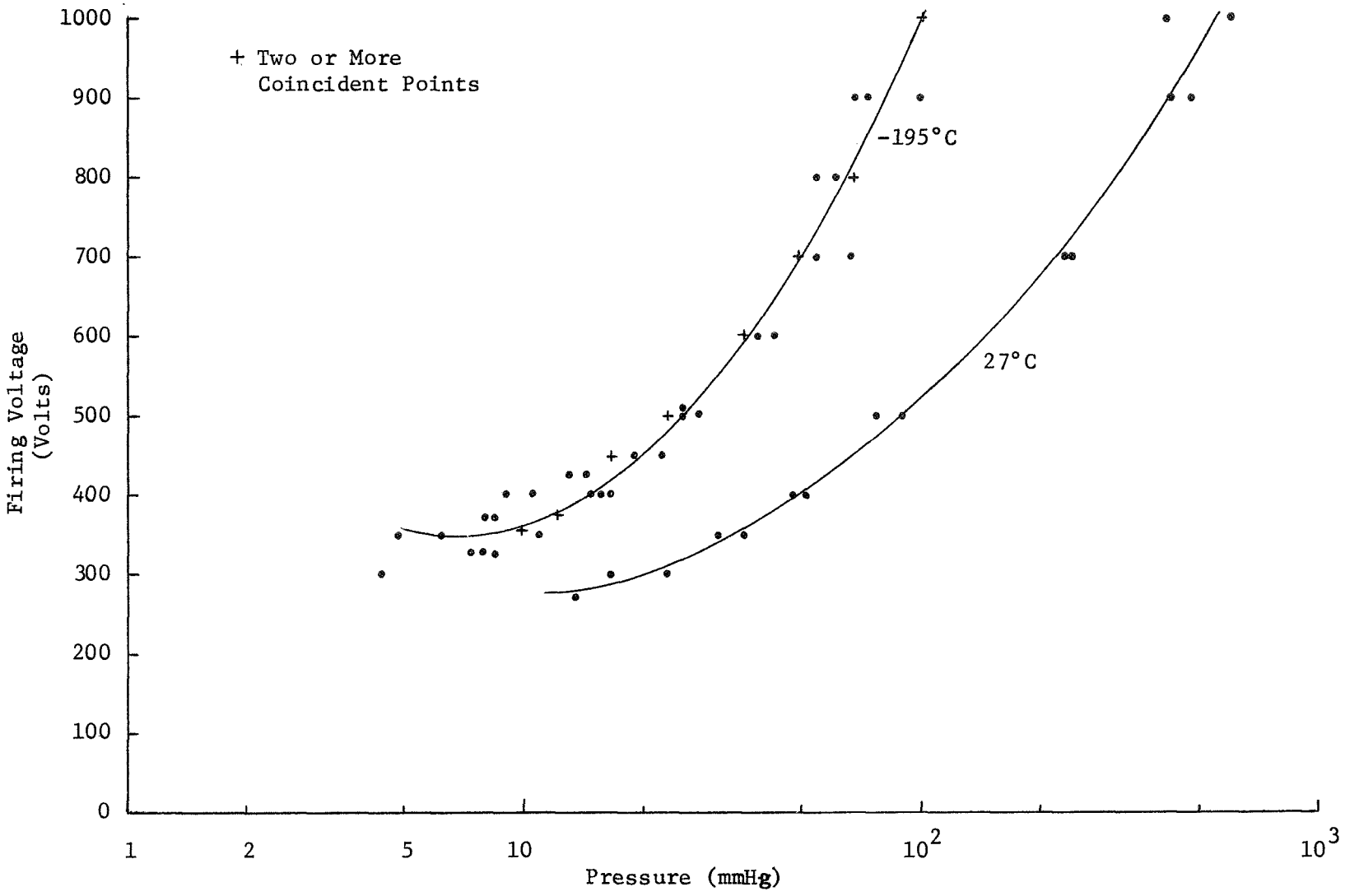

Figure 31. Paschen Curves for 75% Argon-25% Nitrogen Gas

It is of interest to briefly consider the thermal properties of the 75%-25% mixture. The nitrogen, of course, will not liquify at LN_2 temperature. If the sealing pressure at room temperature is 865 mmHg, the partial pressure of nitrogen is 25% of that figure, or 216 mmHg. At LN_2 temperature or -195°C, the partial pressure of nitrogen is further reduced to 55.5 mmHg. Consequently, the nitrogen will not liquify until the temperature is below LN_2 temperatures at 760 mmHg. The partial pressure of argon in this mixture is 650 mmHg at room temperature and 167 mmHg at LN_2 temperature. This is below the 200 mmHg vapor pressure of argon at LN_2 temperature and, consequently, the argon will not liquify.

Paschen Curves. - The Paschen curves presented in this section were determined using a set of four transducers with electrode spacings of 33, 34, 35 and 38 mils. The gas mixtures included argon-nitrogen percentages of 85%/15%, 80%/20%, 75%/25%, 70%/30% and 65%/35%. After taking an initial set of Paschen curve data, these mixtures were doped with 16% dry air and the experiments repeated. A summary of these results are presented in this section.

Figure 32 is a Paschen curve for the 25%/75% argon-nitrogen mixture. (This is a separate mixture from the gas used to determine the Paschen curves of Fig. 31.) These data compare favorably with the results shown in Fig. 31 for earlier experiments. After these curves were determined the gas mixture was doped with air such that the gas percentages were 63% argon, 21% nitrogen and 16% air. Paschen curves determined with this mixture are shown in Fig. 33. These results are essentially identical to the results obtained without the air dopant. Paschen curves for the five gas mixtures determined with one of the four transducers (35 mil spacing) are shown in Fig. 34. These curves are essentially identical, within experimental error, of the results achieved with all combinations of the gases and transducers described in this section.

The multitude of data determined with the 75% argon-25% nitrogen gas mixtures prepared at RTI are summarized by the Paschen curves of Fig. 35.

The MEPF/G Gas Mixture

The argon-nitrogen mixtures discussed previously in this report were mixed at RTI under less than ideal circumstances. The gases were mixed in used gas cylinders that were thoroughly flushed with the gases to be used in the mixture and then pumped to a low pressure. In the absence of equipment for handling or measuring high pressures, only small volumes could be mixed at one time and new mixtures were frequently prepared. It was deemed advisable to purchase an adequate quantity of

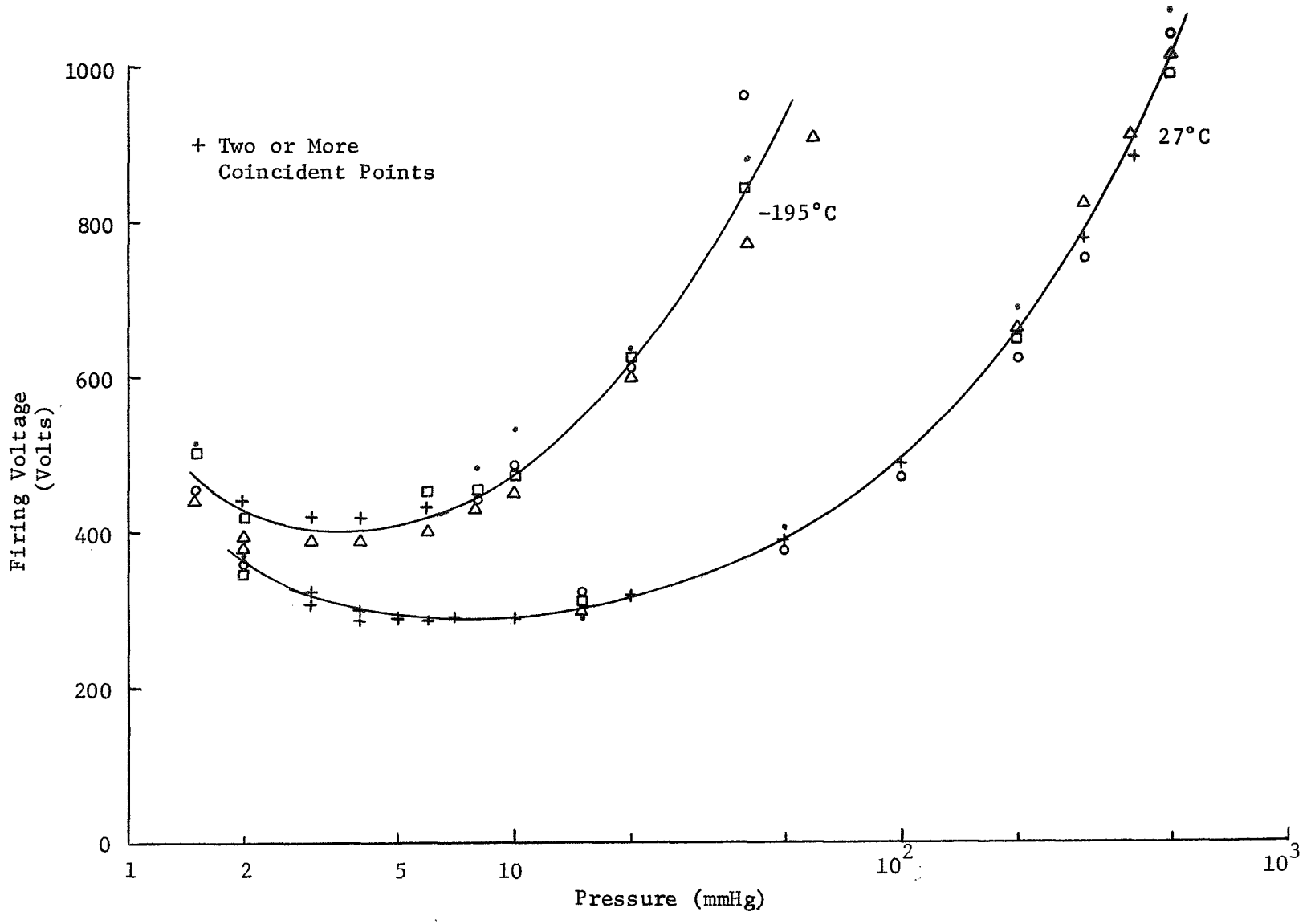

Figure 32. Additional 75% Argon/25% Nitrogen Paschen Curves

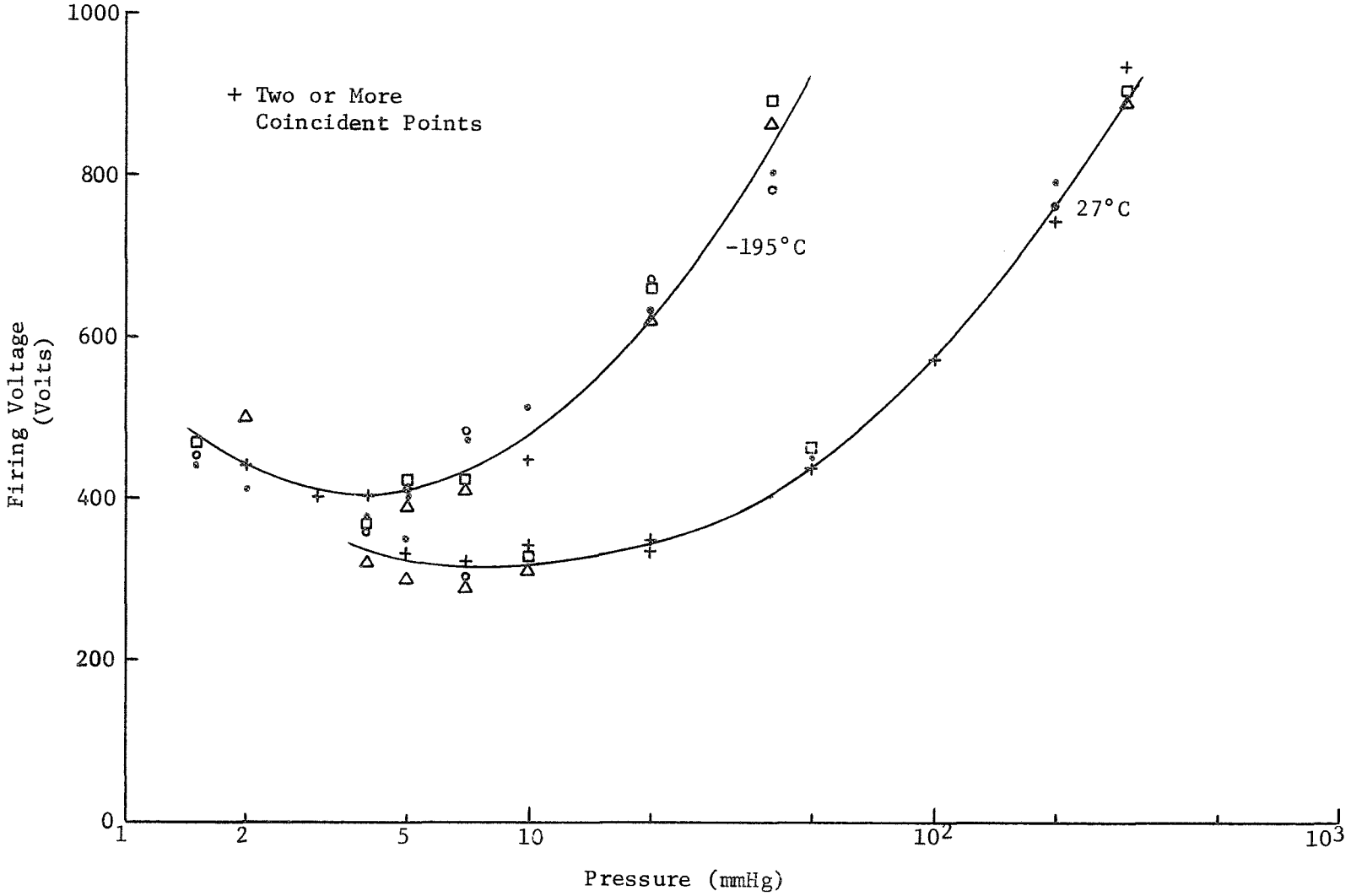

Figure 33. Paschen Curves for a 63% Argon, 21% Nitrogen, 16% Air Mixture

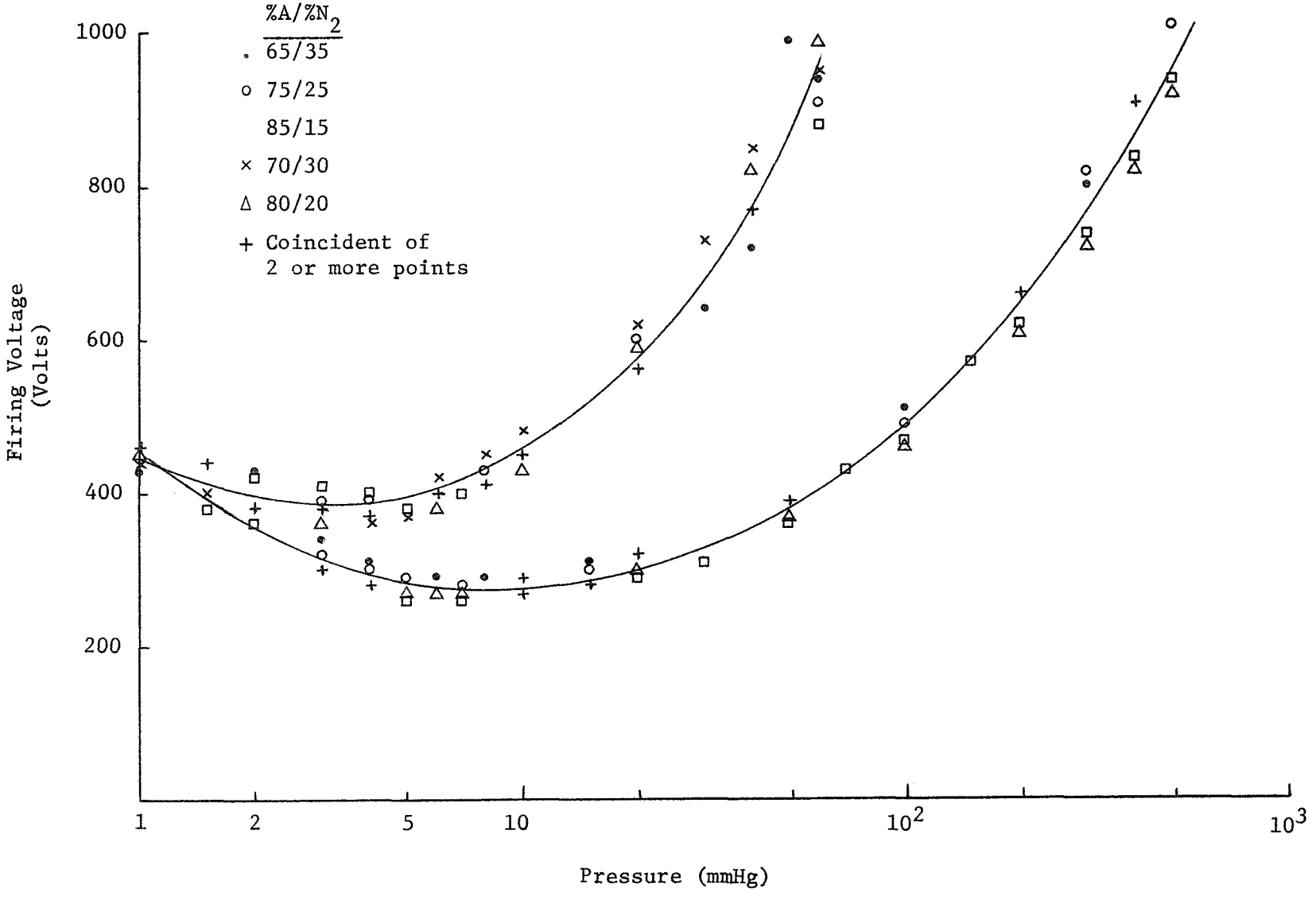

Figure 34. Paschen Curves for Five Argon/Nitrogen Mixtures

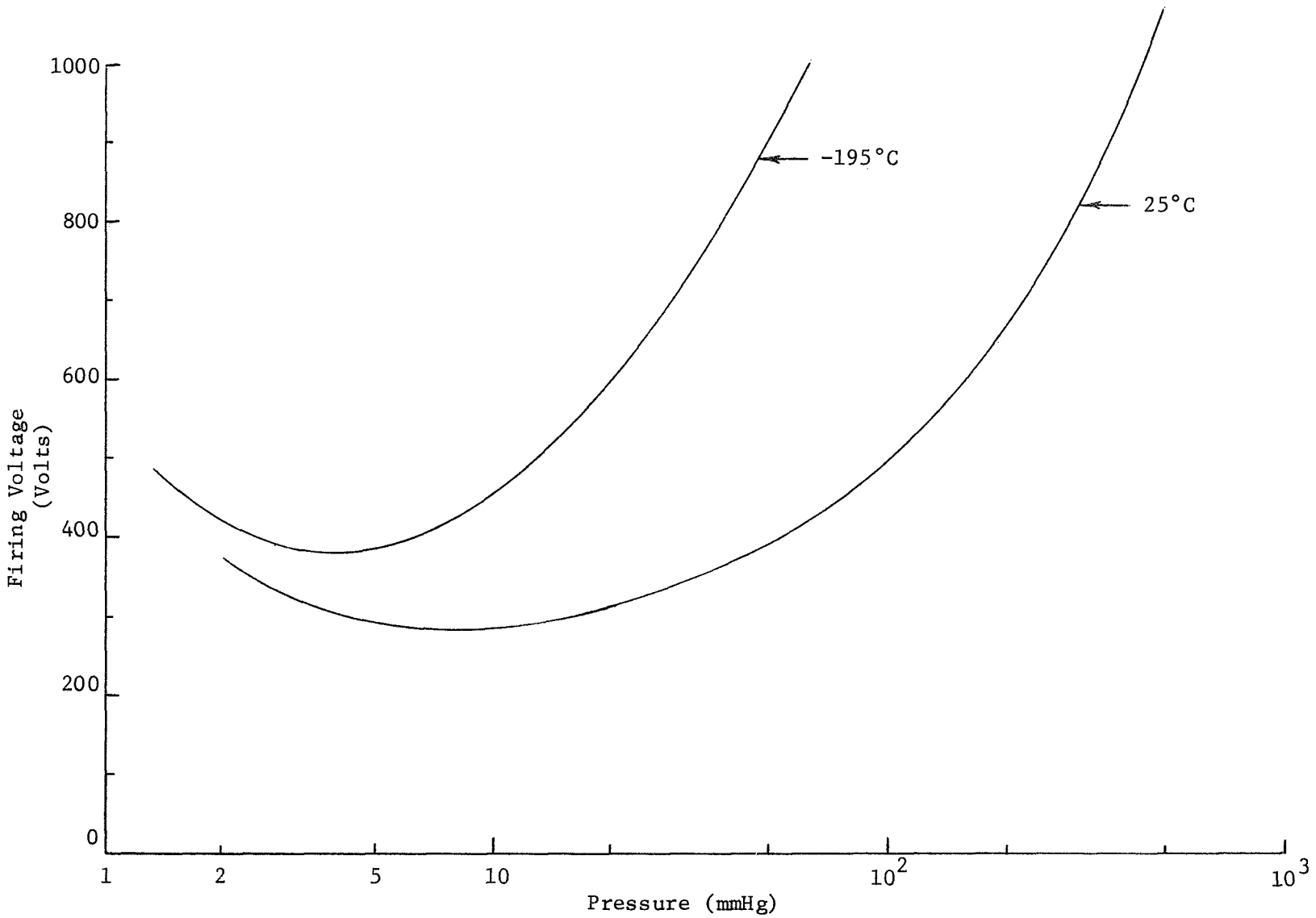

Figure 35. A Summary of Paschen Curves for RTI Mixtures of 75% Argon-25% Nitrogen

the selected argon-nitrogen mixture, i.e., 75% argon-25% nitrogen, from a commercial source to supply the anticipated needs of the MEPF/G experiments. The gas was purchased by LaRC and two cylinders were supplied to RTI for further experimentation. The supplier's analyses of these two cylinders are as follows:

Cylinder No.	Component	Analysis	
SG13536B	Nitrogen	24.5	Molar %
	Oxygen	1.4	Molar ppm
	Carbon Dioxide	<0.5	Molar ppm
	Carbon Monoxide	<1.0	Molar ppm
	Nitrous Oxide	<0.1	Molar ppm
	Methane	<0.5	Molar ppm
	Acetylene	<0.05	Molar ppm
	Total Hydrocarbons	<1.0	Molar ppm
	Water	0.15	Molar ppm
	Water	-125°F	Dew Point
	Argon	Balance	
SG15619B	Nitrogen	24.5	Molar %
	Oxygen	0.5	Molar ppm
	Carbon Dioxide	<0.5	Molar ppm
	Carbon Monoxide	<1.0	Molar ppm
	Nitrous Oxide	<0.1	Molar ppm
	Methane	<0.5	Molar ppm
	Acetylene	<0.05	Molar ppm
	Total Hydrocarbons	<1.0	Molar ppm
	Water	0.15	Molar ppm
	Water	-125°F	Dew Point

Paschen curves for the MEPF/G transducers were determined with the MEPF/G gas mixture, and these results are shown in Figs. 36 and 37. Test circuits, apparatus and procedures were the same as for previous Paschen curves. Data points were determined by both fixing pressure and increasing voltage until a firing event occurred and by fixing voltage and lowering pressure until a firing event occurred. These procedures

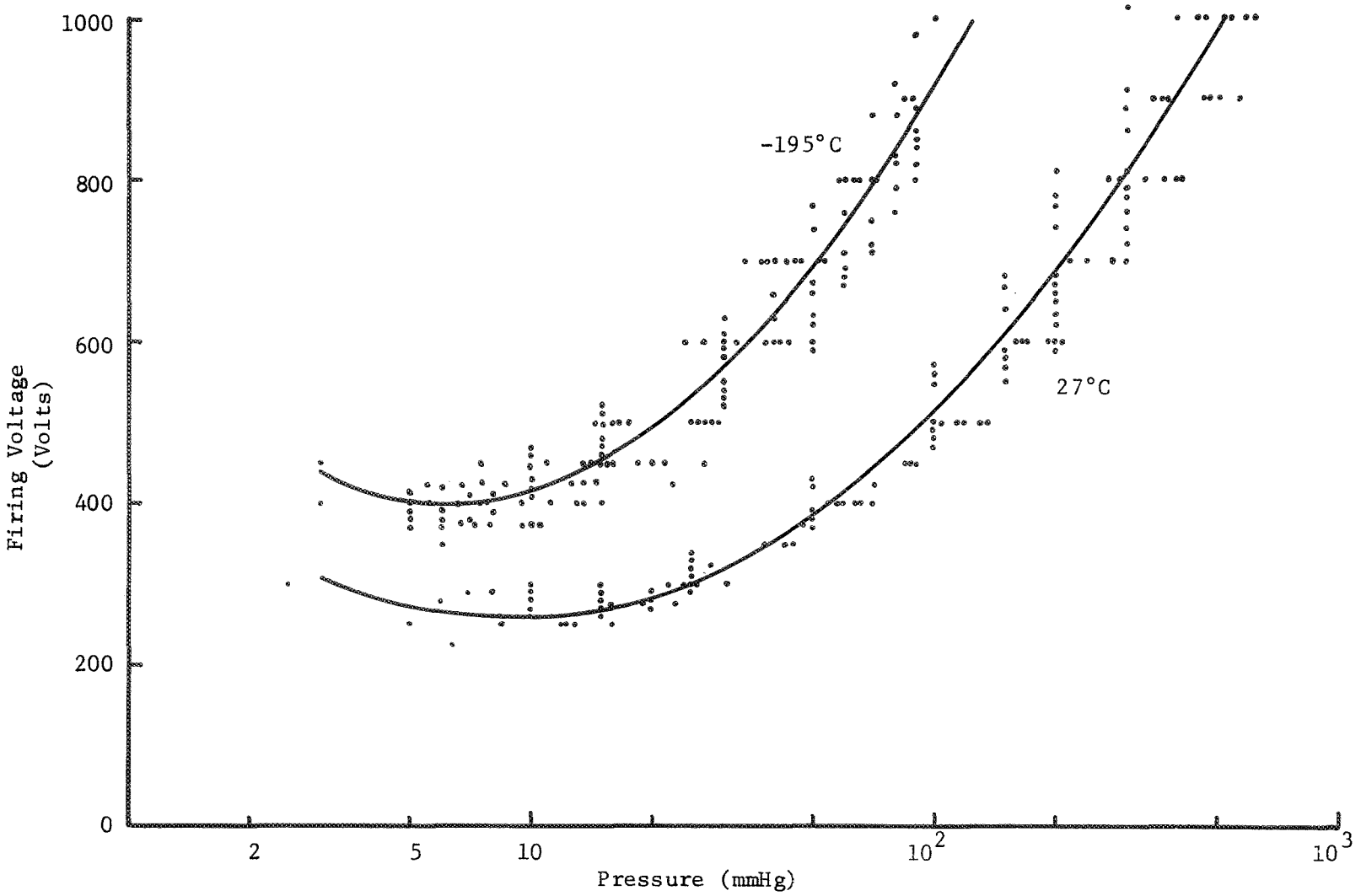

Figure 36. Paschen Curves for the MEPF/G Gas Mixture

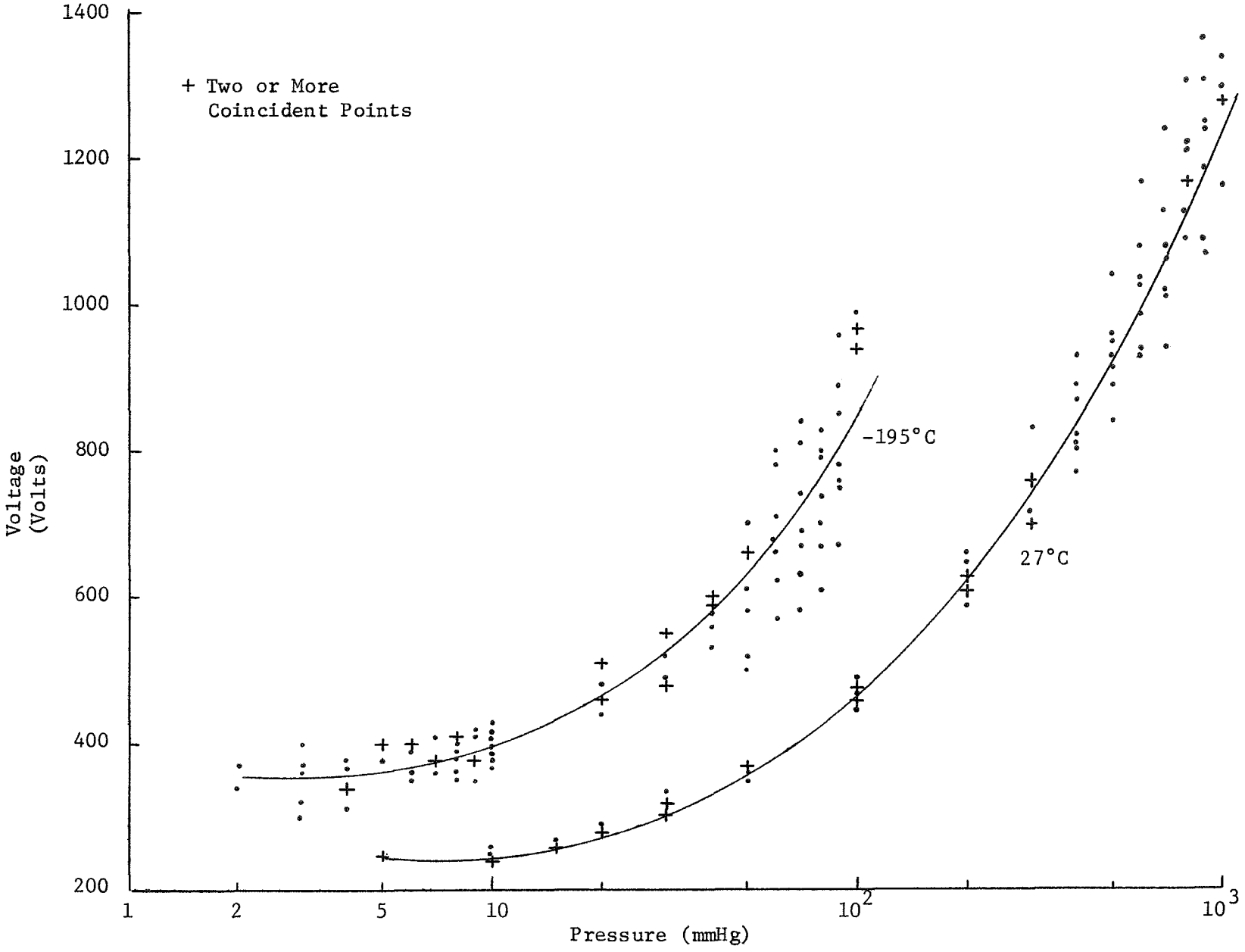

Figure 37. Additional Paschen Curves for the MEPF/G Gas Mixture

are evident in the horizontal and vertical patterns of the data points of Figs. 36 and 37. Reading from these data, V_{hi} for the MEPF/G gas is greater than 1000 V and V_{lo} is approximately 375 V. Oscillograms of the output of the MEPF/G transducer circuitry for the MEPF/G gas are shown in Fig. 38 for room temperature initial firings and in Fig. 39 for LN_2 temperature firings. These were determined by fixing the applied voltage and lowering pressure until a firing event occurred. These waveforms are essentially the same as observed with the other gases investigated. It is concluded from these results that the MEPF/G transducers and gas mixtures are suitable for the planned experiment.

The Paschen curves of Fig. 35 for the RTI mixtures differs from those of Figs. 36 and 37 in that the LN_2 temperature curves of the latter do not turn up as quickly. No explanation for this difference has been determined.

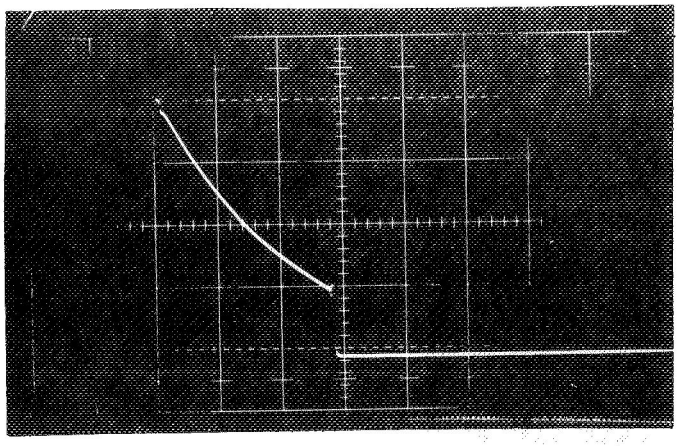

550 V
140 mmHg

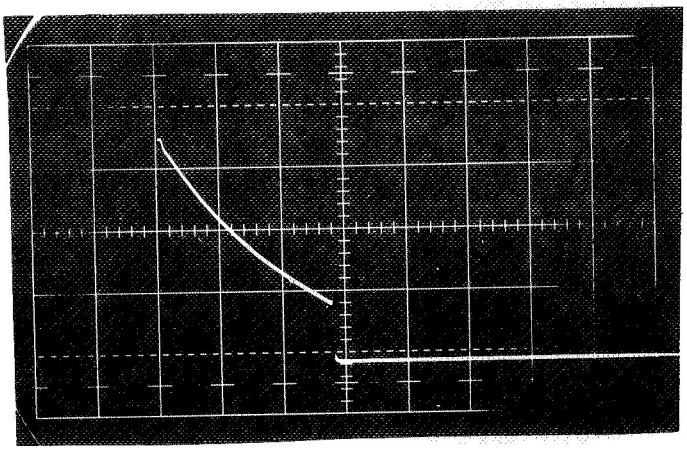

500 V
110 mmHg

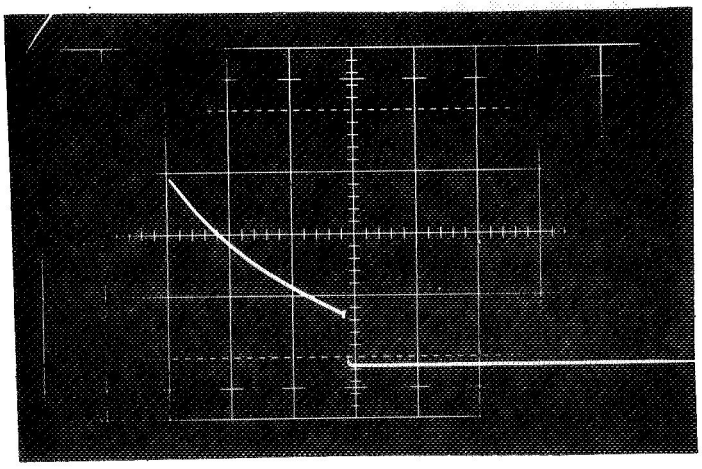

450 V
85 mmHg

Vertical Scale: 5 V/cm
Horizontal Scale: 0.5 mS/cm

Figure 38. Oscillograms of the Transducer Circuitry Output for Initial Firings with the MEPF/G Gas at Room Temperature

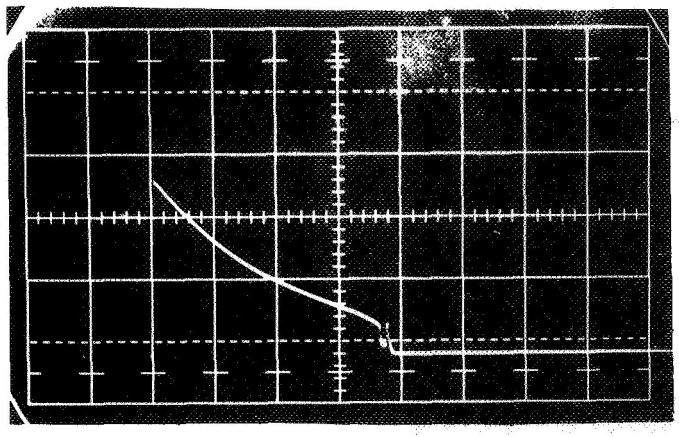

500 V
21 mmHg

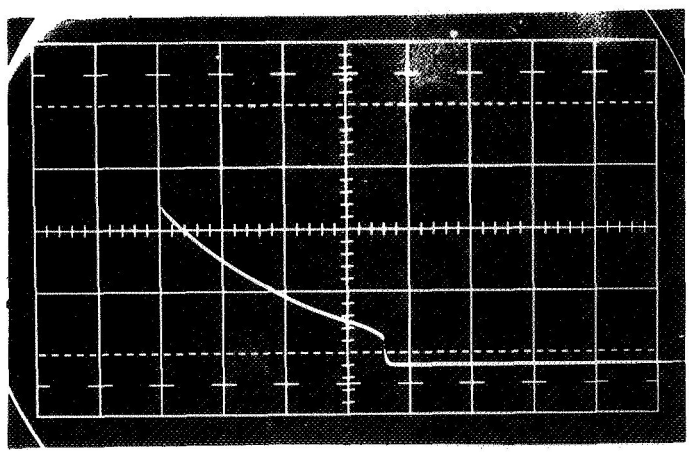

500 V
19 mmHg

Vertical Scale: 5 V/cm
Horizontal Scale: 0.5 mS/cm

Figure 39. Oscillograms of the Transducer Circuitry Output for Initial Firings with the MEPF/G Gas at LN_2 Temperature

SECTION III

THE ELECTRONIC SYSTEM

Summary

The initial objective of the RTI program supporting the MEPF/G experiment was to characterize the transducer and design a compatible electronic system to interface the pressure cells with the spacecraft. As the unreliability of the MEPF/G transducer became evident, additional transducer development replaced electronic system design as RTI's primary objective. Concurrently, the Flight Instrument Division (FID) at LaRC assumed responsibility for the design and fabrication of the MEPF/G electronic system and RTI was relieved of this responsibility to concentrate on transducer development. Before these changes were made, however, a basic electronic system design was completed and a breadboard model was fabricated and tested. This design and test results on the breadboard model are described herein. This work was completed early in the project period.

The Research Triangle Institute's electronic system included a dc-dc converter designed and fabricated by Wilmore Electronics, Inc. on a subcontract. This converter was incorporated into the FID system to become a component of the flight hardware system.

Many features of the electronic system reflect weight, power and volume limitations and other limitations imposed by Pioneer specifications (ref. 2). The experiment was allotted 3.9 lbs weight, 1 watt power and 27 in^3 (3" x 3" x 3") of space. Spacecraft-MEPF/G interfaces are indicated in the block diagram of Fig. 1, and specifications for these interfaces are summarized in the following section. A 32-count recycling counter was specified for the event counter to be read serially to the spacecraft upon command. The number of output lines from the MEPF/G were still to be determined at the time this work was accomplished. One line was required for the counter readout. Other lines could have been committed to other purposes such as redundant counters and the ON-OFF status of the experiment.

The Pioneer specifications include an approved parts list that significantly influenced the electronic design. This parts list was severely restrictive in some areas. Few unijunction transistors and junction FET's were available for selection, for example, and MOSFET's were excluded. Ultimately, the approved parts list was used as a guideline and many exceptions were made, including the use of MOSFET's. The RTI effort, however, was completed early in the program and reflects a commitment to the approved parts list.

Specifications

The interface specifications that pertained to the MEPF/G experiment are discussed below. These specifications are not complete herein. Complete interface specifications are included in PC-220 (ref. 2).

Digital Data. - Unless otherwise specified, a digital "1" or ON signal is 4.5 $\pm$ 1 Vdc and a digital "0" or OFF is 0.25 $\pm$ 0.25 Vdc. Digital data read from the MEPF/G will be a serial, six bit word from a source impedance of 20 kΩ or less.

Input Power. - The MEPF/G experiment is allotted one watt of electrical power to be supplied at 28 Vdc $\pm$ 2%. This voltage is supplied to the dc-dc power converter through an electronic switch. When switched to ON, the power converter must limit the input current such that 1) the current not exceed 500% of nominal steady state current for 10 μs, 2) the current not exceed 200% of the nominal steady state current for 50 ms, and 3) the current not exceed 120% of nominal steady state current for the balance of 1 second.

ON-OFF Command. - The electronic switch incorporated in the power converter turns the MEPF/G experiment ON or OFF upon command. A voltage level of 4 + 1.4, - 1.5 Vdc turns the experiment ON and 0.25 $\pm$ 0.25 Vdc turns the experiment OFF.

Word-Gate Pulse. - A word gate pulse is supplied the MEPF/G from the spacecraft to indicate the time for reading the counter content. A "1" signal is supplied from a 5 kΩ source and the "0" signal is supplied from a 40 kΩ source (these are maximum values). The MEPF/G input impedance must be greater than 50 kΩ and 50 pF.

Bit-Shift Pulse. - Bit shift pulses are supplied the MEPF/G to serially readout the counter content. Impedance levels are the same as for the word gate pulse. A six bit word is read from each digital data line on the MEPF/G.

System Considerations

A simplified block diagram of the MEPF/G experiment is shown in Fig. 1. A more detailed block diagram of the experiment is shown in Fig. 40 to facilitate a description of the system's operation. To begin, consider the spacecraft MEPF/G interfaces. The power converter is supplied 28 Vdc and an ON-OFF command signal from the spacecraft, and supplies the 5, 10 and 525 Vdc required for the experiment. The Digital Telemetry Unit (DTU) supplies word-gate and bit-rate signals to readout the event counter and receives the 6-bit serial count output.

The power converter supplies 525 Vdc to the MEPF/G transducers through the transducer circuitry which was described in Section II of

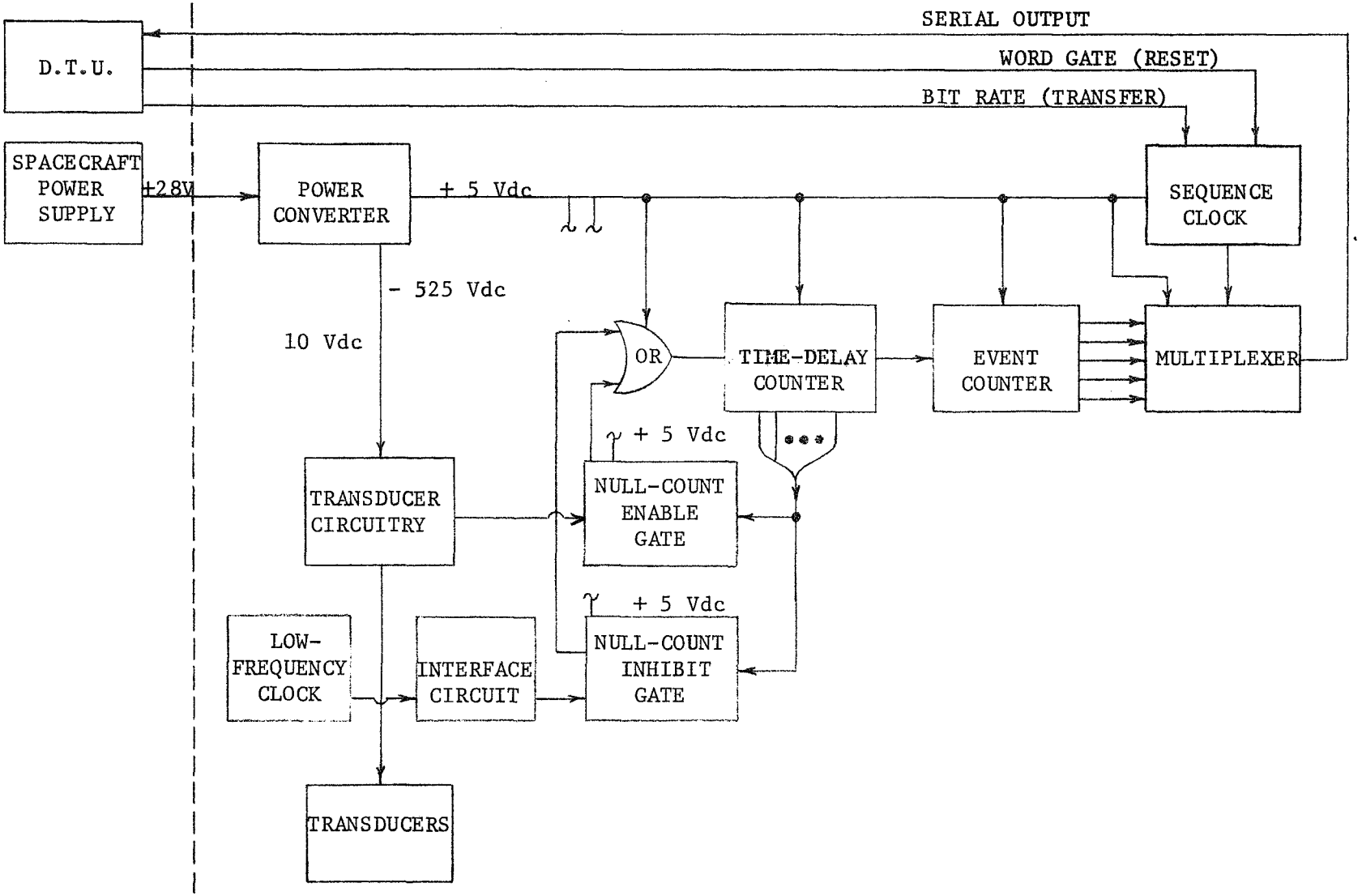

Figure 40. System Block Diagram of the MEPF/G

this report (see Figs. 10, 41). When a transducer firing event occurs, the transducer's circuitry provides an output to the counter circuitry, i.e., to the null-count enable gate of Fig. 40. The transducer is energy limited to turn OFF after the capacitor discharges only to again fire when voltage across the transducer increases to the firing voltage. In this manner, the transducer's circuitry provides a continuous series of output pulses until the cell pressure reduces to a value such that no further firings will occur.

The power converter also supplies 10 Vdc to a low frequency clock which has a period of approximately 20 seconds. The low frequency clock output is supplied to the counter system through the null-count inhibit gate of Fig. 40. The interface circuit is a transistor switching circuit added to "square" the clocks output waveform and assure triggering reliability. The clock output is a spike with an exponential decay.

Except for the transducer circuitry and the low frequency clock, the electronic system principally consists of capatible TTL integrated logic circuitry. This circuitry is supplied with 5 Vdc from the power converter.

In a null condition, the time delay counter of Fig. 40 (a ripple counter) is dormant and supplies seven outputs to the null count enable and inhibit gates. The inhibit gate prevents the low frequency clock from advancing the time delay counter from its null condition. However, the transducer circuitry supplies the time delay counter through an enabled gate such that an output from the transducer circuitry will advance the time delay counter by one count. When the time delay counter is off the null condition, the null count enable gate inhibits any further input from the transducer circuitry and the null count inhibit gate enables the low frequency clock to continue to advance the time delay counter. After approximately 43 minutes, the low frequency clock will have advanced the time delay counter until it again reaches a null condition, and the system is enabled to accept another input from the transducer circuitry.

During the OFF period when the time delay counter is advancing toward its null condition, it is anticipated that the pressure cell which leaked and initiated the cycle will continue to leak to a low pressure such that no further firings can occur. Otherwise, the still firing transducer will advance the time delay counter from null a second time and cause the event counter to register an erroneous count. If a second transducer fires during an OFF period, it will not be counted unless it is still firing 43 minutes after the initial firing of the first transducer, i.e., when the time delay counter returns to null. The actual time delay can be adjusted by changing the period of the low frequency clock or changed by a factor of 2 by adding or removing a flip-flop from the time delay counter.

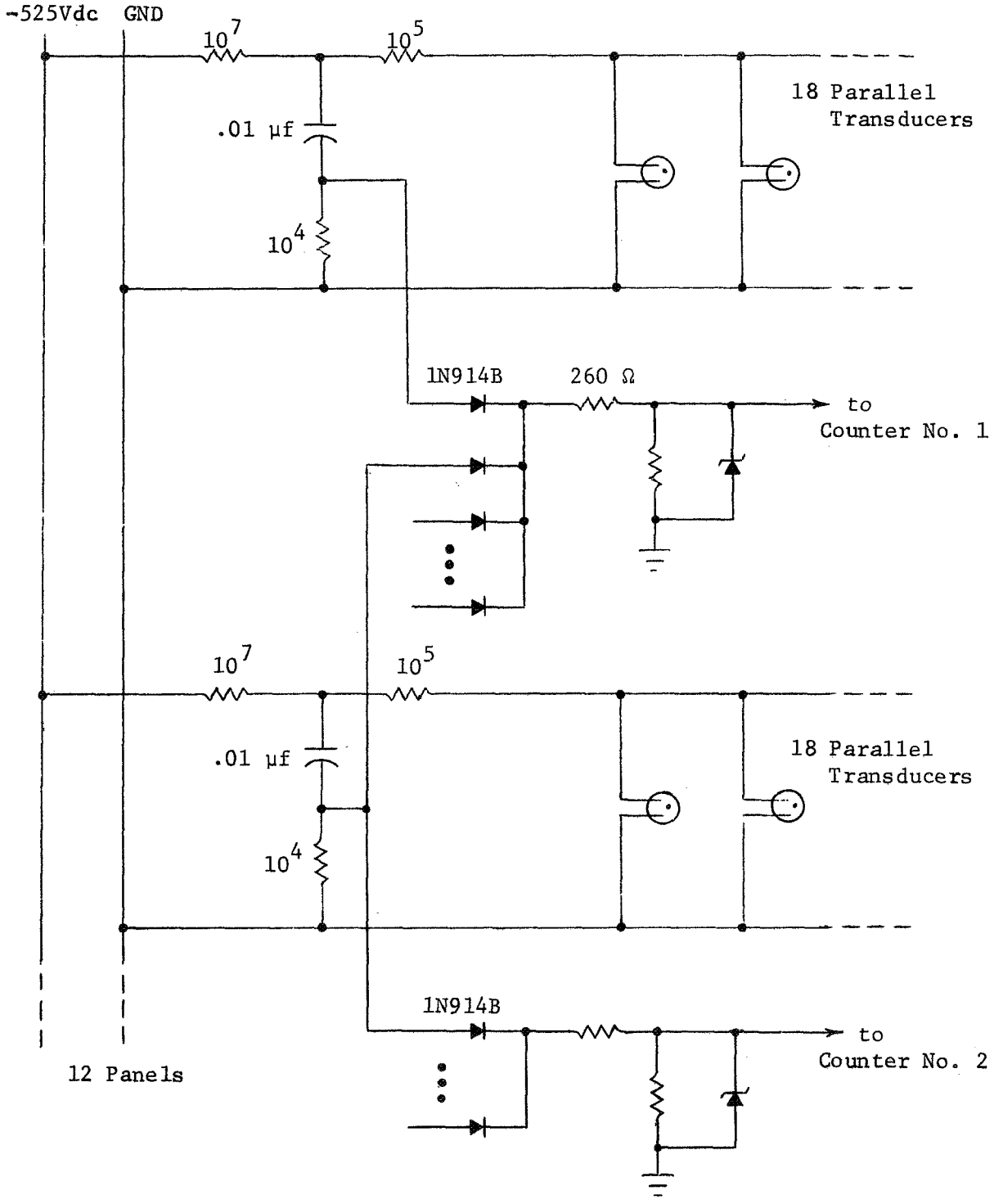

Figure 41. Parallel Transducer Circuits

The event counter advances one count each time the time delay counter advances off the null count. It is a 5-stage recycling ripple counter, and its five outputs store in binary form the number of times the time delay counter has been advanced from its null position. The multiplexer serializes the parallel readout of the event counter and shifts the readout to the spacecraft DTU.

A Redundancy Scheme. - The one watt power allotment is sufficient for a redundant counter system and several parallel transducer circuits. An arrangement for the transducer circuits is illustrated in Fig. 41 where each of the 12 panels has a separate transducer circuit and the 18 transducers on each panel are connected in parallel. The 12 circuits are OR-gated through diodes to two or more transducer interface circuits. (Each of the transducer circuits in Fig. 41 is identical to the circuit of Fig. 10.) One transducer in each of the 12 panels firing would require less than 100 mW. The redundancy scheme is extended in Fig. 42 to include two redundant counters. The counter outputs could be read on separate lines or on a single line as illustrated. The sixth bit in each counter could be used to identify the counter.

Circuit Descriptions

Transducer Circuitry. - The transducer circuitry is described in Section II of this report and is illustrated in Figs. 10 and 41. It is emphasized again that this circuit reflects the necessity of preventing a glowing or fired transducer from dissipating excessive power. (A single transducer glowing at 2 mA of current would require more than 1 W at the power converter input). Energy stored in the 0.01 μF capacitor dissipates across the transducer, R_2 and R_3, whenever a firing event occurs. As the capacitor discharges, voltage across the transducer falls below the running voltage and the glow extinguishes. The transducer voltage again increases to the firing voltages of the transducer at a rate determined by the R_1C time constant.

The Transducer Interface Circuit. - An interface circuit coupling the transducer circuit to the counter is shown in Fig. 41. Other circuits were also used in tests with the electronic system. One was the common emitter circuit illustrated in Fig. 43. Another interface circuit tested was simply a 5 V Zener diode across each of the 10^4 Ω resistors (R_3) in the transducer circuits. The zener diodes act as a limiter to assure that no damaging pulses are transmitted to the counter. Pulses of less than 5 V are transmitted with no attenuation.

Low Frequency Clock. - A schematic of the low frequency clock is shown in Fig. 44. This circuit is the familiar unijunction oscillator

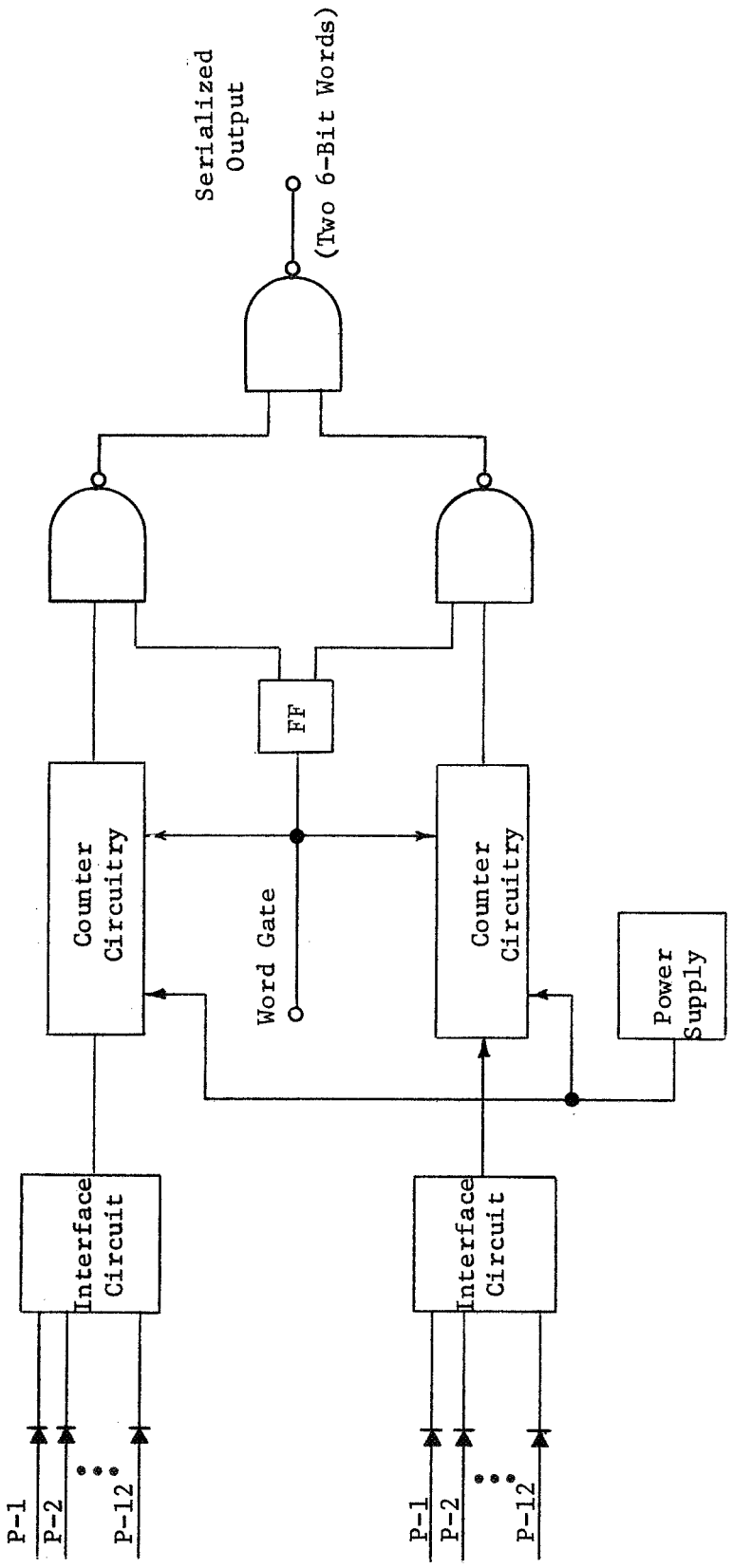

Figure 42. An Illustration of a Redundancy Scheme

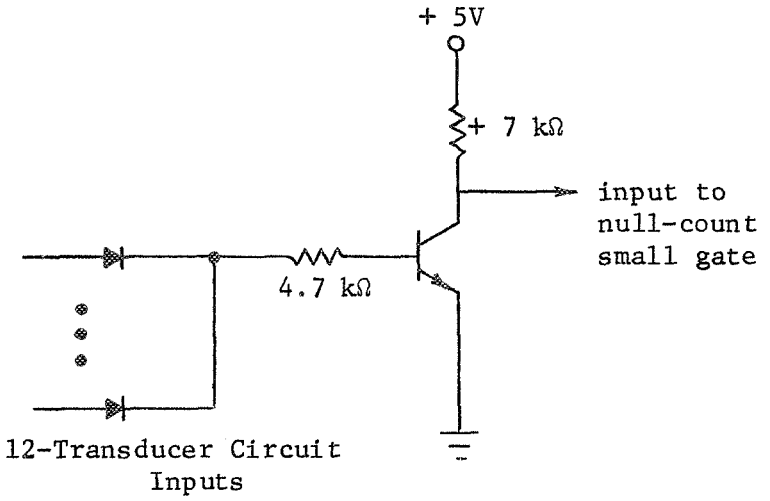

Figure 43. A Transducer Interface Circuit

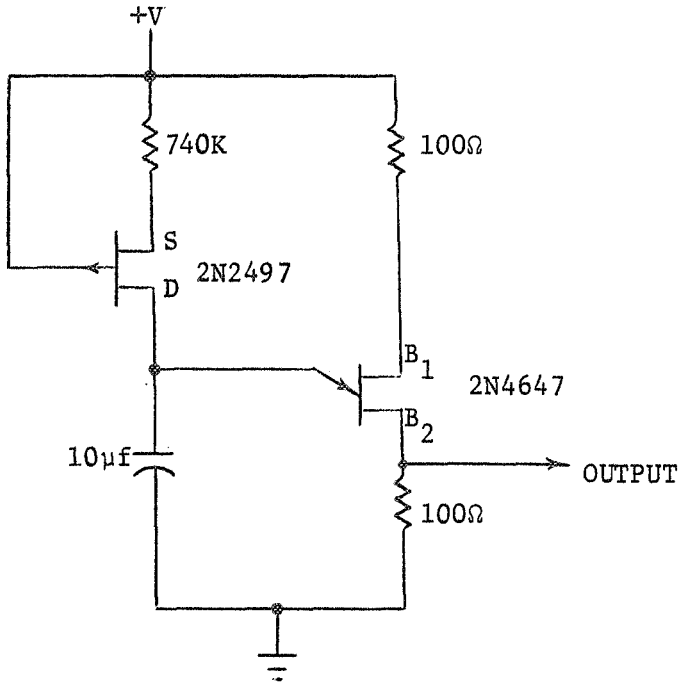

Figure 44. Schematic of The Low-Frequency Clock

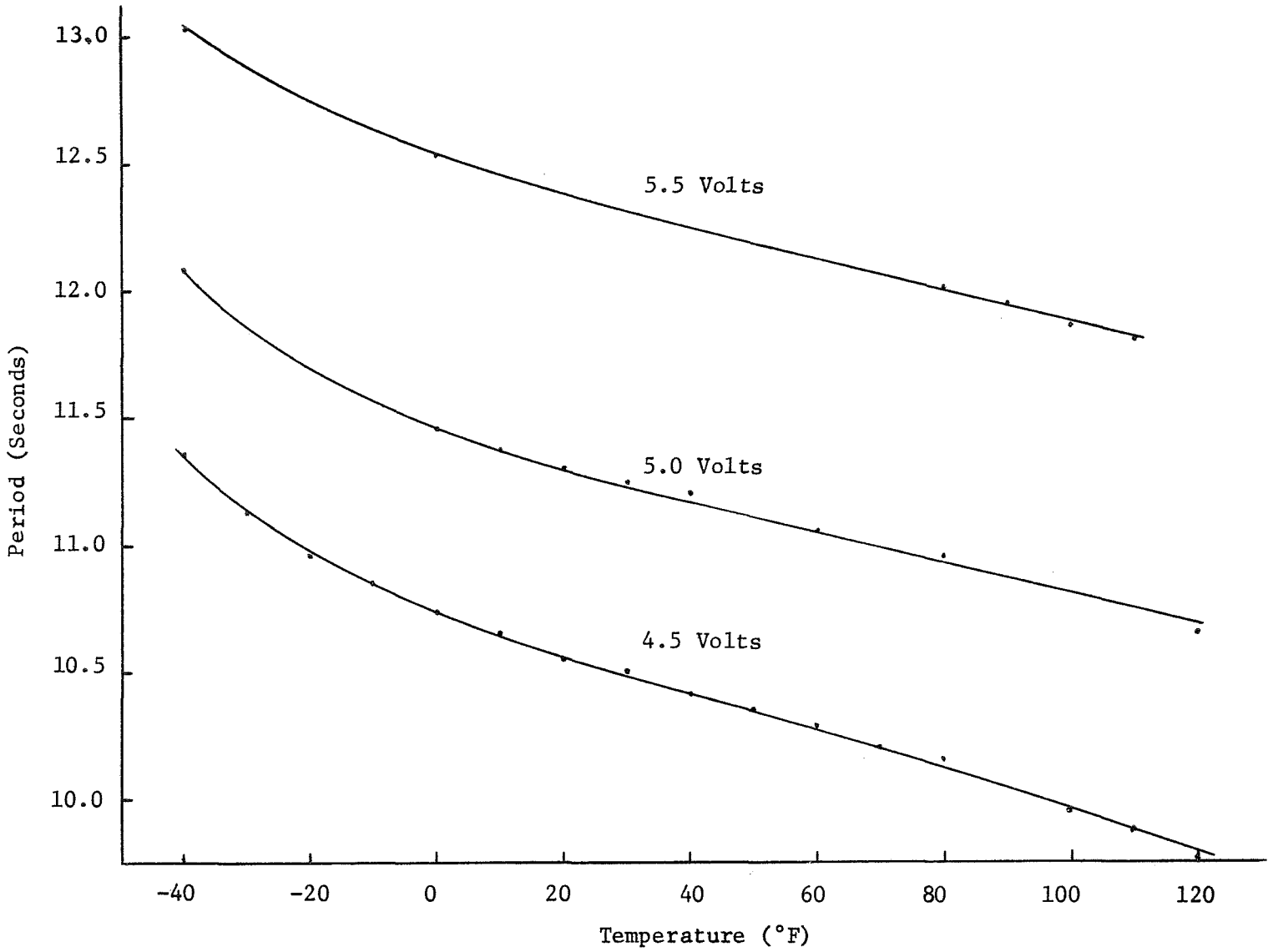

Figure 45. Period of the Low Frequency Clock

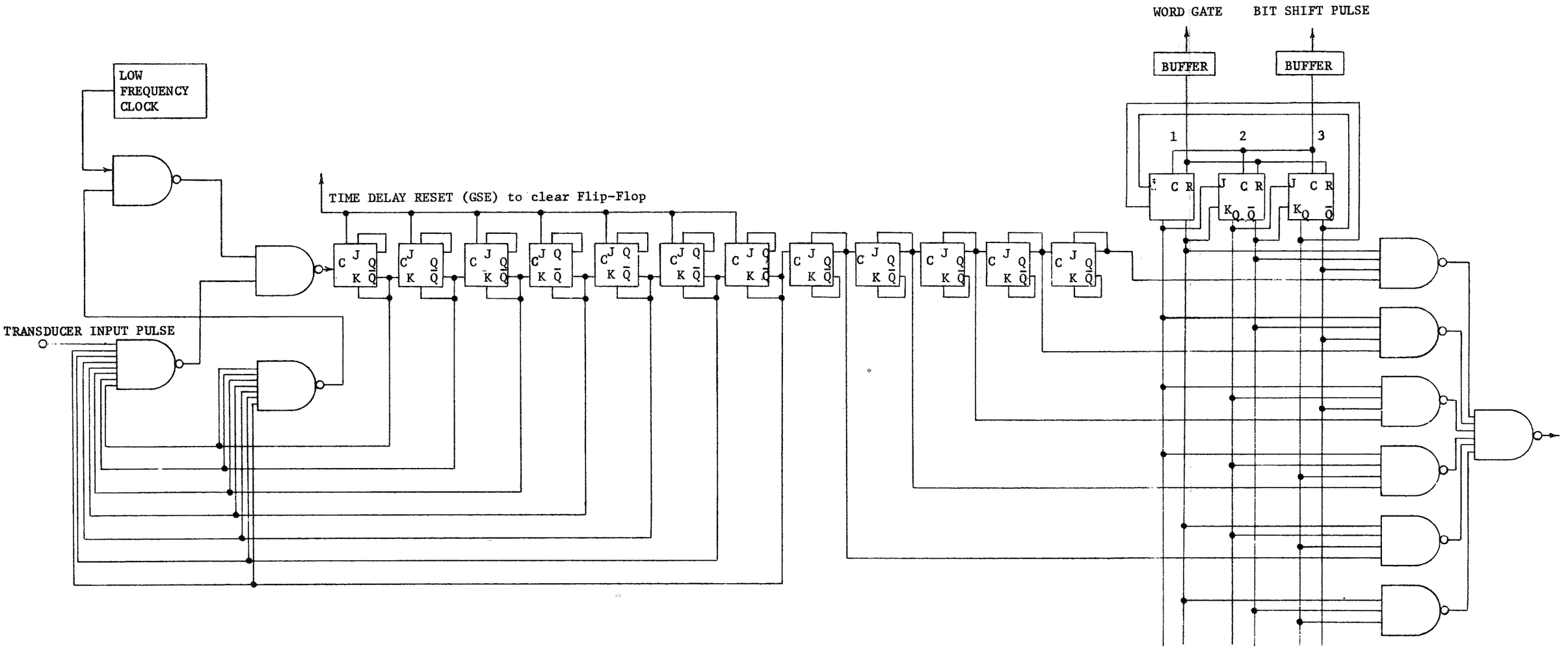

Fig. 46. The MEPF/G Counter System

with a junction FET controlling the charging rate of the 10 μF capacitor. This circuit was originally designed to operate from a 5 Vdc supply, and later operated from 10 Vdc to achieve a longer period. Tests run on the circuit at a nominal 5 V were not repeated with 10 V applied, but the clock was operated over the specified temperature extremes with the complete counter circuit. Figure 45 shows the clock period as a function of temperature with applied voltage as a parameter. This period was increased to approximately 20 seconds by increasing the applied voltage to 10 V and maintaining current through the FET or low as possible.

The Counter Circuit. - The counter circuit is shown in detail in Fig. 46. Each element is a compatible TTL integrated logic circuit interconnected to form the desired counters, shift registers and gates. The logic elements are TI 54L series units selected from the approved parts list. The parts list also included Signetic's SE 400 series of logic elements. A counter breadboard was also fabricated with the SE 400 series units, but these required more power than the TI 54L units.

A photograph of a breadboard model of the counter circuitry is shown in Fig. 47. Individual IC chips are located on printed circuit cards and connected to the breadboard chassis. The discrete component low frequency clock and interface circuitry are in evidence in the photograph. Front and back views of a second breadboard including a model of the power converter are shown in Fig. 48. This model was wired together after the IC chips were mounted on commercially available printed circuit cards. The power converter was reduced in size for the flight hardware models. The electronic circuit models shown in Figs. 47 and 48 were tested over the specified temperature range. Additionally, a breadboard model of the counter using the SE-400 series chips was fabricated and tested.

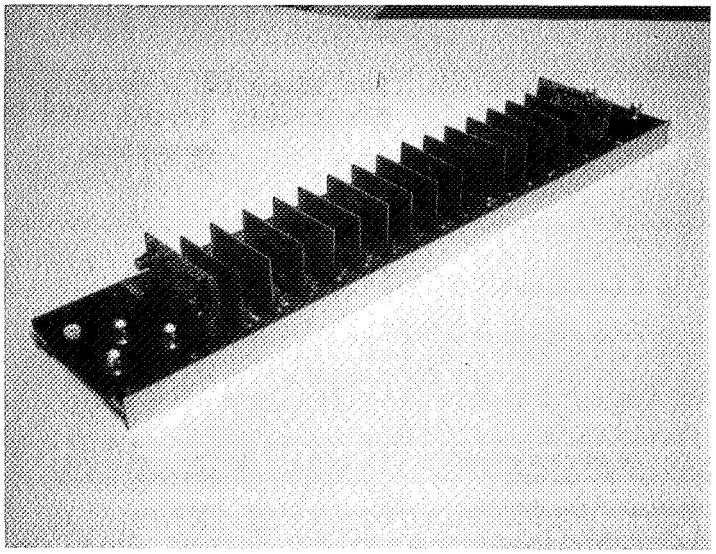

Figure 47. A Photograph of a Breadboard Model of the Electronic System

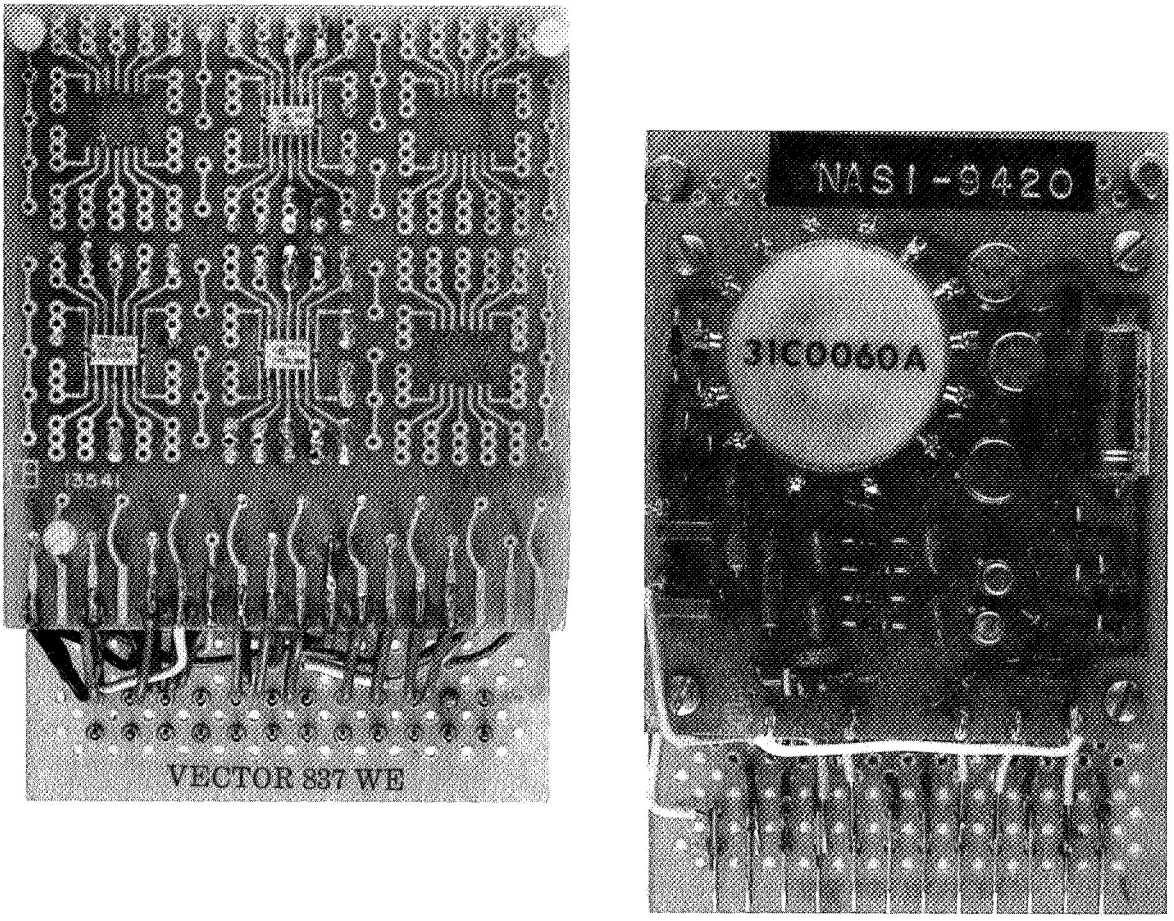

Figure 48. Two Views of a Model of the Electronic System with Power Converter

Power Converter. - The power converter was designed and fabricated by Wilmore Electronics Company, Inc. under an RTI subcontract. The original specifications are tabulated in Table IV. Other specifications were as required by Pioneer Specifications (ref. 2). These specifications were modified on at least two occasions. When helium was rejected as a pressurizing gas for the pressure cells, the high voltage output of the converter was specified to be 375 volts. This was a safe minimum value for neon which was being studied as a replacement for helium. When the argon-nitrogen mixture was selected as the pressurizing gas, it was necessary to again increase the high voltage output of the converter to 525 volts.

Initially, three power converters were fabricated. One of these was included in a breadboard model of the electronic system and is evident in Fig. 48. Two others were used in evaluation tests at LaRC. One of these was significantly reduced in size from the specifications in Table IV and became a prototype for five additional, flight-quality converters. Test results from one of the three original units are included in Tables V, VI and VII. Acceptance tests on the five flight units were run at Wilmore Electronics by Wilmore and LaRC personnel and delivered directly to LaRC.

Test Program

The electronic system breadboard models were cycled through numerous tests at room temperature and the specified temperature extremes of -20°F and +120°F. The facility used to test the electronic models is illustrated in Fig. 49. A pulse generator was used to simulate the input from the transducer circuitry. This same input was also supplied to the bit-shift input on the counter and used to trigger an oscilloscope display of the electronic system serial output. The oscilloscope sweep time was approximately 1/6 the repetition rate of the 222A pulse generator such that each bit of the event counter was multiplexed to display on each sweep of the oscilloscope. Consequently, the content of the event counter was continuously displayed on the oscilloscope. The pulse input to the transducer circuit input has a much higher repetition rate than does the low frequency clock input and was varied from 200 Hz to approximately 9 MHz with satisfactory results.

The facility provided for replacing the low frequency clock with a variable frequency input such that the counter could be cycled quickly for test purposes. The two parallel counters on the low frequency clock input resulted when an earlier discrepancy was traced to a counter on the low frequency input. On subsequent tests, these parallel counters were expected to agree and be compatible with the read-out of the MEPF/G counter. On rare occasions, these counters did not agree. Whenever this condition was observed, the counters were compared with the MEPF/G counter, and the EVEN-ODD status of the counters were compared with the state of the first flip-flop in the time delay counter. Agreement between one of the

Table IV

POWER CONVERTER SPECIFICATIONS

I. Input:

28 Vdc

± 1% Short term error

± 1% Long term drift (Superimposed)

II. Switch:

The converter shall provide for maintaining its own electrical load ON or OFF in accordance with a state signal which is to be supplied. The idling power drawn by the converter during the OFF state shall not exceed 5 mW. The state signal is described below:

A. ON signal -- 4 +1.4, -1.5 Vdc

B. OFF signal -- 0.25 ± 0.25 Vdc

C. Rise time -- 100μS max.

D. Fall time -- 10μS max.

E. Current to control unit shall be 100 μA max.

F. Current from control unit shall be 100 μA max.

G. Voltage supplied from converter to control-unit during off state--5V max.

III. Inrush Current:

When switched to a power bus of 28 Vdc with a source impedance no greater than 1 ohm resistive, the duration of instantaneous load current shall not exceed the following:

A. 250 mA for 5 μS.

B. 100 mA for 50 mS.

C. 110% of normal steady state current for 1 S.

IV. Electrical Outputs:

A. 5.0 Vdc; ± 10% Regulation; ± 2% Ripple P-P

300 mW max. load (converter to be designed such that more power drawn on the output, up to 1.0 watt input, will not damage the unit.)

B. 525 Vdc; ± Regulation; ± 2% Ripple P-P

125 mW max. load (to work continuously into 300 mW load without damage to converter. Able to withstand short circuit for 10 S.)

C. 10 Vdc; ± 10% Regulation; ± 2% Ripple P-P

25 mW load

V. Physical Characteristics:

High quality, printed circuitry construction. Subminature turret or bifurcated terminals for input, output and command signals. Circuit Size: 2 7/8" x 2 7/8" x 1/2" maximum. Weight: 0.4 lb. max.

VI. Temperature:

A. Survival while operating or non-operating, -40°±5°F to +120°±5°F.

B. Outputs voltage regulated to specifications, -20°F to +120°F.

Table V

POWER CONVERTER TEST
Temperature = +76°F Converter 1-W

INPUT		5 VOLT OUTPUT			10 VOLT OUTPUT			525 VOLT OUTPUT		
VOLTS	mA	VOLTS	LOAD	RIPPLE (mV)	VOLTS	LOAD	RIPPLE (mV)	VOLTS	LOAD	RIPPLE (Volts)
28	14.0	5.57	no	7.8	10.17	no	7.7	545	no	3.7
	31.8	4.90	full	26.0	10.06	full	20.0	502	full	8.4
	27.2	4.91	full	26.0	10.09	no	7.7	537	no	3.7
	28.2	4.89	full	26.0	9.96	full	15.	534	no	3.6
27.44	13.8	5.44	no	8.4	9.93	no	7.5	532	no	3.7
	30.9	4.78	full	26.0	9.83	full	22.0	490	full	7.7
	26.6	4.79	full	26.0	9.85	no	8.3	524	no	3.7
	26.8	4.78	full	26.0	9.74	full	14.0	523	no	3.7
28.56	14.2	5.67	no	7.8	10.36	no	7.6	555	no	3.7
	33.2	5.00	full	26.0	10.26	full	22.0	512	full	7.5
	27	5.01	full	26.0	10.28	no	8.4	547	no	3.7
	27.9	5.006	full	26.0	10.17	full	12.0	546	no	3.7

CONTROL SWITCH INPUT

"1" Input Threshold = 1.55 V

"0" Input Threshold = 1.63 V

Control Input ON Current = 89 μA

Coverter OFF Current = 73 μA

Table VI

POWER CONVERTER TEST
Temperature = +120°F Converter 1-W

INPUT		5 VOLT OUTPUT			10 VOLT OUTPUT			525 VOLT OUTPUT		
VOLTS	mA	VOLTS	LOAD	RIPPLE (mV)	VOLTS	LOAD	RIPPLE (mV)	VOLTS	LOAD	RIPPLE (Volts)
28	14.4	5.59	no	7.8	10.18	no	7.8	543	no	3.6V
	32.2	4.90	full	25	10.06	full	19.0	498	full	7.3
	27.2	4.92	full	21	10.10	no	7.1	535	no	3.6
	28.1	4.91	full		9.98	full	11.0	533	no	3.6
27.44	14.3	5.49	no		9.97	no		531	no	
	31.7	4.79	full		9.85	full		487	full	
	26.4	4.81	full		9.89	no		524	no	
	27.3	4.80	full		9.77	full		522	no	
28.56	15.2	5.72	no		10.40	no		555	no	
	33.1	5.00	full		10.26	full		508	full	
	27.9	5.03	full		10.32	no		547	no	
	28.8	5.02	full		10.20	full		547	no	

Table VII

POWER CONVERTER TEST
Temperature = -20°F Converter 1-W

INPUT		5 VOLT OUTPUT			10 VOLT OUTPUT			525 VOLT OUTPUT		
VOLTS	mA	VOLTS	LOAD	RIPPLE (mV)	VOLTS	LOAD	RIPPLE (mV)	VOLTS	LOAD	RIPPLE (Volts)
28	11.4	5.37	no	3.8	10.02	no	7.9	541	no	3.5
	28.3	4.80	full	41	9.88	full	35	485	full	6.0
	23.2	4.82	full	32	9.94	no	41	534	no	3.5
	24.2	4.82	full	31	9.85	full	15	532	no	3.5
27.44	11.1	5.24	no		9.80	no		530	no	
	27.7	4.69	full		9.67	full		473	full	
	22.8	4.71	full		9.72	no		522	no	
	23.8	4.71	full		9.64	full		521	no	
28.56	11.7	5.48	no		10.23	no		553	no	
	29.1	4.92	full		10.10	full		496	full	
	24.0	4.94	full		10.15	no		495	no	
	24.9	4.93	full		10.06	full		494	no	
For temp. = -40°F										
28	28	4.79	full		9.87	full		487	full	

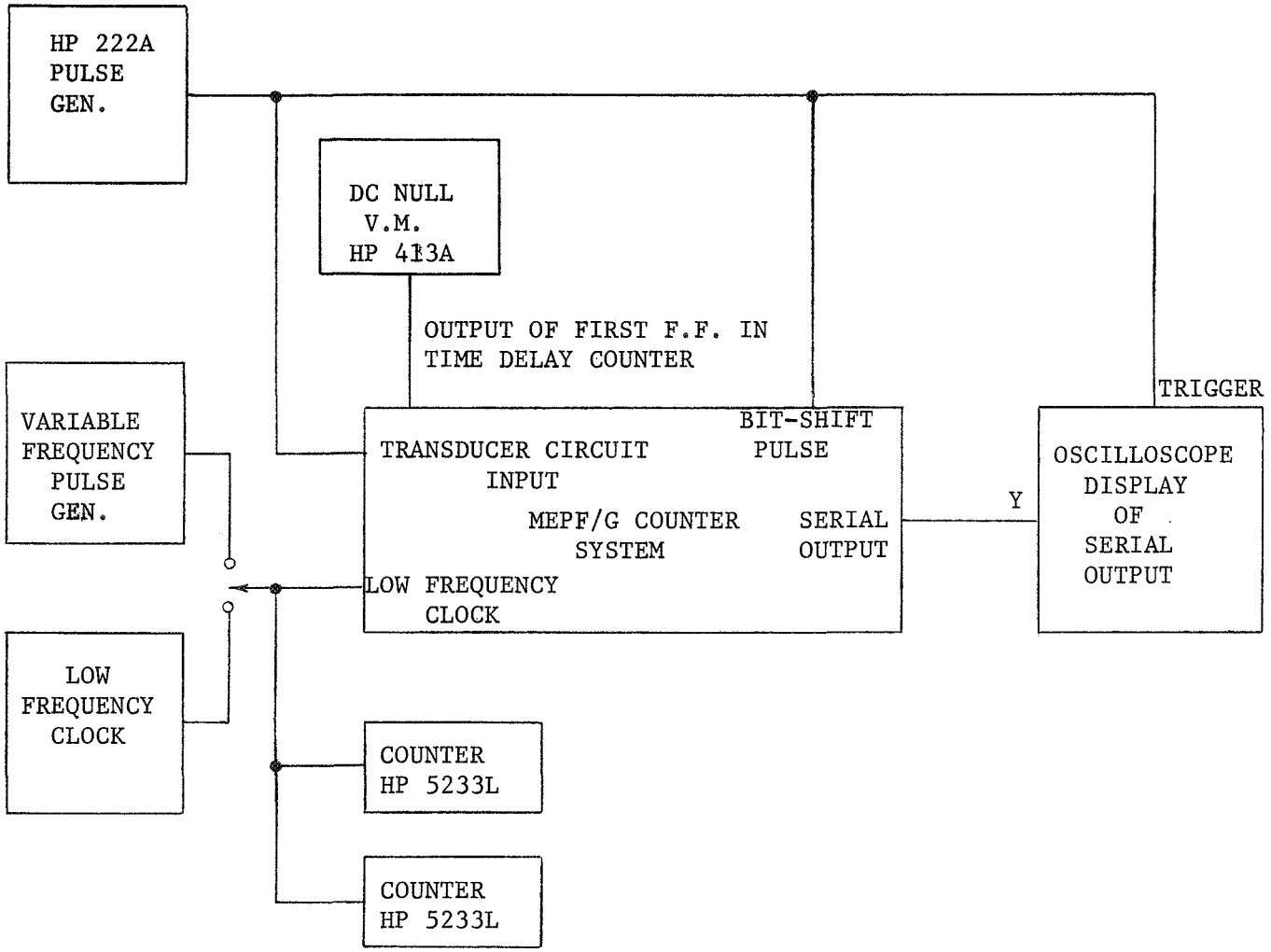

Figure 49. A Test Facility for the MEPF/G Electronic System

two counters and the status of the MEPF/G system was considered a successful test.

The test facility functions as follows. The MEPF/G counter and the low frequency clock counters are set to zero and the transducer circuit input pulse applied during the OFF period of the low frequency clock. Setting the MEPF/G counter system including the 7-bit time delay counter to zero causes the input from the transducer circuitry to be inhibited and the input from the low frequency clock to be enabled. Consequently, the MEPF/G event counter will remain at zero and the low frequency clock will continue to advance the time delay counter. After 127 pulses from the low frequency clock, i.e., $2^7 - 1$ pulses, the time delay counter will return to a null state. Immediately, the first high frequency pulse at the transducer circuit input will advance the MEPF/G counter from the null state and again reject any additional inputs until the low frequency clock again returns the counter to its null state. Consequently, the MEPF/G event counter will advance one count each time the low frequency clock advances 127 counts. (The 7-bit, time delay counter recycles every $2^7 = 128$ counts. In the MEPF/G system, however, the first advance in each cycle is due to either the reset operation or a pulse at the transducer circuit input on subsequent cycles.)

To monitor the test of the MEPF/G electronics, it was necessary to occasionally compare the content of the MEPF/G event counter with the counter monitoring the low frequency clock input. The event counter should read one count for each 127 counts on the low frequency clock counter. Frequently, the MEPF/G counter was monitored as the low frequency clock reached an exact multiple of 127. With a 43 second period low frequency clock, the MEPF/G counter advances every 91 minutes (127 x 43 seconds) and recycles to zero every 48.5 hours (32 x 91 minutes). Numerous error free cycles were observed.

Figure 49 shows a voltmeter monitoring the status of the first flip-flop in the time delay counter. This was simply an additional aid in monitoring the agreement between the MEPF/G counter and the low frequency clock counters. With an even number in the MEPF/G counter event counter, the flip flop (FF-1) reads low or "0" during even counts on the low frequency clock. With an odd number in the event counter, FF-1 reads low or "0" during odd counts on the low frequency clock.

During tests on the electronic system, current to the power converter and current to the 5V load were continuously monitored. The 54L counter nominally drew 16.5 mA from the 5 volt line (83 mW) and the converter drew approximately 22 mA from the 28 V source (616 mW). An earlier breadboard of the counter using the SE400 chips required approximately 120 mW.

Table VIII illustrates observations made during a single cycle of the electronic system. Some of the observations recorded, i.e., currents

and temperatures, are not included in the table. The 6th bit in the read-out is a counter identification bit and was not from the 5-bit, 32 count, recycling event counter.

Table VIII

RECORD OF A COUNTER SYSTEM TEST

Counter Model II, With Converter
Bit Display - 32/16/8/4/2/1

DATE	TIME	LOW COUNTER	MEPF/G	FF-1	REMARKS
1/24/70	9:00 P	0	000000	Lo-Even	Reset-Begin
1/25/70	1:10 P	2503	010011	Lo-Odd	Count 19, Correct
"	1:25 P	2540	010100	Lo-Even	Count 20, Observed Switch
"	10:20 P	3922	011110	Lo-Even	Count 30, Correct
"	10:25 P	3937	011111	Lo-Odd	Count 31, Correct
"	11:15 P	4064	000000	Lo-Even	Observed Correct Switch

SECTION IV

CONCLUSIONS AND RECOMMENDATIONS

The investigations described in this report were conducted in support of the Meteoroid Experiment For Pioneer F/G (MEPF/G). The initial objectives were to characterize the transducer selected for the MEPF/G experiment and design compatible electronics for interfacing with the Pioneer Spacecraft. The transducer proved to be unreliable and the cause and cure of the unreliability became the primary objective. These investigations included different pressurizing gases, altered transducer electrode geometries and materials, the use of initial ionization sources and fabricating procedures. A pressure cell/transducer evolved that utilized the original electrode assembly, electroplated Ni^{63} as an initial source of ionization, and a 75% argon/25% nitrogen gas mixture as a pressurizing gas.

The pressure cell/transducer that evolved from these investigations is suitable for the MEPF/G experiment. Its Paschen characteristics are such that a pressurized cell will not indicate at any expected temperature or power supply voltage, and it will indicate whenever a cell is penetrated and the pressure decreases. There is considerable uncertainty in the locus of the Paschen characteristics of the MEPF/G pressure cells, but the mechanism of a cell indicating or firing is a statistical process and these uncertainties are to be expected. However, the pressure cell/transducer system has an adequate safety margin to assure reliable operation.

The excitation voltage and initial pressure requirements of the MEPF/G pressure cell are moderate and pose no difficult problems for the electronics or the pressure cell fabrication. The Ni^{63} electroplated on the electrodes of the transducers is not hazardous to personnel. Additionally, it is easy to electroplate on the electrodes using standard electroplating procedures, and the amount plated on each electrode is easily controlled. The basic transducer structure is an off-the-shelf component, readily available in large quantitites. This basic structure was originally selected in order to comply with the limited weight allotted to this experiment.

The MEPF/G pressurizing gas was selected after considering several gases and gas mixtures. The two gases, argon and nitrogen, are inert and compatible with each other in that they are not Penning-type mixtures. The gas pressure is low such that the pressure cells will not rupture at the high temperature extreme, and neither gas will condense out at the low temperature extreme. Additionally, the Paschen characteristics of this mixture are suitable for the MEPF/G application.

The electronic system for the MEPF/G was designed and fabricated at LaRC. Early in this program, a similar electronic system was designed and breadboarded at RTI. Some basic characteristics of both designs are as follows: (1) The transducer circuitry does not allow a transducer to continue to glow after it fires. In order to limit the power required by the experiment to less than one watt, a high impedance is seriesed with the paralleled transducer groups to limit current flow. Consequently, the transducer in a leaking cell will "oscillate" as long as the pressure and temperature are within compatible limits. (2) Once a transducer fires, the electronic system ignores any additional transducer firings for a period of time to allow pressure in the penetrated cell to reduce to a low value. The OFF time of the system is a compromise between a short period that would allow a single, leaking cell to be counted twice and a long period that may miss a second event that occurs shortly after an initial event. (3) The content of the event counter is serialized and multiplexed to the spacecraft upon command.

It is concluded that the MEPF/G experiment will adequately perform the function for which it was designed. It is compatible with the Pioneer Spacecraft's specifications and limitations. It will continuously monitor the 216 pressure cells and register a single count in the event counter whenever the pressure in a cell decreases to a significantly lower value and read out to the spacecraft upon command. As the event counter advances it will recycle to 0 and begin anew at the 32^{nd} count.

These investigations were conducted with a sense of urgency. They were conducted in constant support of the MEPF/G experiment and were frequently responding to difficulties that conceivably could abort the experiment. Consequently, many interesting and fruitful areas for investigation were left incomplete in order to seek solutions to more pressing problems. It is recommended that consideration be given to additional investigations into some of these areas.

One of the factors that significantly influences the Paschen characteristics of the MEPF/G transducer and is extremely difficult to control is its past history. The firing voltages and, prior to the use of a source for initial ionization, the probability of a firing changes significantly with time. This "transient" appears to continue for a period as long as several days. It is improbable that it will influence the MEPF/G experiment, but it should be investigated further. An investigation of this transient would be a simple, logical extension of an experiment to monitor the long-term performance of the MEPF/G transducers. A program to study the long-term characteristics of the MEPF/G system is especially recommended.

One mechanism likely to contribute to the influence of past history is changes in the electrode surface with each firing. This mechanism would be extremely difficult to control; however, its influence could

possibly be reduced by using electrodes with highly polished surfaces. Polished electrodes were used in these investigations, but properties of the neon gas in use at that time dominated the transducers characteristics.

The quantity of Ni^{63} on the MEPF/G electrodes was selected so as not to exceed a total of 1 mCi with the maximum number of transducers that would likely be required by the experiment. This amount proved to be adequate and there was no need for further consideration. It is advisable to determine the minimum quantity of Ni^{63} needed to assure reliable operation, however. A program to determine definitive reliability numbers as a function of the quantity of Ni^{63} used would be prohibitive in terms of the number of samples and the quantity of data required. However, if it can be demonstrated that one tenth of the amount currently in use is nominally adequate, for example, one could be confident that an adequate amount is in use. Additionally, this investigation could be of significance to similar future experiments.

LIST OF REFERENCES

1. Kenneth F. Weaver, Voyage to the Planets, National Geographic, Vol. 138, No. 2, August 1970, pp 147-195, National Geographic Society, Washington, D. C.

2. Pioneer F/G Project Specifications (PC-200, PC-213.00-03, PR-200, PS-201, PS-220), NASA, Ames Research Center, Moffett Field, California, April 10, 1969.

3. Cold Cathode Discharge Tubes, J. R. Acton and J. O. Swift, 1963, Academic Press, Inc., N. Y.

4. Fields and Waves in Modern Radio, 2nd Ed. Simon Ramo and John Whinnery, John Wiley & Sons, Inc., N. Y.

5. Gaseous Conductors, Theory and Engineering Applications, 1st Ed. James D. Cobine, McGraw-Hill Book Company, N. Y., 1941.

6. Reference Data for Radio Engineers, 4th Ed. H. P. Westman, Editor. International Telephone and Telegraph Corporation, 1956.

7. D. S. Wollan et al, Gas Density Detector For Use In Space, NASA CR-66834, Physics Department, Virginia Polytechnic Institute, Blacksburg, Virginia 24061, October 1969.

APPENDIX A

PROCEDURE FOR CLEANING, PLATING WITH NI^{63}, COUNTING AND HANDLING THE MEPF/G TIN-PLATED, KOVAR PRESSURE TRANSDUCERS

APPENDIX A

PROCEDURE FOR CLEANING, PLATING WITH NI^{63}, COUNTING AND HANDLING THE MEPF/G TIN-PLATED, KOVAR PRESSURE TRANSDUCERS

PROCEDURE

The following procedure is applied to lots of fifth (50) transducers to allow cleaning and plating in a continuous operation, i.e., storage time between cleaning and plating will be held to a minimum. Following plating, these units will be counted for radioactivity, packaged and labeled individually. All chemicals used for this procedure are "Ultra pure" reagents, and materials that contact the switches, e.g., carrier baskets and tweezers, are stainless steel and are precleaned using Procedure I below:

I. Precleaning to remove Soils and Grease (ref. A-1).

Select a lot of fifty (50) from the prescreened switches. Ascertain that the electrodes are straight and parallel, and remove any bulk debris by wiping with a disposable tissue. Load the lot of 50 in a carrier basket. The 50 units remain in the carrier basket throughout the precleaning process.

(A) Immerse in a boiling trichloroethylene (TCE) bath for 15 minutes.

(B) Immerse in a cold TCE bath for 5 minutes.

(C) Vapor degrease in TCE. (Headway Research Laboratory Vapor Cleaner Model MV 4000).

(D) Rinse in Methanol (Bath 1).

(E) Rinse in Methanol (Bath 2).

(F) Clean in an ultrasonic bath using Methanol.

(G) Rinse in Methanol (Bath 3).

(H) Store in Methanol (Bath 4).

(It is anticipated that storage (Step H) will be held to a minimum and plating will begin immediately).

Figure A-1 shows a precleaning operation in progress. The 50 units are located in the carrier basket on the hot plate (Step A). The ultrasonic bath is not shown in Fig. A-1.

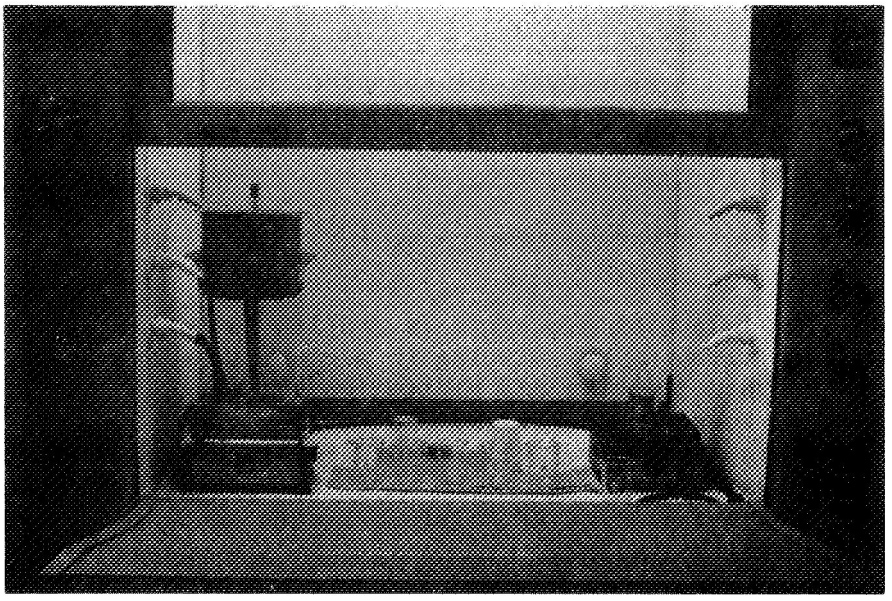

Figure A-1. The Precleaning Process

II. Plating

(A) Remove individual units from the Methanol bath, rinse in distilled deionized water and air dry.

(B) Dip electrodes (only) in 10% (V/V) HCl for approximately 15 seconds. (This step, illustrated in Fig. A-2, activates the surface for plating and is used in preference to an Alkaline cleaning step which is incompatible with tin or an electrolytic cleaning step which is not documented as compatible with tin, ref. A-11).

(C) Rinse each unit in Methanol (Bath 5).

(D) Rinse each unit in distilled, deionized water.

(E) Air dry each unit and place in the plating apparatus.

(Figure A-3 shows the transducer in the holder and posed above the plating bath. Additional details of the plating apparatus are illustrated in Fig. A-4, and the associated instrumentation is shown in Fig. A-5.)

(F) Plate each unit at approximately 0.3 mA until cut-off occurs. (Total plating charge will be determined by the circuit Fig. A-6. The plating circuit is illustrated schematically in Fig. A-7. Referring to Fig. A-6, the high-gain amplifier (μA741) saturates and

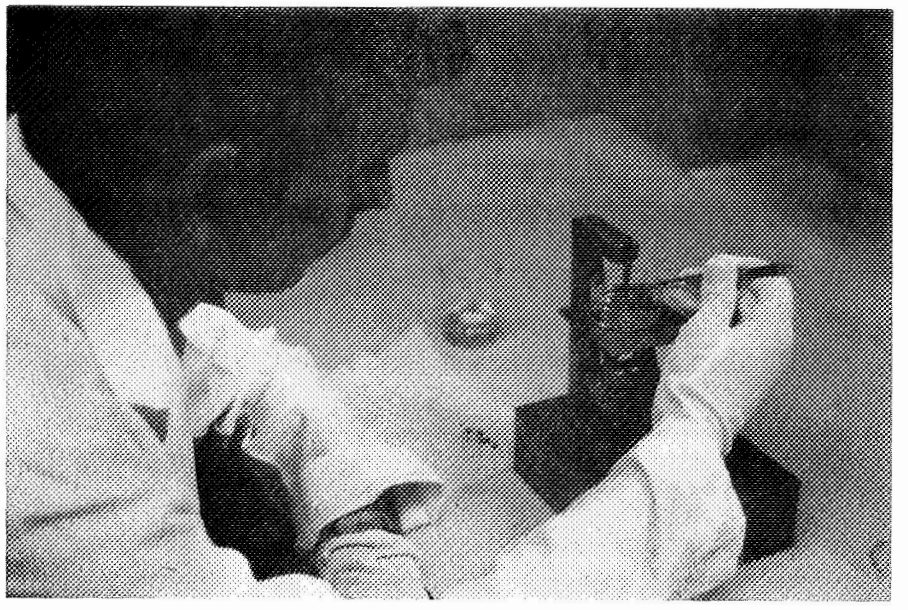

Figure A-2. The Electrode Activation Step Using Hcl

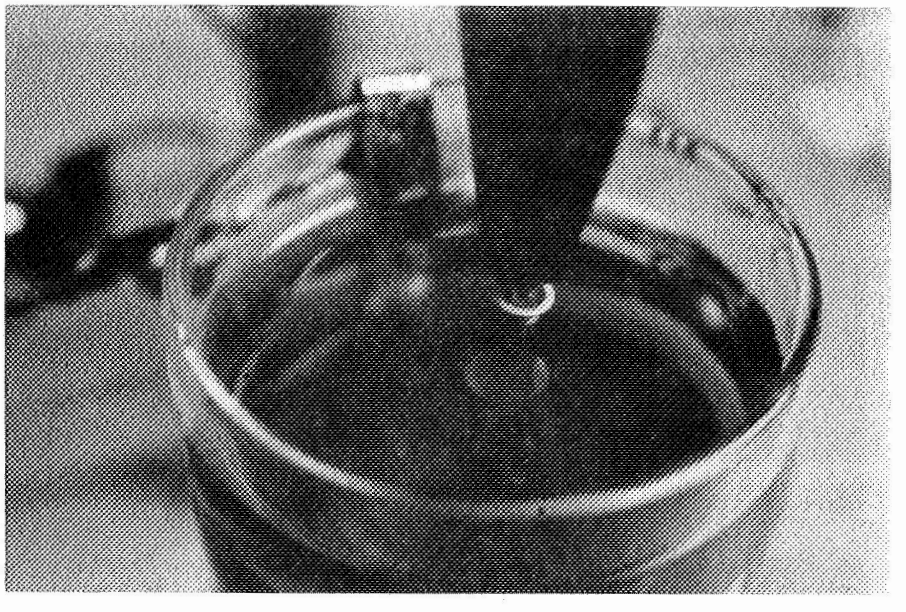

Figure A-3. A Transducer Entering the Plating Bath

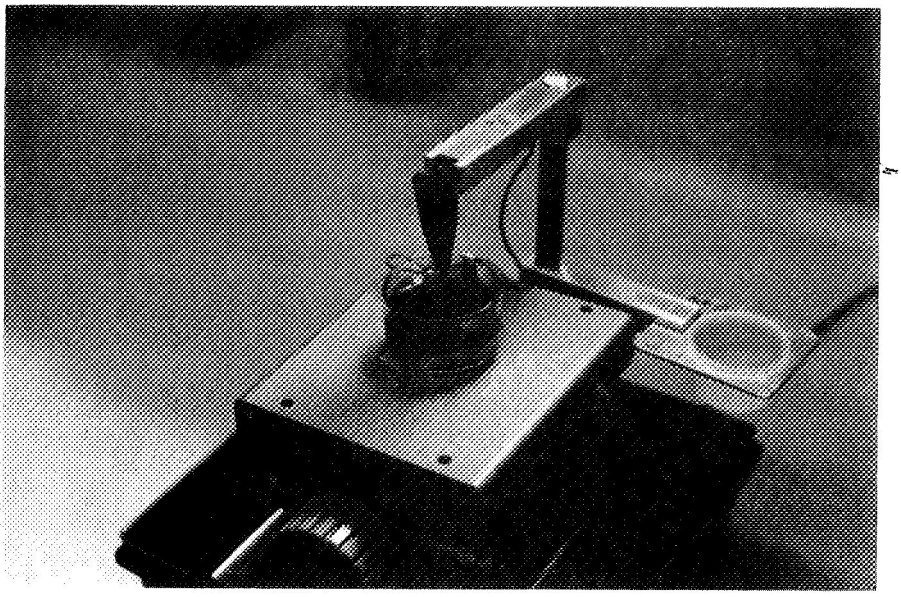

Figure A-4. A Photograph of the Plating Apparatus

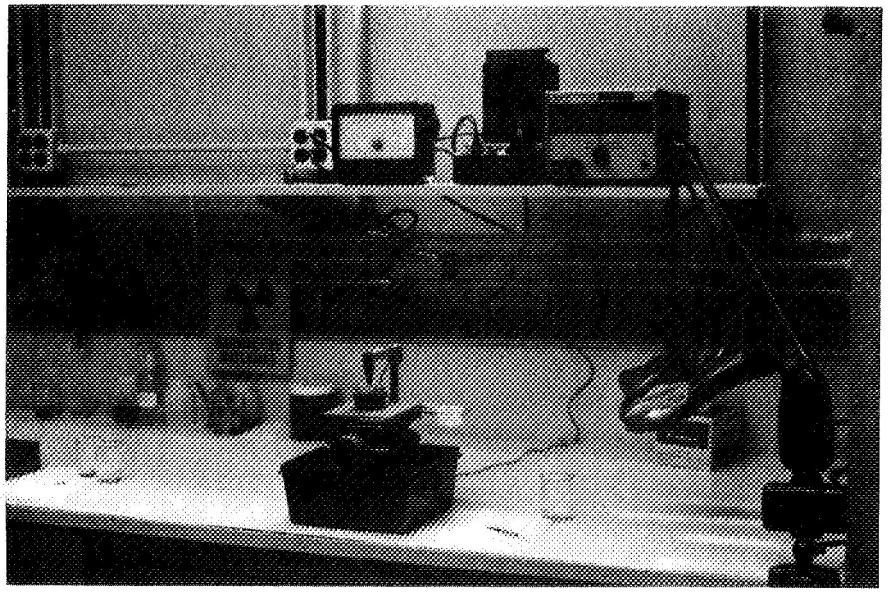

Figure A-5. The Plating Apparatus with Associated Instrumentation

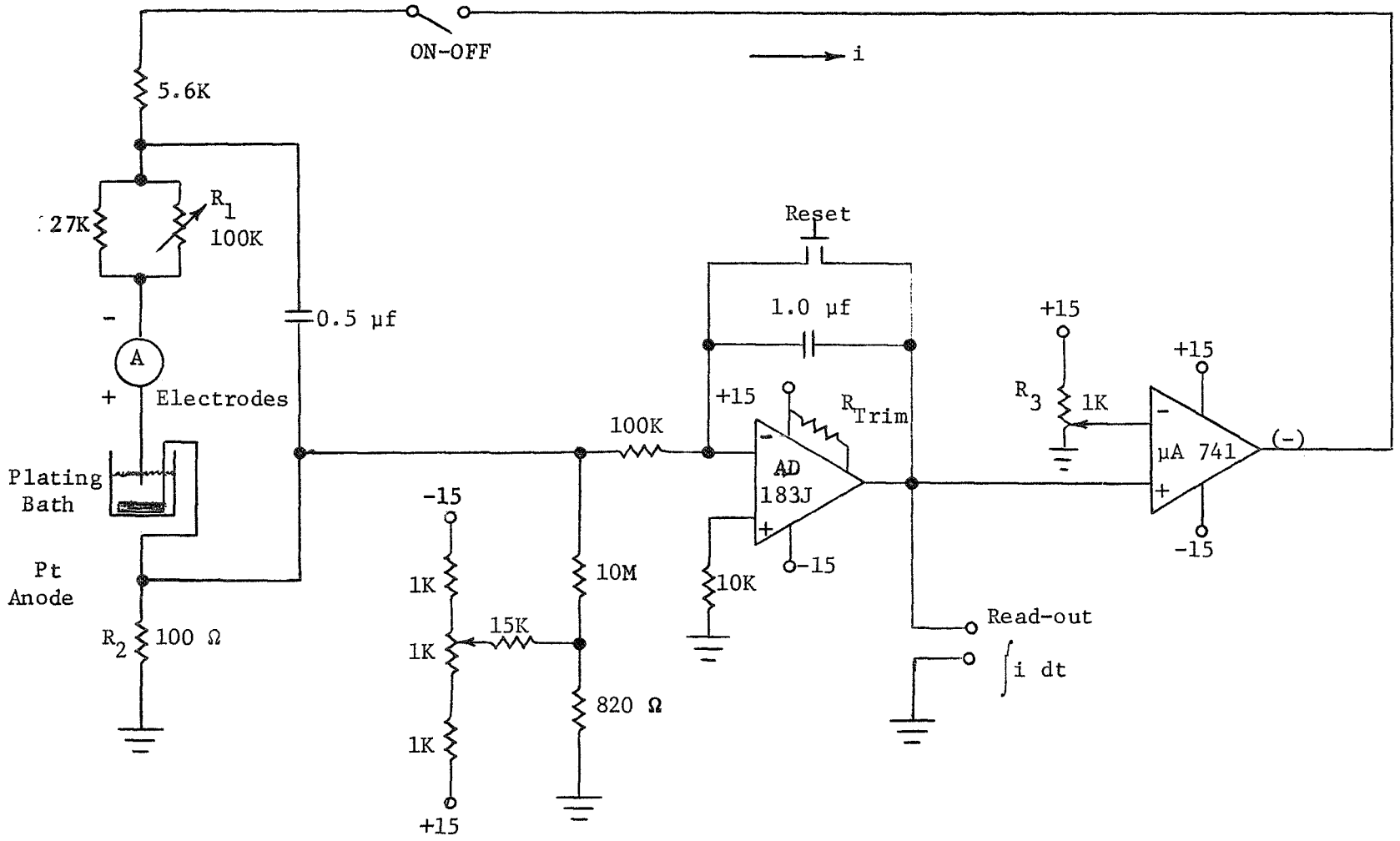

Figure A-6. Circuit to Control i and $\int i\,dt$ in Plating Bath

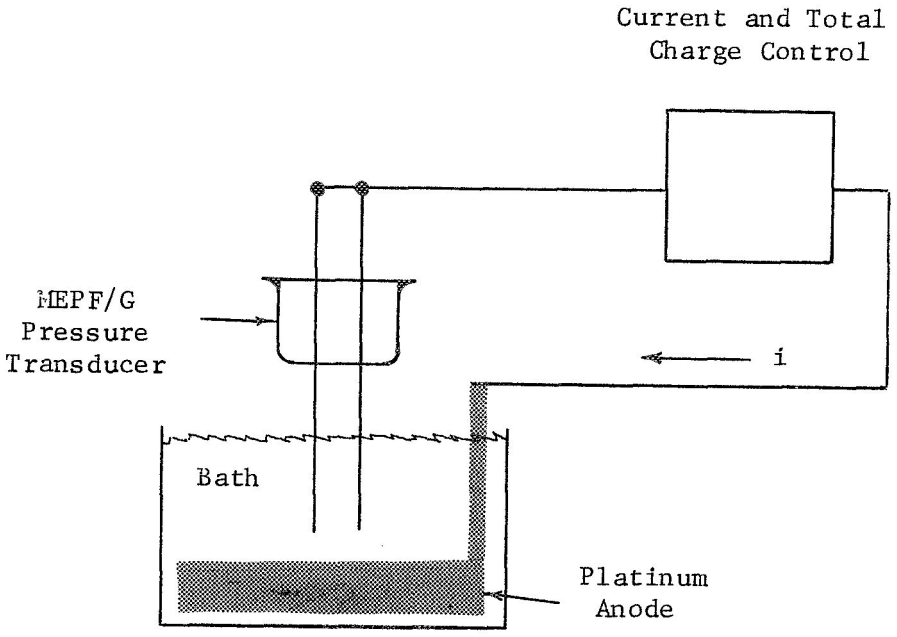

Figure A-7. Schematic of Nickel Plating Apparatus

supplies a relatively constant current to the plating circuit. The current in the plating bath is controlled by adjusting R_1. The total charge that flows in the plating circuit, $\int i\,dt$, is proportional to the Ni^{63} deposited on the transducer electrodes. The integrator (AD183J) integrates the current in the bath, i.e., the voltage across R_2, and causes the voltage source (μA741) to zero at a value determined by R_3. With adjustments such that i = 0.3 mA, and $\int i\,dt$ = 2.0 volts when the voltage supply (and current) zeros, the Ni^{63} distribution illustrated in Fig. A-8 was obtained.

The plating bath is as follows (ref. A-2).

$NiSO_4$ 6 H_2O	12	gms.
H_3BO_3	1.5	gms.
NH_4Cl	1.5	gms.
H_2O_2	5	μℓ

Dissolve these reagents in 100 ml of distilled, deionized water. Add 3 mCi of carrier-free Ni^{63} (Oak Ridge National Laboratory). Operate bath at room temperature, pH of 5 to 5.5 and a current density of 5 to 10 A/ft^2. (0.3 mA per unit)

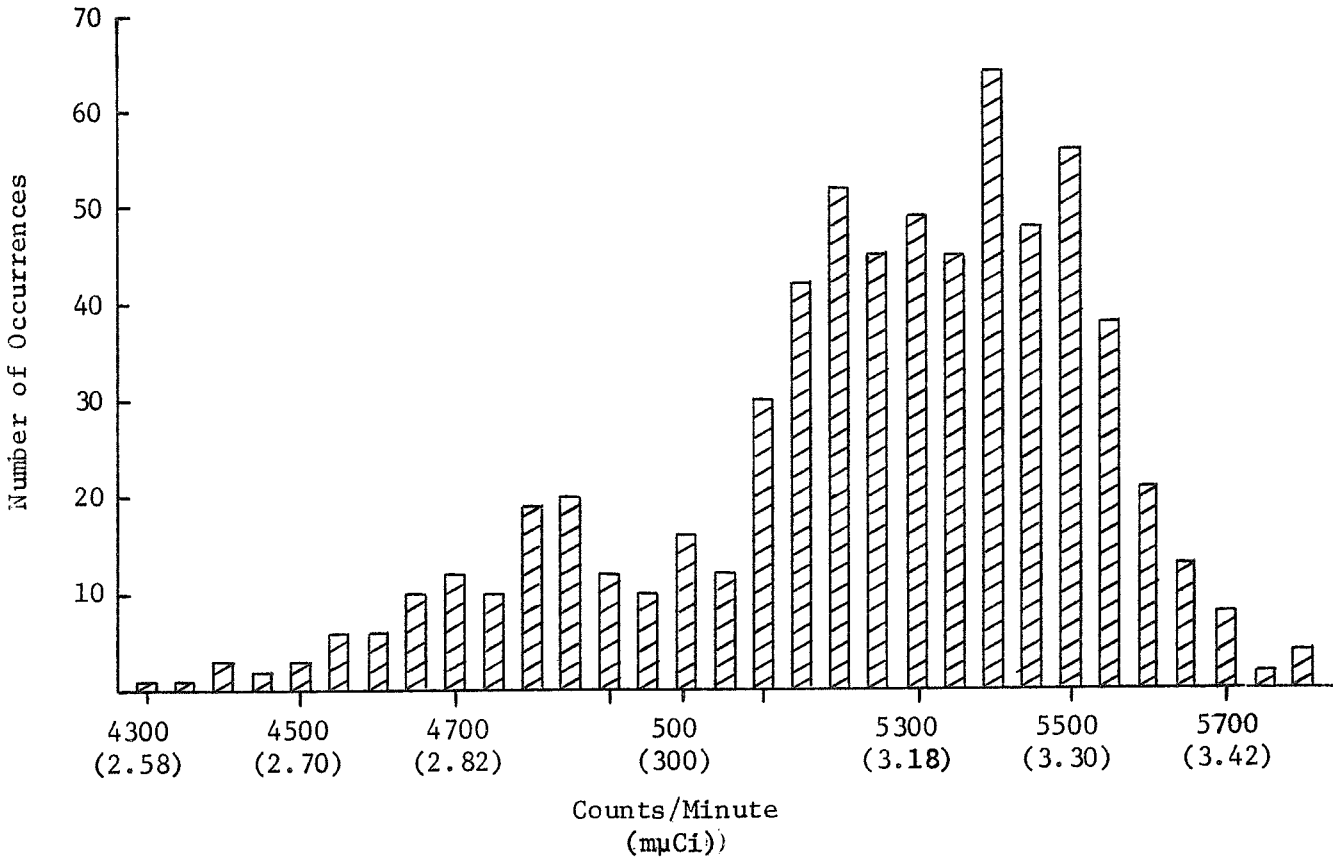

Figure A-8. Distribution of Ni^{63} Activity

(G) Rinse in Methanol (Bath 6).

(H) Rinse in Methanol (Bath 7) and air dry.

III. Counting

(A) After plating is completed, mount each unit in the carrier-planchet. Use precleaned, stainless steel tweezers to grip the outer ring of the transducer.

(B) Stack the planchets in the automatic planchet system. (The planchets are especially prepared, stainelss steel with a stainless steel holder spot welded into the bottom. The carrier/planchet is illustrated in Fig. A-9 with and without a transducer. Figure A-10 shows the carrier-planchet stacked in a columnator that is a part of the counting system. No further manual operations are necessary until counting is completed.)

(C) Operate the counting system to determine a 10-minute count on each transducer. (The counting system is a Nuclear-Chicago Corporation Model 4330 Automatic Planchet System. It consists of a Model 970 Beta detector, a model 1150 Automatic Planchet Changer and a 8703 decade scaler. In the counter, each unit is exposed to P-10 gas in a Model 480 proportional detector operated windowless.

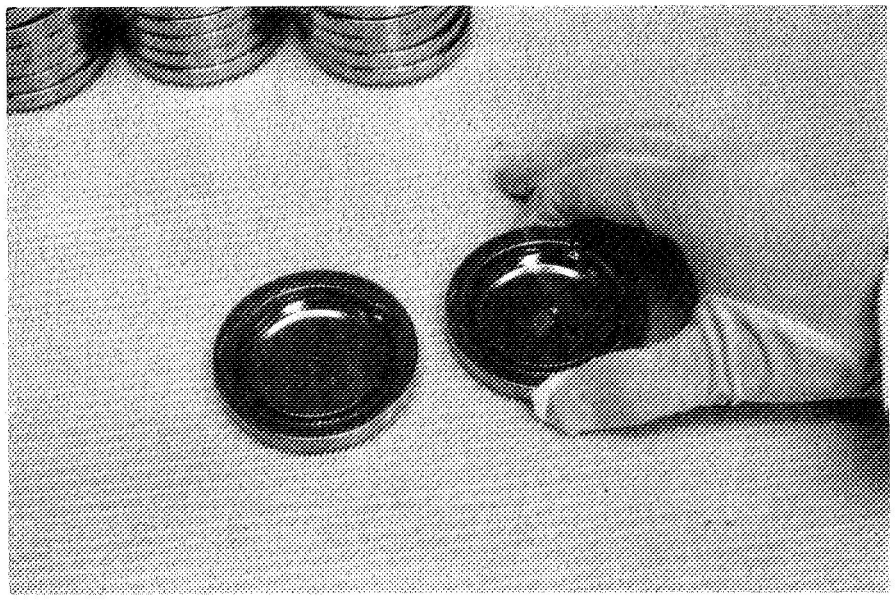

Figure A-9. Carrier-Planchets With and Without a Transducer

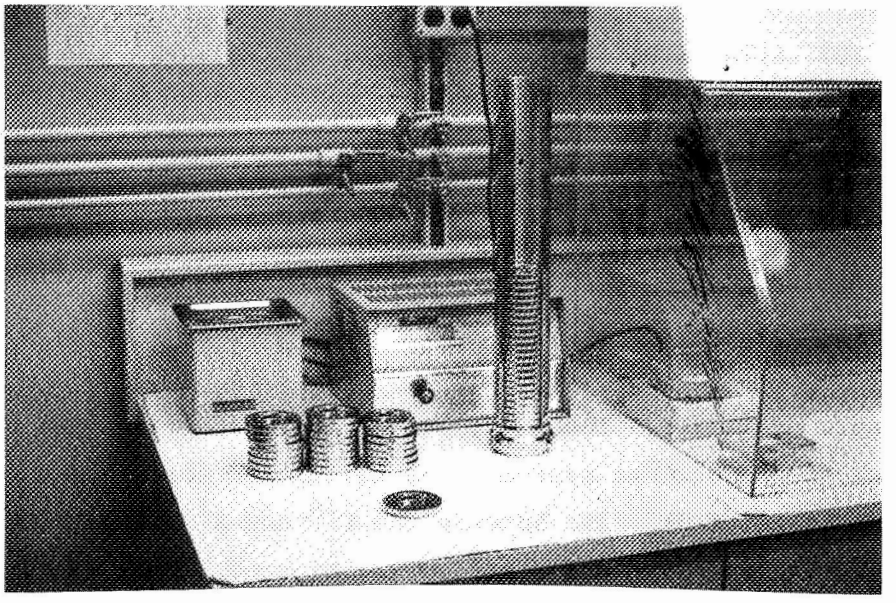

Figure A-10. Carrier-Planchets Stacked in Columnator for Automatic Counting

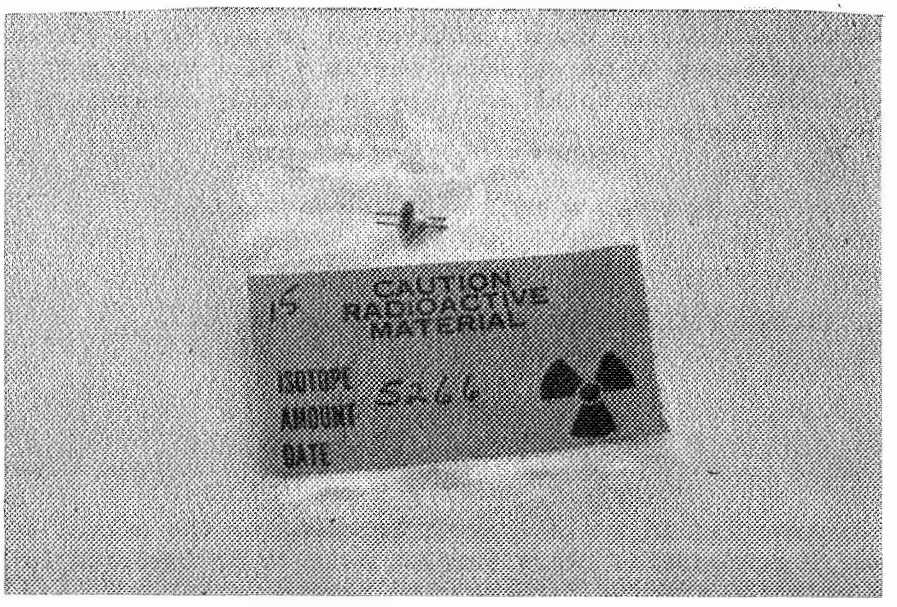

Figure A-11. A Completed and Packaged Transducer.

(D) After counting is completed, unload each transducer from its carrier-planchet directly into a polyethylene bag and seal. Each bag is to be marked with the counter readout in counts per minute. (A completed and sealed transducer is shown in Fig. A-11.)

Counter Calibration

The counting system was calibrated with a Beckman liquid scintillation system for which calibrated carbon-14 (C^{14}) and hydrogen-3 (H^3) samples were available. These calibrated standards permitted the efficiency of the Beckman system to be calculated for C^{14} and H^3. Since the 67 keV betas of Ni^{63} lie between the C^{14} and H^3 betas, the efficiency of the Beckman system for Ni^{63} was estimated. Transducers analyzed with the Beckman scintillation system were also counted with the windowless Nuclear-Chicago system to determine its efficiency. Additionally, a calibrated C^{14} planchet standard was counted in both systems to provide a secondary check on the calibration and to serve as a secondary standard for future counting. The efficiency of the Nuclear-Chicago system was estimated from these calibration counts to be 75% and this estimate is concluded to be accurate within $\pm$ 5%. Knowing the efficiency of the counter, the total activity is readily determined from the definition of a curie (Ci).

$$\begin{aligned} \text{Ci} &\equiv 3.7 \times 10^{10} \text{ disintegrations/sec} \\ &= 2.22 \times 10^{8} \text{ disintegrations/min} \end{aligned}$$

Therefore, if the efficiency of a counter is 75%,

$$C_i = \frac{\text{counts/minute}}{2.22 \times 10^{8} \times .75} .$$

The Beckman liquid system cannot be used for the actual counting of the MEPF/G transducers since samples have to be immersed in a scintillation solution that is difficult to remove.

The Ni^{63} plated on each transducer is such that if every transducer had the maximum amount permissible under worse-case considerations, the total Ni^{63} used in the experiment would be less than 1 μCi.

Ni^{63} Data

Basic:

Half life (T 1/2) = 92 years
Decay Energy (E_β) = 67 keV
Daughter = Cu^{63} (Stable)
Range = 6 mg/cm^2
≈ 5 cm in air
≈ ½ mil in Copper

Maximum permissible body burden for soluble Ni^{63}:

(No physiological effects observable)

Bone = 200 μCi
Total body = 900 μCi
Liver = 10^3 μCi
(No data on insoluble Ni^{63})

AEC Regulations:

(1) Exempt quality for a sealed source = 10 μCi

(2) Exempt quantity for spark gap and electronic tubes is 5 μCi per tube, 10 tubes per person.

The C^{14} planchet standard is identified as follows (ref. A-3):

Model No. - Baird Atomic - No. CTD 14B
Serial No. - 14 B 41
Nuclide - C^{14}
Halflife - 5,568 yr
Principal Radiation - 155 keV β
Date of Standardization - January 3, 1966
Microcurie Content - 0.176 μCi

APPENDIX A

LIST OF REFERENCES

A-1. Recommended Practice for Cleaning Metals Prior to Electroplating, ASTM Designation B-322-68, ASTM Committee B-8, ASTM Standards, Part 7, March 1969.

A-2. Nickel Plating, Metals Handbook, 8th Edition, Vol. 2, American Society for Metals, Metals Park, Ohio, 1964.

A-3. Barid Atomic, Inc., 33 University Road, Cambridge, Mass. 02138.

APPENDIX B

RADIOLOGICAL HEALTH CONSIDERATIONS FOR NI^{63} TRANSDUCERS

Conrad M. Knight
Health Physicist
Radiological Safety Officer
Duke University

J. J. Wortman
Senior Scientist
Research Triangle Institute

APPENDIX B

RADIOLOGICAL HEALTH CONSIDERATIONS FOR NI^{63} TRANSDUCERS

I. Regulatory Aspects:

A. Radioactive Materials Licensing (refs. B-1, B-2): "A general license is hereby issued to transfer, receive, acquire, own, possess, use and import the quantities of byproduct material listed in paragraph 31.100, Schedule A, provided that no person shall at any one time possess or use, pursuant to the general licensing provisions of this section, more than a total of ten such scheduled quantities." Column I of Schedule A (Not as a Sealed Source), reflects a possession of 1 μCi for Ni^{63}. However, as stated above, a total of 10 such quantities may be obtained; therefore a total of 10 μCi Ni^{63} would meet the provisions of a general license. Assuming 0.003 μCi per transducer, possession of 3,333 such devices is licensed.

B. Waste Disposal (refs. B-3, B-4): In the event disposal of one or more sensors is deemed necessary, the most applicable methods are transfer to an authorized recipient; e.g., a commercial waste disposal service, or burial in soil.

C. Transportation (ref. B-5): "Radioactive materials in normal form not exceeding 1 mCi of Group IV (which includes Ni^{63}) are exempt from specification packaging, marking, and labeling, and are exempt from the general packaging requirements of Section 173.393 if the following conditions are met:

(1) The materials are packaged in strong, tight packages such that there will be no leakage of radioactive materials under conditions normally incident to transportation.

(2) The package must be such that the radiation dose rate at any point on the external surface of the package does not exceed 0.5 mCi per hour.

(3) There must be no significant removable radioactive surface contamination on the exterior of the package.

(4) The outside of the inner container must bear the marking "RADIOACTIVE".

A package containing 333,300 devices such as the MEPF/G Ni^{63} transducers would be allowed under this regulation.

It is anticipated that due to new postal regulations soon to be issued, shipment through U. S. Mails will not be possible.

II. Radiological Hazards:

A. Radiological Characteristics: Ni^{63} is a pure beta emitter, with a half life of 92 years. The emitted beta has a maximum energy of 0.067 MeV and decays to stable Cu^{63}. The maximum range of 0.067 MeV beta's is less than 1 cm air.

B. Deposition in Body (ref. B-6): Referenced document B-6 identifies the bone as the organ of interest for internal deposition of Ni^{63} and recommends a maximum permissible burden in the total body of 200 μCi. That is, if the quantity stipulated were deposited in the total body, it would result in the maximum allowable dose-rate to the critical organ. Specifically, for Ni^{63}, 200 μCi whole body deposition would result in a bone exposure of 5 rems per year. Assuming an average concentration of 0.003 Ci per transducer, the total Ni^{63} content of 66,666 such devices could be assimilated. Under the most stringent exposure conditions, i.e., those levels prescribed for non-radiation workers, this figure would be reduced by a factor of 10 to 6,666 devices.

C. Physical and Chemical Properties: Nickel is soluble in Nitric acid; slightly soluble in sulfuric and hydrochloric acids; and has a melting point 1453°C.

D. External Exposure: In view of the low energy beta particle emitted by Ni^{63}, the only type of exposure to be considered would be that received by the hands and fingers during manipulation of the sensors prior to placement in their copper casings. Current regulations specify that the hands should not exceed 18.75 rems per 13 week period. It would be impossible to approach this exposure level even by direct handling of the sensors.

III. Handling Precautions:

Although the external radiation dose-rate is negligible, it must be recognized that the Ni^{63} has been plated onto the transducer electrodes. Such a process does pose a potential source of contamination in that the radioactive material can be physically removed through abrasion or chipping. Therefore, particular attention should be given to the assembly procedure. It is suggested that the

transducers be handled only with disposable gloves; not only to prevent contamination, but to ensure cleanliness. Routine health physics surveys of shipping containers and work surfaces should be conducted.

IV. Conclusions:

In view of the quantities of Ni^{63} proposed in the MEPF/G project, the regulatory and radiological considerations are minimal. Due to the low energy of the emitted beta particles and relatively high melting point of Ni^{63}, the possibility of internal deposition and external exposure is extremely remote under prescribed handling techniques. Even under catastrophic conditions, such that all of the Ni^{63} on 3,000 transducers was assimilated by a single individual, the resulting exposure would be less than that prescribed by existing regulations.

Although the radiation hazards possible under this project are negligible, normal radiological safety techniques should be observed in order to eliminate all unnecessary exposure.

APPENDIX B

LIST OF REFERENCES

B-1. AEC Rules and Regulations, Title 10, Part 31, Section 31.4.

B-2. North Carolina Regulations for Protection Against Radiation, Section B.22, (a), (2).

B-3. AEC Rules and Regulations, Title 10, Part 20, Section 20.301.

B-4. North Carolina Regulations for Protection Against Radiation, Section C.301.

B-5. Department of Transportation, CFR, Title 49, Section 173.391, (a).

B-6. NBS Handbook 69, "Maximum Permissible Body Burdens and Maximum Permissible Concentrations of Radionuclides in Air and Water for Occupational Exposure.

APPENDIX C

ACTIVATION OF COPPER WITH NEUTRONS

APPENDIX C

ACTIVATION OF COPPER WITH NEUTRONS

Ordinary copper contains 69.1% $_{29}Cu^{63}$ and 30.9% $_{29}Cu^{65}$. The following reactions are possible with neutrons:

$$_{29}Cu^{63} + n \rightarrow {}_{29}Cu^{64} + \gamma$$

$$_{29}Cu^{64} \rightarrow {}_{30}Zn^{64}(\text{stable}) + \beta^{-} \; ; \; T_{\frac{1}{2}} = 12.8 \text{ hrs}$$

$$_{29}Cu^{64} \rightarrow {}_{28}Ni^{64}(\text{stable}) + \beta^{+} \; ; \; T_{\frac{1}{2}} = 12.8 \text{ hrs}$$

$$_{29}Cu^{63} + n \rightarrow {}_{29}Cu^{62} + 2n \quad \text{(requires neutron energies > 10 MeV)}$$

$$_{29}Cu^{65} + n \rightarrow {}_{29}Cu^{66} +$$

$$_{29}Cu^{66} \rightarrow {}_{30}Zn^{66}(\text{stable}) + \beta^{-} \; ; \; T_{\frac{1}{2}} = 5.1 \text{ min.}$$

An estimation of the amounts of copper converted to zinc or nickel is as follows: the intensity of neutrons at a distance r surrounding a point of source is

$$I = \frac{I_o}{4\pi r^2} ,$$

where I_o is the source strength in n/sec. For the RTG power supply, a worst case assumption is (ref. 2)

$$I_o = 2.90 \times 10^7 \text{ n/sec.}$$

At a distance of 6 feet,

$$I = \frac{2.90 \times 10^7 \text{ n/sec}}{4\pi \times (6 \text{ ft} \times 30.48 \text{ cm/ft})^2}$$

$$I = 69 \text{ n/sec - cm}^2.$$

The attenuation of neutrons is given by

$$I = I_o \exp(-\sigma Nx) ,$$

where

σ = cross section in cm^2

N = number of absorber nuclei per unit volume, and

x = thickness of absorber.

The only reaction of any significant cross section is the (n, γ) reaction. The cross section for the (n, γ) reaction varies between 6.1×10^{-24} cm^2 and 2.0×10^{-29} cm^2 for neutron energies between 1 and 10 MeV. Assume a cross-section of $\sigma = 1 \times 10^{-24}$ cm^2. The number density for copper is

$$N \quad 8.5 \quad 10^{22}/cm^3 .$$

If the thickness of the copper tubing is assumed to be 0.25 cm, for example, the intensity of given by

$$I = I_o \exp(-10^{-24} \times 8.5 \times 10^{22} \times 0.25)$$

$$= I_o \, 0.98$$

The change in the intensity with time is, of course, the activation rate, A, and is given by

$$A \equiv \Delta I = I - I_o = .69 \ (0.02)/\text{sec } cm^2 = 1.38/\text{sec } cm^2.$$

For a 1 cm^2 area, the number of copper atoms activated per sec is 1.3. This quantity is of absolutely no consequence even after a period 10^{10} years.

Any ionization radiation which may pass through the area near the MEPF/G transducer will only aid the breakdown phenomena. The γ energy is large enough to pass through the chamber; however, there will be only a few per second so that they will not aid significantly.